EXAMINATION COPY

Assessing the effects of site preparation treatments on erosion processes and sediment yield on a commercial *Eucalyptus* plantation - A case study at Two Streams, KwaZulu-Natal

Jordan Michael Bull

[redacted]

Submitted in partial fulfilment of the

requirements for the degree of MSc (Hydrology)

As the candidate's Supervisor I agree to the submission of this dissertation

School of Agriculture, Earth and Environmental Sciences

University of KwaZulu-Natal

Pietermaritzburg

26 August 2020

FRONTISPIECE

ABSTRACT

Soil erosion monitoring and modelling is critical in the face of climate change, as erosion is detrimental to environmental and human health. It reduces soil productivity through degradation, compromises water quality through nutrient loading freshwater sources, and decreases reservoir capacity through sedimentation. This is a global challenge which is being amplified by increased levels of soil erosion on cultivated lands (e.g. commercial forestry), the combined effects of which hinder the success of several United Nations Sustainable Development Goals. However, commercial forestry is essential for human survival, providing a host of resources for human consumption, and expanding in its global coverage each year; although, this expanding need for commercial forestry creates a paradox, as it has the potential to damage environmental health and biodiversity (systems which humans rely on for survival), particularly through soil erosion and sedimentation of freshwater systems. Afforestation of plantations has been widely considered a land-use activity which reduces soil erosion; although, this is dependent on the management of the commercial plantations, where certain commercial forestry management techniques exacerbate soil erosion, such as the well-used site preparation technique of burning. Therefore, an investigation into the effect of commercial forestry site preparation techniques such as burning (at different severities) and mulching on soil erosion and the modelling thereof is required, as only a paucity of research has reported on this.

Soil erosion measurements were conducted on a newly planted *Eucalyptus dunnii* stand, which consisted of three different site preparation techniques, namely a hot burn, a cold burn and a mulch treatment, in the Two Streams catchment, Kwa-Zulu Natal, South Africa. Micro-runoff and runoff plots were used to respectively measure splash and rill erosion of sediment, nitrogen, phosphorous, dissolved organic carbon, particulate organic carbon loss and runoff on each treatment at different slopes. In addition, soil erosion and runoff of this catchment and treatments were modelled using the ArcSWAT model, and the observations were used to validate the simulated outputs. The mulch treatment had the most consistent reduction in runoff and erosion, while the burn treatments of different severities generated greater respective runoff and erosion quantities through different erosional processes (splash vs rill). The ArcSWAT model over-simulated runoff on the hot burn and mulch treatment, while under-simulating on the cold burn treatment; however, the model consistently over-simulated sediment and nutrient loss on all treatments, indicating the model's inability to simulate soil erosion on the defined land-use treatments. The reduced runoff and erosion produced by the mulch treatment is

attributed to the protection that the mulch provides to the soil from splash erosion and the resistance posed to overland flow reducing rill erosion. The burn treatments generating more erosion and runoff through different erosional processes was attributed to the differing nature of debris produced by each burn severity. This research will contribute towards the data sets necessary to refine the land-use management tools of the ArcSWAT model to better model soil erosion on different land-use treatments. Furthermore, this research demonstrates the erosion processes that differing site preparation treatments are susceptible to, and what this means for future research and protecting soil and downstream water quality in the face of climate change.

DECLARATION

I Jordan Michael Bull declare that:

i. The research reported in this dissertation, except where otherwise indicated, is my original work.

ii. This dissertation has not been submitted for any degree or examination at any other university.

iii. This dissertation does not contain other persons' data, pictures, graphs or other information, unless specifically acknowledged as being sourced from other persons.

iv. This dissertation does not contain other persons' writing, unless specifically acknowledged as being sourced from other researchers. Where other written sources have been quoted, then:
a) their words have been re-written but the general information attributed to them has been referenced;
b) where their exact words have been used, their writing has been placed inside quotation marks, and referenced.

v. Where I have reproduced a publication of which I am an author, co-author or editor, I have indicated in detail which part of the publication was actually written by myself alone and have fully referenced such publications.

vi. This dissertation does not contain text, graphics or tables copied and pasted from the Internet, unless specifically acknowledged, and the source being detailed in the dissertation and in the References sections.

21/08/2020

Jordan Michael Bull Date

21/08/2020

Prof. Trevor Hill Date

23/08/2020

Prof. Colin Everson Date

ACKNOWLEDGEMENTS

My utmost gratitude goes out to my supervisors, Professor Trevor Hill and Professor Colin Everson, for the support, freedom, guidance and patience that they have provided me with throughout this research. I have been privileged to have supervisors who were so dedicated and passionate about my research, and I have you to thank for my growth as an academic throughout this project, and my successful pursuit of a PhD. Colin, you have provided me with invaluable support and leadership by not only guiding me in the academic realm, but by encouraging me to broaden my horizons through travelling and adventuring, whilst ensuring that I did not lose sight of my primary objective of furthering my education. Trevor, you have provided me with eternal support, guidance and mentorship in my academic career and outside of academia, encouraging me to adventure and explore the world, whilst still maintaining a strong academic focus and standing. The incredible experiences that I have been allowed to have throughout this research, have shaped me into the person and academic I am today, and for this I am forever grateful.

This research is a part of a larger research project (WRC K5/2402) which is funded and managed by the Water Research Commission, entitled 'Assessing the impact of erosion and sediment yield from different land uses in farming and forestry systems and their effect on water resources in selected catchments of South Africa'. I would like to thank the Water Research Commission for funding this research, and Mondi for their collaborative efforts with this research, and in particular David Mhlongo, Silviculture Forester at Mondi for overseeing the implementation of the forestry treatments required for this research.

To those who contributed their technical expertise towards the success of this research, thank you Sanele Ngubane, Dr Khatab Mohammed Abdalla, Vivek Naiken, Matthew Dickey, Jarryd Gillham, and Mr Cobus Pretorius. A special thank you to Dr Bruce Charles Scott-Shaw, Post-Doctoral Student, School of Agricultural, Earth & Environmental Science, for his invaluable support and guidance with the SWAT modelling phase of this research. To my fellow students and friends who assisted with fieldwork: Gugulethu Tshabalala, Kyle Trent Cameron Reddy, and Keanu Singh, Ruvekh Singh, and Corny Dellwisch; your effort, time and motivation throughout my research are tremendously appreciated. I would also like to extend my deepest appreciation to Dr Hewer, Dr Delport, and the UKZN Discipline of Biochemistry, for giving me access to their vacuum pump and filter papers during the lab-work phase of this research.

I would like to show my greatest appreciation to Mannilall Sewcharran and Umgeni water, for their outstanding assistance with laboratory work vital for this research. My thanks are also extended to the Department of Agriculture and Rural Development, Soil Science Analytical Services laboratory, Cedara, for their impeccable assistance in analysing soil samples.

To my loving parents Catherine Bull, Sean Bradshaw and Emma Bradshaw, my wonderful siblings Hudson, Jimothy, and Cassidi, and my beautiful dog Biscuit, I would like to thank you for your eternal love and support. The happiness, encouragement and chaos you have brought to my life throughout this research were imperative for the success of this research.

I would like to express my deepest love and appreciation to my loving girlfriend Sarah Wilson Kemsley for your unwavering patience, support and encouragement throughout my research. You have stood by me through the most difficult parts of this research, where at times my patience has been little, and my mind absent. You have been a pillar of strength throughout my life, and the success of this research is largely owing to you. For everything that you are, I am eternally grateful. I would also like to extend this appreciation to Kate Kemsley, for her love, support and always providing me with the encouragement needed to complete this research, which has helped me produce research of the highest possible quality.

To Dirty-Mike and the boys (Brad, Jadin, Steve, Mariah, Kayle, Dean, Josh, Tyler, Vince, and Dee), I would like to thank for the endless support, light-heartedness, and chaotic joy you have given me throughout this project. You have always been a source of unending love, happiness and encouragement within my life.

Lastly, I would like this research to serve as a commemoration of Mariah Amy George, the most beautiful soul I have ever had the privilege of loving and being loved by. The happiness and joy you gave to others was unmatched and of the purest and kindest form. Every memory I have with you is cherished dearly, and a day does not pass where you are not missed or longed for. In my heart, you are always with me.

TABLE OF CONTENTS

LIST OF TABLES

LIST OF FIGURES

LIST OF PLATES

Chapter One

Introduction

1.1 Introduction

The cultivation of trees under commercial forestry provides a range of products for human use, such as fibre and pulp for the production of paper, and charcoal used in the production of steel (Jewitt, 2005). Commercial forestry primarily consisting of exotic/alien species is used to provide wood for the timber industry (Nambiar, 1999; Jewitt, 2005). Forestry plantations cover approximately 10 million ha worldwide, with this area having an estimated growth rate of 1 million ha year^{-1} (Jewitt, 2005). The predominantly cultivated species are those which have a short rotation and fast growth rates, typically belonging to the *Eucalyptus* and *Acacia* genera (Montagnini and Nair, 2004). Despite the economic benefits provided by commercial forestry, these plantation species tend to be a paradox species, providing vital resources; however, compromising environmental health, in particular biodiversity, river sedimentation, and exacerbating soil erosion directly through growth or indirectly through planting and harvesting (Blackburn *et al*., 1986; Carpenter *et al*., 1998; Fernández *et al*., 2004; Chaplot *et al*., 2011; Oliveira *et al*., 2013).

Globally, and in South Africa, soil erosion by water is the most significant form of land degradation (Laker, 2004). Natural global erosion rates range from 0 – 64 t ha^{-1}, while cultivated lands exacerbate soil erosion, producing erosion rates from 0.1 – 200 t ha^{-1} (Morgan, 2009). Soil erosion has far-reaching effects on a range of life supporting systems, namely food supply and security, natural ecosystems, public health, and economic development (Knox *et al.*, 2010; Chaplot *et al*., 2011; Schaller *et al.*, 2016). This obstructs the attainment of several sustainable development goals set out by the United Nations aimed at, *inter alia*, improving environmental sustainability and ensuring peace, prosperity and an end to poverty (United Nations, 2015).

The processes of soil erosion by water function at different spatial scales, beginning with the impact of raindrops on the soil surface driving splash erosion, followed by concentrated and channelized runoff causing linear erosion ranging from inter-rill to gully erosion, and having several off-site impacts (siltation of reservoirs, and compromised water quality) (Blackburn *et al*., 1986; Salles and

Poesen, 2000; Cantón *et al*., 2011; Chaplot *et al*., 2011). In addition, there are *in situ* effects of soil erosion, such as a reduction in water holding capacity and productivity of the soil, through the removal of fertile soil horizons (Toy *et al.*, 2002; Chaplot *et al*., 2011). However, soil erosion can be regulated by vegetation cover, which reduces raindrop kinetic energy, entraps eroded soil particles, and reduces the slaking of aggregates (Podwojewski *et al*., 2011). In addition, soil erosion can be controlled through conservative land management practices such as, contour cropping, mulching, and maintaining soil organic matter (SOM) (Pimentel *et al*., 1995; Rickson, 2014).

Commercial forestry has the potential to increase the vulnerability of a landscape to soil erosion and sediment loss through site preparation techniques (Blackburn *et al*., 1986). These techniques disturb the soil, affecting soil productivity and downstream water quality (Blackburn *et al*., 1986). Despite the threat it poses to soils, commercial forestry site preparation techniques are used by forest managers, as they aid in the preparation of a seedbed, control competing species, and assist in planting (Blackburn *et al*., 1986). Site preparation methods include burning mulching, mechanical preparation (brush chopping, shearing and windrowing, bedding on the contour), and shallow harrowing (Beasley, 1979; Robichaud and Waldrop, 1994; Piirainen *et al*., 2007; Lakel et al., 2010). A well-used method for preparing forestry sites is the burning of the site after harvesting of the previous rotation (Robichaud and Waldrop, 1994; Lakel *et al*., 2010). However, this has the potential to produce water-repellent layers within the soil, and surface sealing, which reduces soil infiltration and increases runoff, leading to increased soil erosion (DeBano *et al*., 1976; Neary *et al.*, 1999; Scott, 2000; Martin and Moody, 2001). Robichaud and Waldrop (1994) note that the severity of the post-harvest burns affects the quantity of the sediment loads which are transported from forestry sites.

Commercial forest plantations have the potential to increase runoff and erosion, by inhibiting the growth of the understory, which is responsible for increasing soil infiltration, resulting in increased runoff (Geißler *et al.*, 2012). There are several factors which affect soil erosion within a plantation, namely raindrop fall velocity and size distribution, precipitation intensity, leaf and crown attributes, canopy density and height, LAI (Leaf Area Index), and the soil cover (litter) (Geißler *et al.*, 2012). *Eucalyptus* plantations experience increased levels of erosion and runoff in comparison to natural grazing lands, and burned macchia, and an inverse relationship with the age of the tree and the observed soil erosion (Vacca *et al.*, 2000; Oliveira *et al*., 2013).

This study investigates site preparation and soil erosion on a young *Eucalyptus* stand in KwaZulu-Natal, South Africa. The focus being commercial forestry because of its potential to disrupt natural erosion processes and soil nutrients, affecting soil productivity and water quality. The observations of this study are used to validate a sediment yield model.

1.2 Research Aim and Objectives

The research question was: how do commercial forestry site preparation techniques influence soil erosion processes?

The research aim was to assess the effect of site preparation techniques of a commercial *Eucalyptus* plantation on the generation of runoff volume, sediment and nutrient load from rain splash and rill erosion and assess the accuracy of modelling. The research aim was achieved through the following objectives:

i. Set up of an experiment carefully designed to measure soil erosion and nutrient loss at the scales at which rain splash and rill erosion operate.
ii. Determination of sediment yields, nutrient losses and runoff generation on differing site preparation treatments at the spatial scales that each erosion process functions.
iii. Identifying the causes of varying runoff, nutrient loss and sediment yield generation of different site preparation treatments.
iv. Use the observed results to verify modelled soil erosion of the same site preparation treatments.

The natural landscapes which support human life are subject to land degradation resulting from land management practices (Blackburn *et al.*, 1986; Knox *et al.*, 2010; Geißler *et al.*, 2012). This is of particular importance as soil erosion, coupled with land degradation, is detrimental to the *in situ* location and has off-site impacts (Blackburn *et al*., 1986; Salles and Poesen, 2000; Laker, 2004; Chaplot *et al*., 2011). The resultant decline in environmental and human well-being is in direct conflict with several sustainable development goals (Knox *et al.*, 2010; Chaplot *et al*., 2011; United

Nations, 2015; Schaller *et al.*, 2016). This justifies the importance of conducting research into better understanding the impacts of large-scale land management and how land management can align with commercial needs, while supporting environmental conservation. This project was a component of a larger research project (WRC K5/2402) funded by the Water Research Commission entitled 'Assessing the impact of erosion and sediment yield from different land uses in farming and forestry systems and their effect on water resources in selected catchments of South Africa'.

Chapter Two

Literature Review

2.1 Introduction

The literature review chapter consists of an amalgamation of recent literature sources pertaining to soil erosion and sediment yield, and the described project. First, the different types of soil erosion and assessing its scalar variation was investigated in 'Types and Assessment of Soil Erosion', followed by the primary factors which drive soil erosion rates in 'Governing Factors of Soil Erosion Rates'. The environmental impacts of soil erosion and implications for human life can be expected in 'Effects of Soil Erosion'. The section 'Soil Erosion and Commercial Forestry' provides an insight into the linkages between soil erosion and commercial plantations and the management thereof. The different methods for preparing commercial forestry sites and their implications are reviewed in 'Plantation Management'. Soil erosion reduction methods are discussed in 'Soil Erosion Mitigation'. A review of the ACRU, SWAT, and USLE models, which are commonly utilised in the modelling of soil erosion, can be found in 'Sediment Yield Modelling'. Finally, a synthesis of the literature review is presented.

At a global scale, soil erosion by water is a major threat to ecosystem health, leading to global land degradation (Podwojewski *et al.,* 2011). Contemporary rates of erosion has been accelerated by human activities, and is greater than the rate of soil formation, reducing soil productivity and removing soil nutrients such as nitrogen and phosphorous (Carpenter *et al*., 1998; Toy *et al.,* 2002). Soil erosion and land degradation is a critical environmental issue in South Africa, where more than 70% of the country is affected with soil erosion of varying severities (Le Roux *et al*., 2008). It is estimated that soil erosion costs South Africa R2 billion per year, which includes the costs of remediating the off-site impacts of soil erosion, such as dredging reservoirs which suffer from siltation (Le Roux *et al*., 2008).

Soil erosion has far-reaching effects on several important facets of human survival, namely food supply and security, natural ecosystems, public health, and economic development (Blackburn *et*

al., 1986; Salles and Poesen, 2000; Chaplot *et al*., 2011). Soil irreversibly damaged as a consequence of soil erosion has reduced water holding capacity, in conjunction with reducing the productivity of the soil, through the removal of fertile soil horizons (Blackburn *et al*., 1986; Chaplot *et al*., 2011). Soil erosion results in catchment-scale consequences, such as sedimentation of reservoirs (jeopardizing water security and quality), and debris flows (Chaplot *et al*., 2011). The rise in exploitation of the upper reaches of catchment land resources leads to an increase in observed sediment yields, accompanied by nutrient loading of water courses, which ultimately reduces catchment water quality (Valentin *et al.*, 2005).

2.2 Types and Assessment of Soil Erosion

There are several agents which are responsible for providing energy for the erosion and sedimentation process, namely physical (wind, water and ice), gravity, chemical reactions, and anthropogenic disturbances such as tillage (Lal, 2001; Toy *et al.*, 2002). The process of erosion and sedimentation consists of soil particle (along with other earth particles) detachment, entrainment, transportation, and finally deposition (Toy *et al.*, 2002). Where the sediment yield/load is defined as the quantity of sediment which is transported to a particular point of measurement (Toy *et al.*, 2002).

In South Africa, water is the primary soil erosion agent, and results in the generation of various stages of the erosion process, which is determined by the interaction between the soil and water (Salles and Poesen, 2000; Le Roux *et al*., 2008). The impact of raindrops on the soil surface is a dominant instrument for soil erosion by water (Salles and Poesen, 2000; Rumpel *et al*., 2009). As the raindrops hit the soil surface, they cause soil detachment, which is transported by splash and overland flow (surface runoff) (Salles and Poesen, 2000; Rumpel *et al*., 2009). The generation of overland flow is strongly influenced by rainfall intensity, antecedent soil moisture, and slope steepness, whereby an increase in either of these factors increases runoff production (Ziadat and Taimeh, 2013). Runoff is generated through saturated and Hortonian overland flow (Parsons and Abrahams, 1992). Saturated overland flow occurs when the soil reaches its volumetric infiltration capacity due to rainfall, becoming saturated, resulting in water accumulating on the soil surface and running off (Parsons and Abrahams, 1992). Hortonian overland flow is the result of rainfall

intensity surpassing the soil infiltration rate, resulting in overland flow (Parsons and Abrahams, 1992). As runoff increases, so too does the risk of sheet and rill erosion, which has the potential to harm the natural environment (Le Bissonnais *et al.*, 1998). Inter-rill erosion consists of uniform sheet erosion on the inter-rill area, the runoff and eroded material takes a lateral flow path towards adjacent rills (Toy *et al.*, 2002). Rill erosion occurs as erosion rates increase, whereby erosion takes place in concentrated incisions, known as rills (Toy *et al.*, 2002). The formation of gullies is the next successional phase of erosion, where severe erosion rates lead to the development of deep incised channels (Toy *et al.*, 2002). Upon the commencement of channelized runoff, linear erosion occurs, consisting of rill and gully erosion (Chaplot *et al.*, 2005). At any stage of the erosion process, transportation of sediment can cease because of changes in slope or ground cover, reducing the erosive energy of the agent, and causing deposition (Lal, 2001; Ziadat and Taimeh, 2013).

The mitigation and recovery from soil erosion requires an understanding of the spatial extent of the soil erosion (Le Roux *et al*., 2007). It is understood that at smaller spatial scales the primary detachment and transport process are being driven by rain splash which can be measured at the plot scale of 1 m^2 (Rumpel *et al*., 2009; Chaplot and Poesen, 2012). Runoff detachment becomes the dominant erosive process at a larger surface area, being measured at a scale of several m^2 (Chaplot and Poesen, 2012). This scalar variation in soil erosion processes makes it a necessity to measure soil erosion at varying spatial scales to determine the dominant processes (Cantón *et al*., 2011; Chaplot and Poesen, 2012). Therefore, conducting research on a multi-scale basis appears to be a promising method for the identification and quantification of the relative erosion processes, which are acting on and dominating a landscape at varying spatial scales, such as splash, inter-rill, rill, and gully erosion (Cantón *et al*., 2011; Chaplot and Poesen, 2012).

2.3 Governing Factors of Soil Erosion Rates

Soil erosion is a naturally occurring process; however, it is deemed ‘accelerated soil erosion’ when the erosion taking place is viewed as being detrimental to the environment (Beckedahl and De Villiers, 2000). This section focuses on the factors which affect the rate at which soil erosion occurs, namely rainfall erosivity, soil erodibility, topography, vegetation cover, soil management techniques, and soil conservation practices (Singh *et al*., 1992; Lal, 2001).

The potential ability of rainfall to cause erosion is regarded as the rainfall erosivity and is an interaction between the kinetic energy of rainfall and the soil surface (Obi and Salako, 1995; da Silva, 2004). Rainfall erosivity is governed by several factors, which can be divided into two distinct groups, those which are directly related to the precipitation, and those which are related to the surrounding environment (Obi and Salako, 1995; Lal, 2001). Factors that are directly related to the precipitation consist of drop size distribution, terminal velocity, rainfall duration, frequency, and intensity (Obi and Salako, 1995; Lal, 2001). Factors which are extraneous to precipitation consist of slope angle, and wind velocity (Obi and Salako, 1995; Lal, 2001).

The soil's susceptibility to be eroded by the aforementioned agents of erosion is indicated by its erodibility (Lal, 2001; Buttafuoco *et al.,* 2012). This is dependent on several soil characteristics, namely physical, and chemical characteristics, and organic matter (OM) content (Lal, 2001; Buttafuoco *et al.,* 2012). The physical characteristics consist of soil texture and structure, porosity, shear strength, aggregate stability, soil water retention, infiltrability, clay minerals, and transmissivity (Lal, 2001; Buttafuoco *et al.,* 2012). Chemical characteristics consist of cation and anion exchange, and present cations, where potassium enriched soils have an increase in soil erodibility, runoff generation, and erosion (Auerswald *et al*., 1996; Lal, 2001). In addition, soil erodibility is influenced by management practices employed on the landscape, as it is a dynamic attribute of soils (Lal, 2001). Soil erosion rates are further influenced by the topographical characteristics of a landscape (Lal, 2001; Buttafuoco *et al.,* 2012), the characteristics include: the gradient of the slope, slope length, aspect, and slope shape (Lal, 2001; Buttafuoco *et al.,* 2012). In South Africa, highly erosive dispersive and duplex soils are abundant in some regions (Rienks *et al*., 2000; Hardie *et al*., 2009; Fey, 2010). Duplex soils have a hard and dense B horizon, which has a notably high clay content, leading to a clear boundary between the overlaying horizon (Fey, 2010). Duplex soils are highly erodible, as clay dispersion in this soil results in surface crusting, increasing runoff and erosion, while subsurface erosion (piping) is a potential for this soil type, where the low permeability of the B horizon encourages subsurface flow and subsequent erosion along the inter-boundary line (Fey, 2010). Subsurface erosion is a common trait within dispersive soils, which is the result of clay platelets separating from aggregates in the presence of fresh water (Hardie *et al*., 200). The result is the suspension of clay platelets which are transported via cracks and pores and finally entering a water source, where they can be observed as 'muddy' or 'milky' water (Hardie *et al*., 200).

Soil cover significantly influences soil erosion, as it dissipates the energy provided by the various agents of soil erosion (Lal, 2001; Mohammad and Adam, 2010). This is achieved through several measures; however, the magnitude of control is governed by the vegetation type, root system, size, litter components, and shape of the vegetation (Mohammad and Adam, 2010; Podwojewski *et al*., 2011). Soil cover reduces raindrop kinetic energy and runoff velocity, increasing soil infiltration and preserving soil aggregates via root structures, cumulatively leading to a reduction in runoff and soil detachment (Podwojewski *et al*., 2011). The entrapment of fine soil particles which have been eroded is increased by soil cover, as it functions as a filter (Podwojewski *et al*., 2011). However, a lack of soil cover (resulting from the removal of residue or burning) ultimately results in an increase in soil erosion rates (Lal, 2001; Mohammad and Adam, 2010).

There is a strong link between soil erosion and land management, where soil erosion is exacerbated by anthropogenic, social, and political factors, such as high-density populations, and intensive land-use activities such as overgrazing (Pimentel *et al*., 1995; Podwojewski *et al.*, 2011; Gillham, 2016). Maintenance of a permanent and dense vegetation cover is the most effective method for reducing soil erosion, the loss of which results in significant increases in soil erosion (Pimentel *et al*., 1995; Laker, 2004). Furthermore, the conversion of steep natural landscapes to agricultural lands results in increased soil erosion rates but continues to occur due to the needs of a rising human population (Pimentel *et al*., 1995). However, it is possible to protect soils and curb erosion rates on cultivated land though conservative land management practices (Pimentel *et al*., 1995; Ekholm and Lehtoranta, 2012; Rickson, 2014). These include *inter alia* the employment of reduced tillage, afforestation (such as commercial forestry), planting on the contour, cultivating cover crops, mulching, strip cropping, and terracing (Pimentel *et al*., 1995; Ekholm and Lehtoranta, 2012; Geißler *et al*., 2012; Rickson, 2014).

Despite the availability of several conservative techniques, a commonly employed method for managing landscapes is the use of fire (Snyman, 2003; Strydom, 2013). The method alters soil characteristics and vegetation, reducing soil infiltration rates, which affects the partitioning of water into runoff, and subsurface throughflow, at the soil surface (Doerr *et al*., 1996; Shakesby and Doerr, 2006; Cerda and Robichaud, 2009). Reductions in infiltration rates of soils stem from chemical and physical alterations of the soil subsequent to burning (Saá *et al.*, 1994; Neary *et al.*, 1999; Martin and Moody, 2001). Fire-driven physical alterations of soils which lead to reductions in soil infiltration include: changes in soil structure, post-fire ash, and exposure of bare soils (Neary *et al*.,

1999). The combustion of SOM affects soil structure and can lead to the reduction of soil infiltration and increased soil nutrient loss (Saá *et al.*, 1994; Neary *et al.*, 1999). Severe catchment burns leave deposits of ash and charcoal, which, aided by small soil particles, seal larger soil pores, reducing infiltration (Morin and Benyamini, 1977; Neary *et al.*, 1999; Martin and Moody, 2001; Strydom, 2013).

Prescribed burns utilised for catchment management have been found to exhibit no significant impacts on nitrogen and dissolve organic carbon concentrations in runoff (Knoepp and Swank, 1993; Clay *et al*., 2009). The bare soil surface becomes susceptible to rain splash, which destroys soil aggregates at the soil surface, and seals pores, resulting in the development of a surface crust, further reducing infiltration (Morin and Benyamini, 1977; Martin and Moody, 2001; Strydom, 2013). The reductions in infiltration following a burn lead to increases in surface runoff, total discharge, peak discharge, soil erosion, and sedimentation (Rycroft, 1947; Van Wyk, 1986; cited by Toucher *et al.*, 2016; Scott and Van Wyk, 1990; Doerr *et al.*, 1996; Neary *et al.*, 1999). In addition, burn severity has been shown to affect soil phosphorous loss due to soil erosion, whereby the greater the burn severity, the greater the degree of phosphorous loss (Saá *et al.*, 1994).

2.4 Soil Erosion Impacts

Clean water is crucial for human survival, as it is necessary for drinking, cropland irrigation, supporting ecosystems and biodiversity, industry, and transport (Carpenter *et al*., 1998). Water resources are compromised by erosion that leads to the pollution and sedimentation of water bodies (such as reservoirs), which is a growing threat in South Africa, impacting ecosystem health and human well-being (Carpenter *et al*., 1998; Le Roux *et al*., 2013). Pollution and sedimentation of freshwater sources has led to a decline in water quality and security of many rivers, lakes, and dams (Carpenter *et al*., 1998; Le Roux *et al*., 2013). The impacts of soil erosion are diverse and sweeping, and compromise the success of several United Nations sustainable development goals namely ‘zero hunger’, ‘good health and well-being’, ‘clean water and sanitation’, ‘decent work and economic growth’, ‘responsible consumption and production’, ‘life below water’, and ‘life on land’ (Carpenter *et al*., 1998; Le Roux *et al*., 2013; United Nations, 2015).

In situ water erosion impacts landscapes by removing nutrient rich soil horizons, ultimately reducing the productivity of the soil (Blackburn *et al*., 1986; Chaplot *et al*., 2011). However, the sediment which is transported off the erosion site (such as forestry plantations) leads to nonpoint source pollution, resulting in water quality decline and the sedimentation of reservoirs and valley bottoms (Carpenter *et al*., 1998; Curriero *et al*., 2001; Chaplot *et al*., 2011). Furthermore, soil erosion, and the resultant suspended sediment load in the fluvial system has the potential to damage hydrological structures (Van Wyk, 1986; cited by Toucher *et al.*, 2016). This sediment load reduces water quality by increasing the turbidity of the water, which has been directly correlated to increasing ailment in communities, as it shields microbes from disinfection mechanisms such as solar UV radiation (Curriero *et al*., 2001; Thompson *et al*., 2003). A significant off-site issue is eutrophication, stemming from nutrient loading of phosphorus and nitrogen in freshwater bodies, causing excessive algal blooms (Carpenter *et al*., 1998). These blooms of blue-green algae (cyanobacteria) can be aggressive and result in significant water quality deterioration (Carpenter *et al*., 1998).

Soil erosion has the potential to remove soil organic carbon, which is crucial within soils, as it aids in soil aggregation, vegetation nutrient supply, and acts as a carbon sink for the greenhouse gas carbon dioxide (Le Bissonnais and Arrouays, 1997; Zinn *et al*., 2002; Mohammad and Adam, 2010; Oliveira *et al*., 2013). The sustainability of land-use activities is dependent on the conservation of soil organic carbon; however, land-use activities have the potential to negatively affect soil organic carbon (Le Bissonnais and Arrouays, 1997; Zinn *et al*., 2002; Oliveira *et al*., 2013). The consequences are a steady rise in concentrations of atmospheric carbon (contributing to greenhouse gases), stemming from land-use activities which release carbon from the soil (Lal, 2001). The erosion driven loss of soil carbon is responsible for contributing towards the observed increases in the pool of atmospheric carbon (Lal, 2001).

In South Africa it is projected that future climate change will result in increased extreme rainfall events (Mason *et al.*, 1999), where summer rainfall over the eastern and interior part of the country is expected to increase, while winter rainfall over the western part of the country is expected to decline (Hewitson and Crane, 2006). It is expected that changes in the future climate will impact soil resources, as soil erosion and transportation of sediments are governed by precipitation and runoff (Chaplot, 2007).

2.5 Soil Erosion and Commercial Forestry

Afforestation has been widely regarded as a land management measure that aids in the prevention of soil erosion, and is continuously being utilised through the introduction of commercial forest plantations (Geißler *et al*., 2012). Commercial plantations can reduce soil erosion by dissipating the energy of raindrop impact, stabilizing the soil with root systems and a litter layer, and improving soil infiltrability (Kort *et al*., 1998; Geißler *et al*., 2012; Gillham, 2016). This is not to say that commercial forestry guarantees a reduction in soil erosion (Nanko *et al*., 2004, 2008; Geißler *et al*., 2012; Oliveira *et al*., 2013). The density and management practices of a commercial forest are crucial in determining quantity of soil erosion on a landscape (Fernández *et al*., 2004; Geißler *et al*., 2012; Oliveira *et al*., 2013). There are, however, additional controlling factors of soil erosion under a forested canopy namely, raindrop fall velocity and size distribution, precipitation intensity, leaf and crown attributes, canopy height, LAI (Leaf Area Index), vegetation age, and the soil cover (litter) (Geißler *et al*., 2012; Oliveira *et al*., 2013).

It has been demonstrated that the throughfall which occurs in plantations, is more erosive than rainfall which occurs in an open field (Nanko *et al*., 2004, 2008). This is due to the raindrops coalescing and increasing in diameter as they travel via throughfall, leading to an increase in their erosive energy compared to rainfall in an open field (Nanko *et al*., 2004). This is the result of the throughfall raindrops falling at a lower frequency, but having a larger diameter (Nanko *et al*., 2004). Ultimately, this leads to the throughfall having a greater potential to cause splash erosion (Geißler *et al*., 2012). *Eucalyptus* plantations have been found to increase soil erosion and nutrient loss (P, K, Ca, Mg, organic carbon) during the early stages of growth, and decline in erosion with increasing tree size (Oliveira *et al*., 2013). During the early stages of growth, the canopy cover produces little cover for the soil surface, leaving the bare soil exposed, increasing soil erosion, nutrient loss, and organic carbon loss (Oliveira *et al*., 2013). In addition, soil erosion removes nitrogen from landscapes transporting it downstream, affecting water quality (Carpenter *et al*., 1998).

Despite these shortcomings, South Africa is dependent on the commercial farming of exotic species, *Eucalyptus* in particular (Albaugh *et al*., 2013). Soil erosion in South African timber plantations is exacerbated by soil water repellency, which reduces soil infiltrability, and enhances overland flow, and thus erosion (Le Bissonnais *et al.*, 1998; Scott, 2000). Water repellency on

Eucalyptus plantations in South Africa is a frequent occurrence, where soil texture or class plays no part in preventing the development of water repellent soils (Scott, 2000).

2.6 Plantation Management

Burning is commonly used as a form of site preparation when planting a new commercial forestry stand (Blackburn *et al*., 1986; Swift *et al*., 1993; Vose and Swank, 1993; Robichaud and Waldrop, 1994). There are several types of burns which can be employed, such as the brown-and-burn, fell-and-burn, and a burn based on seasonality (Blackburn *et al*., 1986; Swift *et al*., 1993; Vose and Swank, 1993; Robichaud and Waldrop, 1994). Burning has the potential to be coupled with other site preparation methods such as shearing and windrowing, and roller chopping (Blackburn *et al*., 1986). The use of burning as a site preparation method is relied upon for its ability to prepare the seedbed, facilitate planting, and control competing species (Vose and Swank, 1993; Blackburn *et al*., 1986). It has been noted by Robichaud and Waldrop (1994), that greater severity site preparation burns produce significantly larger quantities of sediment loads which are transported from forestry sites. Water-repellency in soils can develop from the burning of OM, leading to the production of organic gas, which envelopes soil particles, and reduces soil infiltration due to its hydrophobic nature (DeBano *et al*., 1976; Scott, 1994; Martin and Moody, 2001).

Several studies have assessed the effect of mulching forest soil after the occurrence of a wildfire in an attempt to control soil erosion (Bautista *et al*., 1996; Prats *et al*., 2012: Robichaud *et al*., 2013). Mulching attempts to reduce erosion through increasing the effective ground cover on the soil surface, and by covering the soil with one of several materials (Bautista *et al*., 1996; Prats *et al*., 2012: Robichaud *et al*., 2013). Bautista et al. (1996) found that following a wildfire, a straw mulch reduced runoff and soil erosion by approximately 720 % compared to un-mulched soils, in a mature pine forest in semi-arid Spain. In Portugal, the mulching of a *Eucalyptus* plantation following a wildfire using chopped *Eucalyptus* bark was able to reduce the runoff coefficient from 26 to 15%, and soil erosion from 5.41 to 0.74 Mg ha^{-1} (Prats *et al*., 2012). Despite the ability of mulching to significantly reduce soil erosion, few studies have been conducted which assess the performance of mulching, as a site preparation technique on soil erosion (Fernández *et al*., 2004). In Spain, it was found on a post-harvest forestry site that the slash scatter treatments had the greatest effect on

the prevention of soil erosion, and burn treatments resulted in the greatest sediment losses (Fernández *et al*., 2004).

2.7 Soil Erosion Mitigation

The continual process of soil erosion is complex and dynamic, having both *in situ* and *ex situ* impacts; however, it is more desirable to control erosion at its source, protecting the soils, and downstream water quality (through reduced pollution) (Carpenter *et al*., 1998; Chaplot *et al*., 2011; Rickson, 2014). Furthermore, the costs of proactive mitigation (such as increasing soil cover) of soil erosion are far less than the reactive costs (such as dredging), emphasising the importance of controlling erosion at source (Rickson, 2014). A key factor in the regulation of soil erosion is the vegetation type and degree of vegetation cover (Laker, 2004). Vegetation provides an aerial canopy cover, and a surface basal cover, which protects the soil surface. Below the surface, SOM and root systems stabilize soil aggregates, reducing soil erosion (Guerra, 1994; Laker, 2004; Podwojewski *et al*., 2011).

Reducing soil erosion at its source in cultivated lands will protect water resources from water quality decline by preventing freshwater nutrient loading and eutrophication (Ekholm and Lehtoranta, 2012). This can be established by introducing on-site preventative measures, which can be used individually or coupled with other measures (Pimentel *et al*., 1995; Ekholm and Lehtoranta, 2012; Rickson, 2014). These measures include, inter alia, contour cropping, cover crops, constructing settling ponds, check dams, and wetlands, establishing in-field and edge-of-field grass buffer strips, mulches, terracing, and maintaining SOM (Pimentel *et al*., 1995; Ekholm and Lehtoranta, 2012; Rickson, 2014). The majority of these methods maintain a protective cover over the soil, which intercepts and reduces the kinetic energy of raindrops (Pimentel *et al*., 1995; Ekholm and Lehtoranta, 2012; Rickson, 2014). In addition to providing a protective cover, mulches release nitrogen and organic carbon into the soil through decomposition (Youkhana and Idol, 2009). Hydrological models can be utilised as a pre-emptive method to mitigate and reduce the potential impacts of soil erosion on a landscape caused by human activity (Le Roux *et al*., 2013; Nearing, 2013). This is achieved by using model outputs to aid in the regulation of land-use activities to

ensure compliance with conservation regulations (Nearing, 2013). Models are designed to be used for soil erosion predictions either on or off-site or both (Nearing, 2013).

2.8 Sediment Yield Modelling

Our understanding of the physical laws of the processes which are taking place in the natural environment forms the foundation upon which soil erosion models are built (Oeurng *et al.,* 2011). Soil erosion models are categorized into different classes which is usually determined by the complexity of the model, and the models spatial and temporal resolution (Le Roux *et al*., 2007). The main model categories are: physically based, empirical, and conceptual (Le Roux *et al*., 2007).

Soil erosion models are limited, as there is generally a poor prediction of the spatial patterns of erosion (Le Roux *et al*., 2007). In addition, most models are unreliable when it comes to producing accurate predictions of quantities of soil erosion/sediment yield which are absolute (Le Roux *et al*., 2007). Model data requirements significantly increase as the more spatial and temporal complexities are introduced (Le Roux *et al*., 2007). Nevertheless, soil erosion models have been reworked and used at regional scales in South Africa to produce objective comparisons, which are crucial for identifying areas requiring soil conservation efforts (Le Roux *et al*., 2007).

The Agricultural Catchment Research Model (ACRU) model is an example of a physical conceptual model, which is utilized in South Africa (Jewitt and Schulze, 1999; Le Roux *et al*., 2007). This model simulates sediment yields by integrating elements of the soil water budget with modules (Jewitt and Schulze, 1999). The ACRU model is limited as the outputs require verification against observed data sets to be confidently used (Jewitt and Schulze, 1999).

In contrast, the Soil and Water Assessment Tool (SWAT) is a conceptual model developed in the United States, which is employed in South Africa, and commonly used in catchments which contain agricultural areas, to evaluate water quality and hydrological processes (Oeurng *et al.,* 2011). The transportation of sediments, and the ArcSWAT GIS interface, make SWAT an effective model for use in commercial forestry, which has a high degree of spatial complexity (Scott-Shaw *et al.,* 2020). The SWAT model simulates the impacts in ungauged rural basins that differing land management decisions have on water and sediment yields (Le Roux *et al*., 2007). The SWAT model, once

calibrated, has been used successfully to model sediment yield and streamflow on an *Acacia mearnsii* plantation in the Two Streams catchment, South Africa (Scott-Shaw *et al.*, 2020). However, prior to calibrating the SWAT model, Scot-Shaw et al. (2020) found that the model was under-simulating streamflow. To improve calibration of the SWAT model a greater number of measured sediment and nutrient loss values are required for use in the calibration process of the model (Scott-Shaw *et al.*, 2020). Despite being developed in the USA, the SWAT model has been successfully used in South Africa, and in many other places around the globe, including Europe, China, and central Africa, demonstrating its ability to model runoff, streamflow, erosion and nutrient cycling in a range of regions (Govender and Everson, 2005; Panagopoulos *et al.*, 2007; Wu and Chen, 2009; Setegn *et al*., 2010; Gyamfi *et al*., 2016; Scott-Shaw *et al.*, 2020).

The Universal Soil Loss Equation (USLE) is an empirical model, which relates soil erosion to several natural factors (Lal, 2001; Buttafuoco *et al.*, 2012). Originally developed to predict soil erosion which occurred on hillslopes and cultivated areas, but was later modified to enable the prediction of soil erosion under different circumstances (Lal, 2001). The prediction of soil erosion on several different landscapes on a single storm basis, namely rangelands, forests, and flatlands, was incorporated into the modified model, producing the Modified Universal Soil Loss Equation (MUSLE) (Lal, 2001). The USLE has seen another revised version, the Revised Universal Soil Loss Equation (RUSLE), which includes concepts from soil erosion models, which are process-based (Lal, 2001; Buttafuoco *et al.*, 2012). This enables the RUSLE to estimate certain input values of the various factors that it requires to run (Lal, 2001).

2.9 Synthesis

Soil erosion is a global occurrence, and has considerable impacts on catchments, operating with high spatial variability (Carpenter *et al*., 1998; Laker, 2004; Cantón *et al*., 2011). The degree to which soil erosion occurs is governed by several factors, such as land and soil management, which is controlled by anthropogenic actives and can have profound effects on soil erosion (Pimentel *et al*., 1995; Fernández *et al*., 2004; Podwojewski *et al.*, 2011). However, the use of soil conservation practices (such as mulching) on plantations, reduces soil erosion rates, protecting soil productivity, water quality, and environmental health (Blackburn *et al*., 1986; Chaplot *et al*., 2011; Prats *et al*.,

2012). The use of fire as a management practice may be necessary as a forestry site preparation method; however, burning forested landscapes leads to a reduction in vegetation cover and exposes soils to elevated levels of erosion (Blackburn *et al*., 1986; Lal, 2001; Mohammad and Adam, 2010). Furthermore, fire has been shown to have significant adverse impacts on soil infiltrability, enhancing runoff and erosion (DeBano, 1981; Fernández *et al*., 2004).

South Africa is reliant on commercial forestry, despite already suffering from severe and wide-spread soil erosion, and having cognisance of the vulnerability of *Eucalyptus* plantations to exacerbate soil erosion, and the resultant decline in soil productivity and downstream water quality (Blackburn *et al*., 1986; Chaplot *et al*., 2011; Oliveira *et al*., 2013). South Africa remains undeterred by the environmental, climatic, and economic repercussions, of soil erosion; thus, a sustainable and conservative method for employing forestry is critical; one which can help curb climate change and preserve soil and water resources, achieving the aforementioned Sustainable Development Goals (Zinn *et al*., 2002 Le Roux *et al*., 2008; Chaplot *et al*., 2011; United Nations, 2015).

The influence of burning and mulching treatments, or a combination of both, on the influence of soil erosion on *Eucalyptus* plantations with varying spatial scales in South Africa has not yet been established. The outcomes of which would aid in the sustainable management of commercial *Eucalyptus* plantations in South Africa. This is vital in the wake of climate change, and the potential feedback loop between increased extreme precipitation events, exacerbating soil erosion, leading to increased soil carbon loss, and greenhouse gas emissions (Le Bissonnais *et al.*, 1998; Mason *et al.*, 1999; Lal, 2001; Ziadat and Taimeh, 2013). Furthermore, the results of research in this field will provide soil erosion models with a basis for validating outputs of erosion on *Eucalyptus* plantations consisting of varying site preparation techniques in South Africa (Scott-Shaw *et al.*, 2020).

Chapter Three

Methods

3.1 Introduction

Soil erosion can be monitored *in situ* – on the site itself, using runoff plots of varying sizes to assess the different stages of soil erosion (Hartanto *et al*., 2003; Chaplot *et al*., 2011; Chaplot and Poesen, 2012). Micro-runoff plots (1 m^2) provide a measure of the contribution of splash erosion and raindrop impact, while runoff plots (several m^2) are used to assess erosion generated by overland flow (Hartanto *et al*., 2003; Rumpel *et al*., 2009; Chaplot and Poesen, 2012; Oliveira *et al*., 2013). In field experiments, inter-rill erosion has been measured on plots ranging from 2 m^2 – 2.5 m^2, while rill erosion has primarily been measured on plots greater than 5 m^2 (Smets *et al.*, 2008; Chaplot and Poesen, 2012). The use of runoff plots in the monitoring of soil erosion is a cost-effective approach, while still providing valuable data on the soil erosion at the plot locations (Hartanto *et al*., 2003). Installing several smaller and larger plots at differing hillslope positions will result in a study which is able to indicate the processes of soil erosion and the spatial scales at which they operate (Chaplot and Poesen, 2012). Continuous monitoring provides valuable information on the temporal scales at which soil erosion operates, such as the changes in soil erosion throughout a rainfall event (of a particular intensity), and the seasonal variations of soil erosion (Vandaele and Poesen, 1995; Chaplot *et al*., 2011). Although, there is a limitation associated with the use of runoff plots, as on shorter runoff plots, mulch is notably less effective at decreasing relative soil erosion in comparison to longer plots (Smets *et al.*, 2008).

Observing soil erosion by water is dependent on precipitation which occurs over the study area; therefore, the simulation of rainfall has been a viable method for observing soil erosion (Chaplot *et al*., 2011). The simulation of rainfall means that the rainfall intensity, duration, and raindrop kinetic energy can all be controlled (Chaplot *et al*., 2011).

3.2 Study Site

This study was conducted in the Two Streams catchment (29°12'13.1"S 30°39'14.6"E) located within the Mondi Mistley/Canema forestry estate (Clulow *et al*., 2011; Google Maps, 2018). The catchment is situated on the east coast of South Africa in the province of Kwa-Zulu Natal, approximately 20 km outside of Greytown (*Figure 3.1*). This study site allowed for frequent data collection as it is 70 km north-east of the University of Kwa-Zulu Natal (Pietermaritzburg campus), which allowed for quick response times to precipitation events.

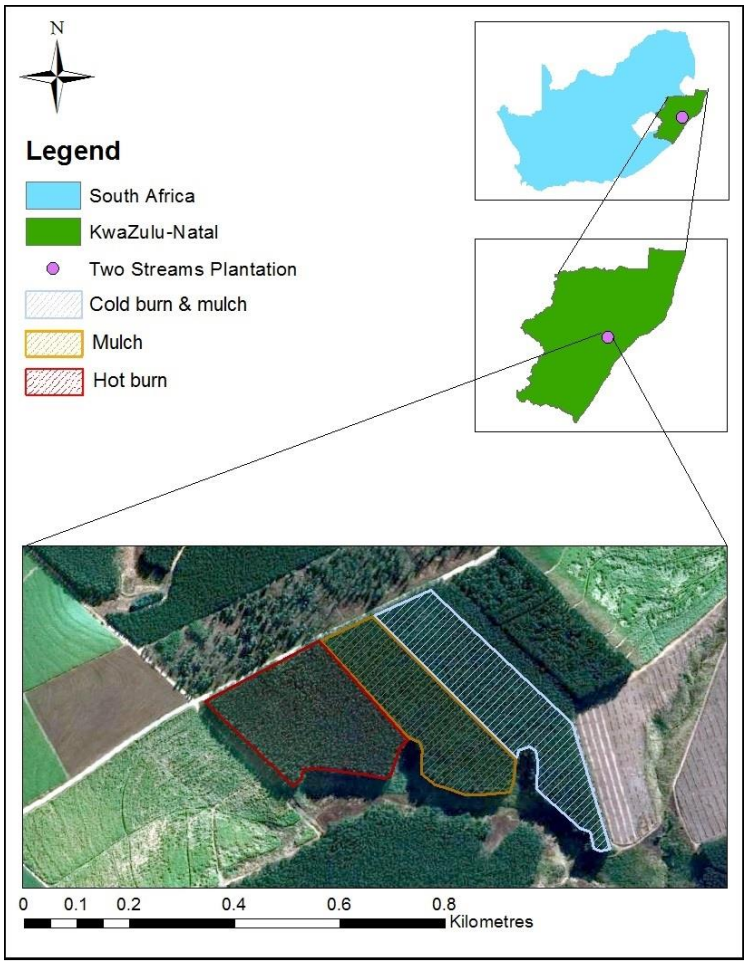

Figure 3.1: Location and site treatments of the Two Streams forestry plantation, Mistley Canema estate, South Africa (Google Earth Pro; Google Maps, 2018).

The Two Streams catchment (34 hectares) is situated in a summer rainfall region (receiving most of its rainfall between October and March), with a MAP (Mean Annual Precipitation) ranging from 659 to 1139 mm (Clulow *et al*., 2011). This location receives little precipitation from cold fronts and mist (Clulow *et al*., 2011). Extensive research output from the catchment has improved the overall monitoring of the catchment, such as a gauging weir being established in the catchment in 1999, and the installation of an Automatic Weather Station (AWS) in 2006.

The catchment has a mean slope of 16%, with soils that are generally 2 m deep, highly permeably, considerably weathered, reside under the Ecca group of dolerite dykes and sills, and is apedal and plinthic (Clulow *et al*., 2011; Le Roux *et al*., 2015). The strong weathering in the Inanda profile has led to significantly leached and highly acidic soils, while mottling in the subsoil of the Magwa indicates a decline in the permeability of the soil (Le Roux *et al*., 2015).

The area, which is now under commercial plantations was previously a natural grassland, consisting of *Themeda triandra*, of which only a small portion remains (Bulcock and Jewitt, 2012). The natural vegetation is seen to have little value from a commercial forestry viewpoint, due to many arable areas having a significant potential for cultivation of several species, namely pine (*Pinus*), wattle (*Acacia*), and gum (*Eucalyptus*) (Bulcock and Jewitt, 2012). The proposed study site was previously a black wattle (*Acacia mearnsii*) stand, which was felled at the beginning of 2018, and was reforested with a gum (*Eucalyptus dunnii*) stand, planted in April 2018, under which this study was conducted.

3.3 Experimental Design

Three site preparation treatments were investigated, namely a cold burn treatment (CBT) (*Plate 3.1 A*), a hot burn treatment (HBT) (*Plate 3.1 B*), and a mulch treatment at which no burning took place (*Plate 3.1 C*). Each of these treatments was monitored and sampled throughout the study. The treatments were established on the forestry site in the last week of February 2018. The cold burn took place under moderate soil moisture and air temperature conditions (*Plate 3.2 A*), while the hot burn took place on a day with low soil moisture and high air temperature (produced by several hot dry days preceding the day of the burn) (*Plate 3.2 B*). The fuel for both burns consisted of debris which remained after the felling of an *Acacia mearnsii* stand that preceded the new *Eucalyptus*

plantation. The mulch was comprised of hand-spread debris remaining from the felling of the *Acacia mearnsii* stand, and the mechanical chipping of remaining tree stumps. After the treatments were established, herbicides (Glyphosate) and pesticides (Alphathrin) were applied evenly to each treatment to control competing weeds, grasses and insect pests.

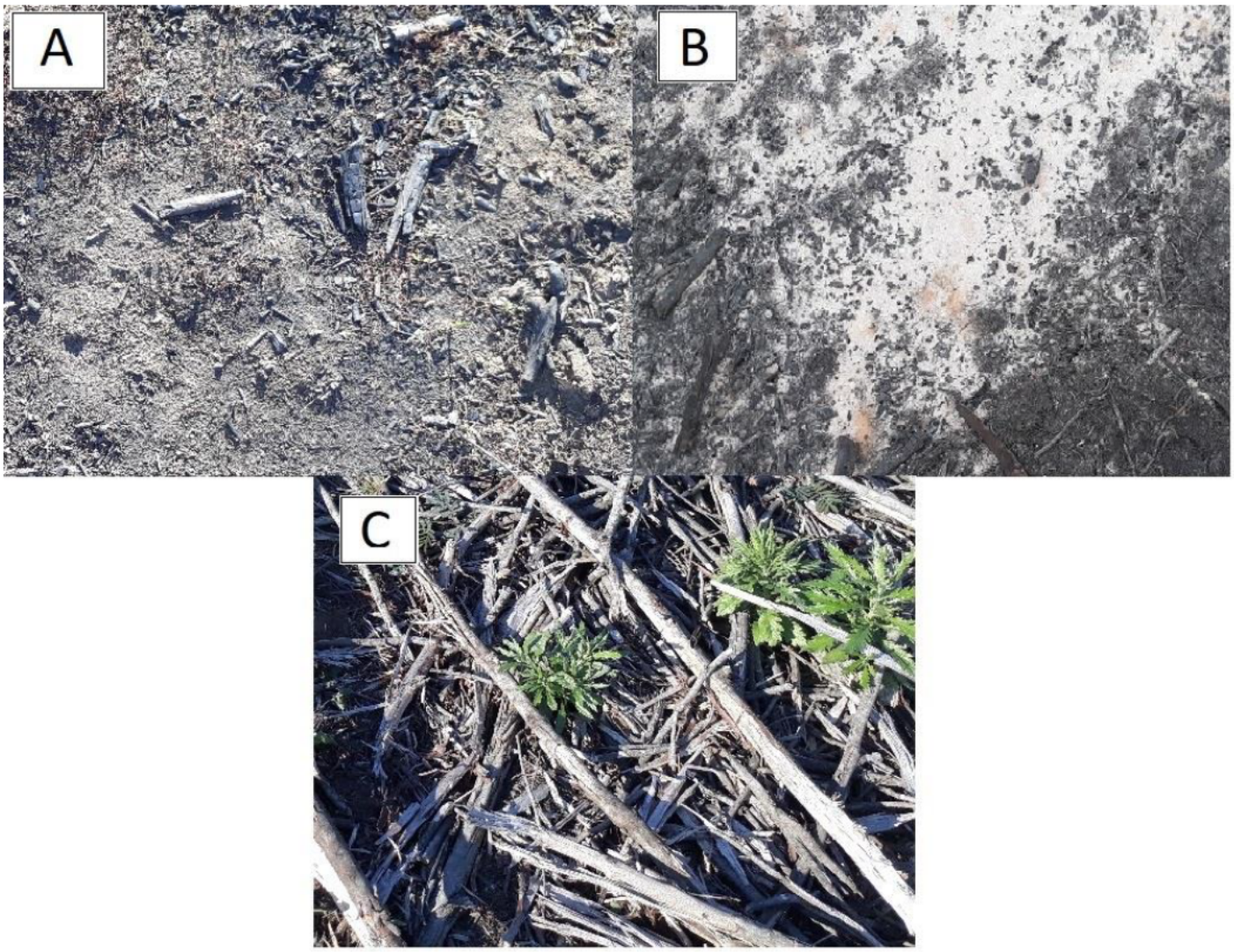

Plate 3.1: Prescribed site preparation treatments, cold burn (A), hot burn (B), mulch (C).

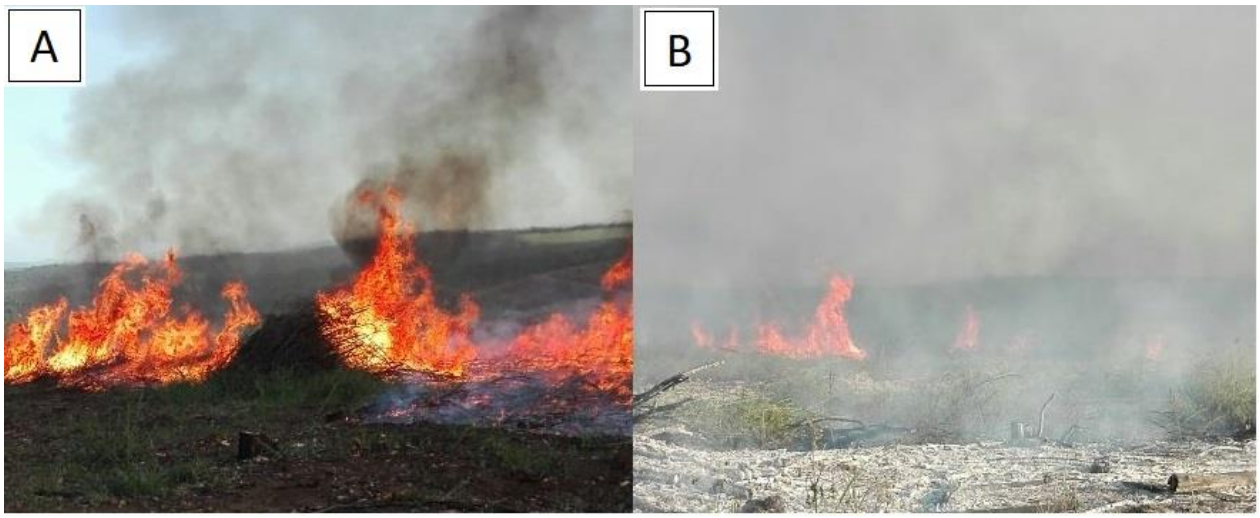

Plate 3.2: Burning of the cold burn treatment (A), and the hot burn treatment (B).

Runoff plots, and micro-plots were installed at various locations on the slope (upper and lower) of
80 the catchment within each treatment. Six of each runoff plot types were placed within each treatment; three at the top of the slope, regarded as the gentle slope, and three at the bottom of the slope, regarded as the steep slope (*Figure 3.2*).

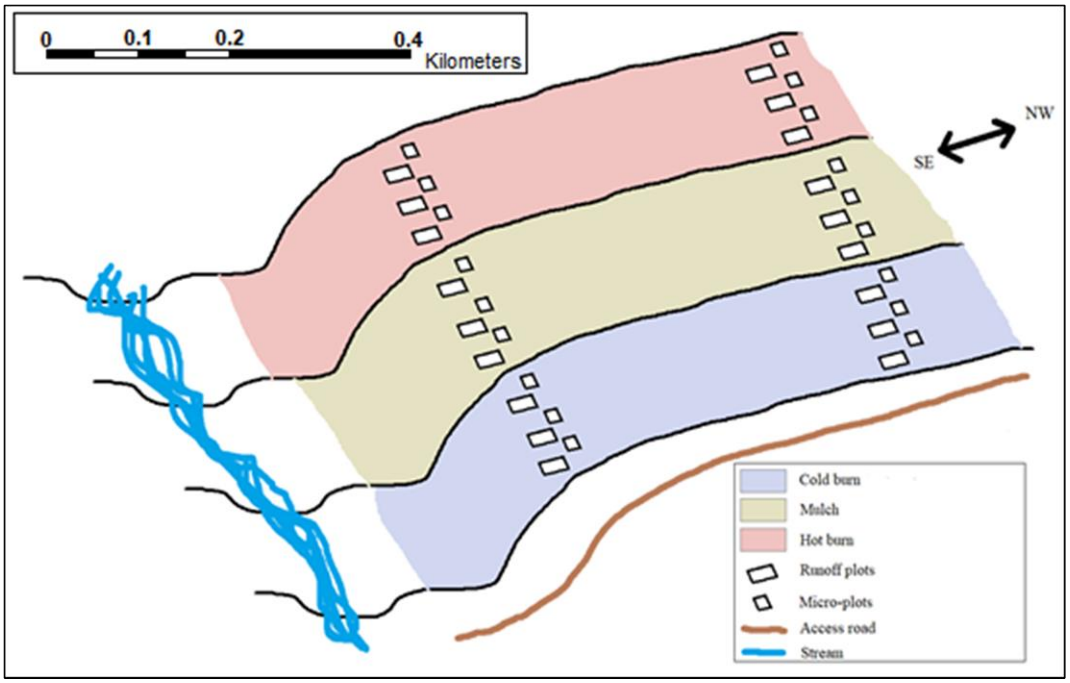

Figure 3.2: Layout and orientation of micro-runoff and runoff plots.

3.4 Rainfall data

Manual rain gauges were installed at each plot location (*Plate 3.3*), to measure rainfall depth (a point measurement of the total depth of accumulated rainfall that would otherwise hit the ground and runoff or infiltrate into the soil). In addition, these gauges measured the spatial variability of rainfall between the different plot locations (gentle slope vs. steep slope), and between the different treatments. The rain gauges were installed 1.5 m above the soil surface, as per Gillham (2016). Water samples from rain gauges at this research site in a prior study concluded that the rainfall in this area produced concentrations of phosphorus, nitrogen, DOC and POC that were too low to impact the levels measured in the runoff from each plot (Gillham, 2016). Therefore, the rain gauges were only used for measuring the precipitation depth at each treatment site. Precipitation data were acquired from an AWS located approximately 500 m from the site.

Plate 3.3: Manual rain gauge installed at the research location.

3.5 Water and Nutrient Flux Assessments

Water and nutrient fluxes were measured on each treatment type from October 2018 – March 2019 and were subjected to multiple scales of spatial assessment. A total of 18 micro-runoff plots (1 m^2) and 18 runoff plots (10 m^2) were set up in replicates of three at two different hillslope classes (gentle and steep) across three different site preparation treatments (CBT, HBT, mulch) (Chaplot and Poesen, 2012). Both plot types were assumed to be closed systems, whereby there were no conveyance losses or external runoff enter the measuring system which had not originated on the designated plot areas.

3.5.1 Micro-runoff plots

The micro-runoff plots provided measurements of splash erosion and runoff generated by rain splash (Chaplot and Poesen, 2012). Plots (1 m x 1 m) were constructed and manufactured from galvanised steel sheets. The 1 m^2 plots were inserted vertically into the ground to an approximate depth of 0.1 m, so that the upper edge was parallel to the surrounding slope (*Plate 3.4*) (Chaplot and Poesen, 2012). This ensured that rainfall which occurred on the plot was entrapped, and directed downslope (within the plot), into the plot gutter. The gutter connected to the plot, channelled water into a storage bucket (20 L). The total volume captured by each of the micro-runoff plots was measured at each site visit. Site visits after each recorded rainfall event >10 mm were initiated by a telemetry alert from the AMS (Chaplot and Poesen, 2012). A measuring cylinder was used to measure the total volume. The same water was used to flush the trapped sediment out of the gutters and into the storage bucket. Following flushing, the storage bucket was stirred to produce an even distribution of sediments, and a representative 500 ml grab sample was taken. Samples were returned to the laboratory and analysed for sediment load and chemical concentrations (see Chapter 3.7 Water Quality Assessment for details) (Chaplot and Poesen, 2012).

Plate 3.4: Micro-runoff plot (1 m^2).

3.5.2 Runoff Plots

The runoff plots provided measurements of rill erosion and the runoff generated by overland flow (Smets *et al.,* 2008). Rill erosion is assumed to be the primary form of erosion being measured at the runoff plot scale, although it is possible that the process of inter-rill erosion will be operating within this scale (Smets *et al.,* 2008; Chaplot and Poesen, 2012). The 10 m^2 plots were constructed as a 5 m x 2 m rectangle, made from galvanised steel sheets and were inserted vertically into the ground to an approximate depth of 0.1 m, with the long side positioned parallel to the direction of slope (*Plate 3.5*) (Chaplot and Poesen, 2012). This ensured that rainfall which occurred on the plot was entrapped, and directed downslope (within the plot), into the plot gutter.

Plate 3.5: Runoff plot (10 m^2).

Holes were manually dug (*Plate 3.6*) to sink storage tanks to capture the total volume of runoff and erosion. The plot gutter, channelled water through piping into a storage "Jojo" tank (300 litre volume) (*Plate 3.7 A*). Smaller (20 litre) buckets were placed within these tanks making it easier to measure and sample smaller precipitation events (*Plate 3.7 B*). The total volume captured by each of the runoff plots was measured at each site visit (outlined in Chapter 3.5.1 Micro-runoff plots) (Chaplot and Poesen, 2012). A measuring cylinder was used to measure the total volume if only the smaller bucket contained water; however, if the smaller bucket had overflowed and the large tank was full, the total water volume was calculated using the depth of the water within the tank, after the smaller bucket was emptied into the tank. Once measured the same water was used to flush the trapped sediment out of the gutters and into the storage bucket. Following flushing, the storage bucket was stirred to produce an even distribution of sediments, and a 500 ml grab sample was taken. This sample represented the total water and sediment collected in the storage tank, which was then analysed for sediment load and chemical concentrations (Chaplot and Poesen, 2012).

Plate 3.6: Storage tank hole being dug by Jordan Bull.

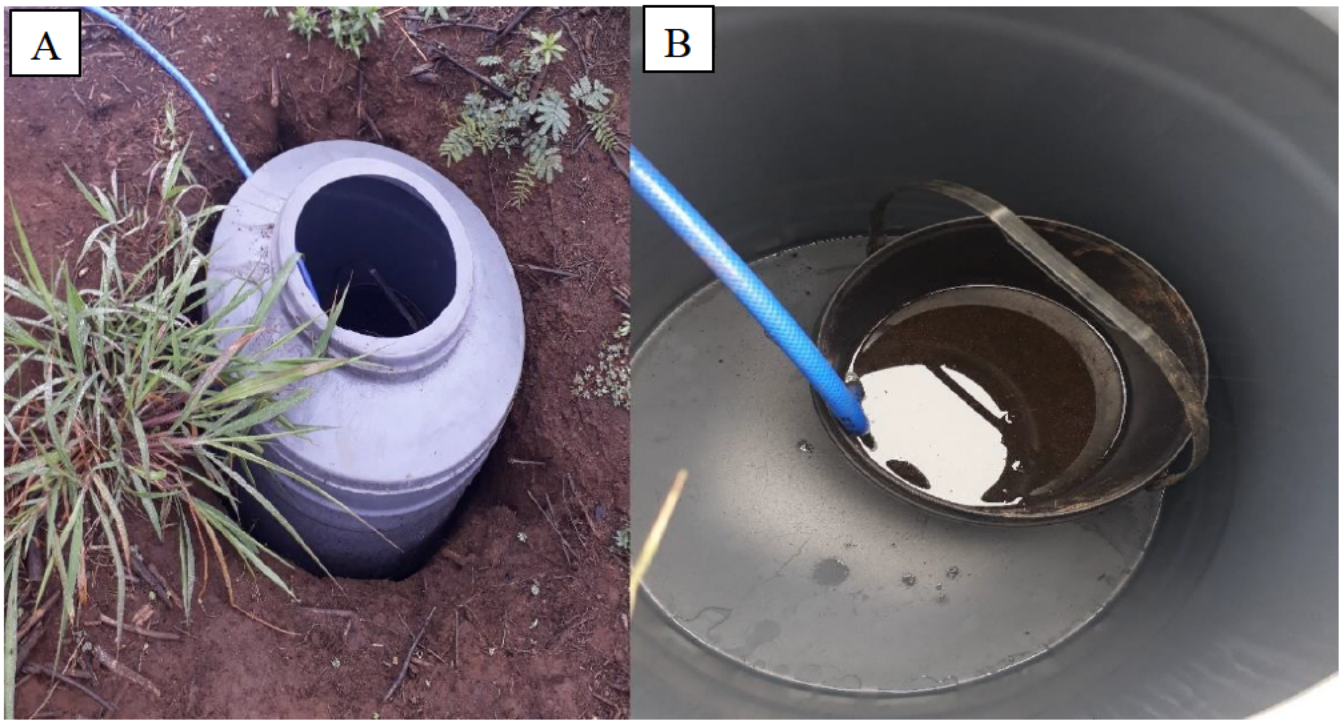

160

Plate 3.7: Jojo tank sunk to ground level (A) and a collecting bucket within Jojo tank (B).

At each slope class (gentle and steep) on each treatment type, a single runoff plot had its gutter fed into a tipping bucket gauge system (*Plate 3.8*), which recorded the total water volume which ran off the plot, before being routed into a storage Jojo tank for sampling. Each tipping bucket system was calibrated to tip every two litres. In addition to indicating a total volume, the tipping buckets provided an indication of the temporal overland flow response of each plot to the commencement of a rainfall event. Each tipping bucket was coupled with a HOBO event-logger which recorded and stored the measured data.

Plate 3.8: Tipping bucket gauging system for measuring surface runoff.

3.6 Site Visits and Sampling Procedure

It was necessary to visit the Two Streams catchment site after rainfall events to collect samples (Chaplot and Poesen, 2012). The regularity of site visits was determined by precipitation frequency and depth, as laid out in Chapter 3.5.1. All water samples which were taken from the field were stored in a cooler box, transported to the laboratory, placed in a refrigerator and kept at 4 ^{o}C until they were analysed (Plumb, 1981; Müller-Nedebock *et al*., 2016).

3.7 Water Quality Assessment

Water quality of the runoff was assessed through sampling at various spatial scales (micro-plots, runoff plots, upper and lower hillslopes). The water quality was assessed in terms of soil particles, nitrogen, phosphorus, Dissolved Organic Carbon (DOC) and Particulate Organic Carbon (POC).

3.7.1 Sediment load measurement

A Ø47 filter paper was used to filter water samples. Once filtered, the remaining sediment samples were dried for 24 hours at 110 ^{o}C, after which it was placed in a furnace which heated the samples to 550 ^{o}C for two hours, ensuring combustion of all OM (Plumb, 1981). The dried sediment load was then weighted, and the concentration (g L^{-1}) was determined for the sample (sediment weight x 2, as the sample volume was 500 mL). Sediment yield (g m^{-2}) was determined for each monitoring scale, by multiplying the sediment concentration by the runoff flux per unit area (L m^{-2}).

3.7.2 Particulate organic carbon (POC)

POC was determined by drying sediment remaining from filtered water samples at 110 ^{o}C for 24 hours, leaving behind only sediments. This was then weighted (g), before placing it in a furnace for two hours at 550 ^{o}C to ensure combustion of all POC (Plumb, 1981). The sample was then weighted after combustion of the particulate OM. The POC was the difference in weight of the sample, which was converted from grams to grams per litre (g L^{-1}), and converted to the POC content per unit area (g m^{-2}), by multiplying the POC concentration by the runoff flux per unit area (L m^{-2}) for each monitoring scale.

3.7.3 Dissolved organic carbon (DOC)

DOC assessments were conducted by Umgeni water, using a Shimadzu TOC-5000 analyser in conjunction with an ASI-5000 autosampler and Balston 78-30 high purity total organic carbon (TOC) gas generator (Müller-Nedebock *et al*., 2016). The method employed converted organic solutes in the water samples to CO_2, which was then measured (mg L^{-1}), and subsequently converted to a DOC content per unit area (mg m^{-2}), by multiplying the DOC concentration by the runoff flux per unit area (L m^{-2}) for each monitoring scale.

3.7.4 Nitrogen and phosphorous measurements

An AQUALYTIC spectrophotometer AL800 was used to determine nitrogen (N) and phosphorus (P) concentrations in water samples (mg L^{-1}), which was converted to nutrient content per unit area (mg m^{-2}), by multiplying the nutrient concentration by the runoff flux per unit area (L m^{-2}) for each monitoring scale. The nutrient concentrations were determined using a less than 10% error. A prior study in the area found that nitrite concentrations were too small to detect, therefore nitrites were not sampled (Gillham, 2016).

3.8 Environmental Assessment

3.8.1 Measurement of slope, soil and vegetation

Slope angle (in degrees) of each plot was measured using an inclinometer at the bottom of each plot in conjunction with a ranging rod at the top of each plot. The change in slope was read off the inclinometer.

Soil properties were measured by taking soil core samples of the first 10 cm of soil using a cylinder with a height of 10 cm and a diameter of 7 cm. These samples were taken after all three treatments had been established, but prior to the commencement of erosion monitoring. The samples were taken to the Department of Agriculture and Rural Development, Soil Science Analytical Services laboratory, Cedara, where they were chemically analysed. This test provided information on several

elements and properties which were found in the soil, namely: soil density, phosphorus (P), potassium (K), calcium (Ca), magnesium (Mg), acidity exchange, total cations, acid saturation, pH, zinc (Zn), manganese (Mn), and copper (Cu).

Leaf area index (LAI) was measured using a LI-COR 2200 plant canopy analyser at all of the plot locations throughout the growth of the stand. At each plot (both micro-runoff and runoff) the vegetation cover and abundance was measured using the Braun Blanquet classification method. This method employs measurements of the tree number, mean diameter and breast height of trees, the aerial cover, and the litter and grass cover (Gillham, 2016).

3.8.2 Soil water repellency

The procedure outlined by Scott (2000) for testing water repellency of soils was employed in this study. Where water drop penetration time (WDPT) was measured as the time required for a drop of water to infiltrate the soil (Scott, 2000). Soil water repellency tests were conducted on each treatment type. A total of six locations were tested per treatment (three at each hillslope position).

The soil was prepared by smoothing the surface at each sample location (Scott, 2000). The average recorded time of six drops at each sampling point was used to represent that sample point (maximum allowed time of 300 seconds) (Scott, 2000). At each sample location, repellency tests were conducted on the soil surface. Soils at sample locations were each cut as flat as possible ensure consistent testing conditions at each location that tests were conducted (Scott, 1994). Soil repellency tests were carried out at each location when a site visit to sample a rainfall event took place.

3.9 Arc-SWAT Setup and Modelling

The Soil and Water Assessment Tool (SWAT) was used to model sediment transport of the catchment which was studied. This model was chosen for its ability to model sediment yield in relation to land-use management, and its success in modelling soil erosion on an *Acacia mearnsii* plantation in the Two Streams catchment, South Africa (Le Roux *et al*., 2007; Scott-Shaw *et al.*,

2020). The results from this study were compared with the output of the model, to determine how the model performs with regards to soil erosion processes on differing site treatments of a commercial *Eucalyptus* plantation.

Arc-SWAT was setup by first importing a Digital Elevation model (30 m resolution), land-use data, and soil data for the study site into a new SWAT project within the ArcGIS program (*Figure 3.3*). All data was projected to the WGS 1984 UTM coordinate reference system. The DEM used was from the 30 m Shuttle Radar Topography Mission (SRTM) 1 Arc-Second Global radar. The land-use data was adapted from the land-use shapefile used by Scott-Shaw et al. (2020). The soils data consisted of an amalgamation of data from NRCS (1996), Soil Classification Working Group (1991), Everson et al. (2014), and Le Roux et al. (2015). The long-term weather data were acquired from two AWS stations situated within the Two Stream catchment. The research site treatments were delineated in the land-use layer by importing a google earth image of the research site and georeferencing it to the chosen Geographic Coordinate System and clipping the treatments to the current land-uses and defining each treatment.

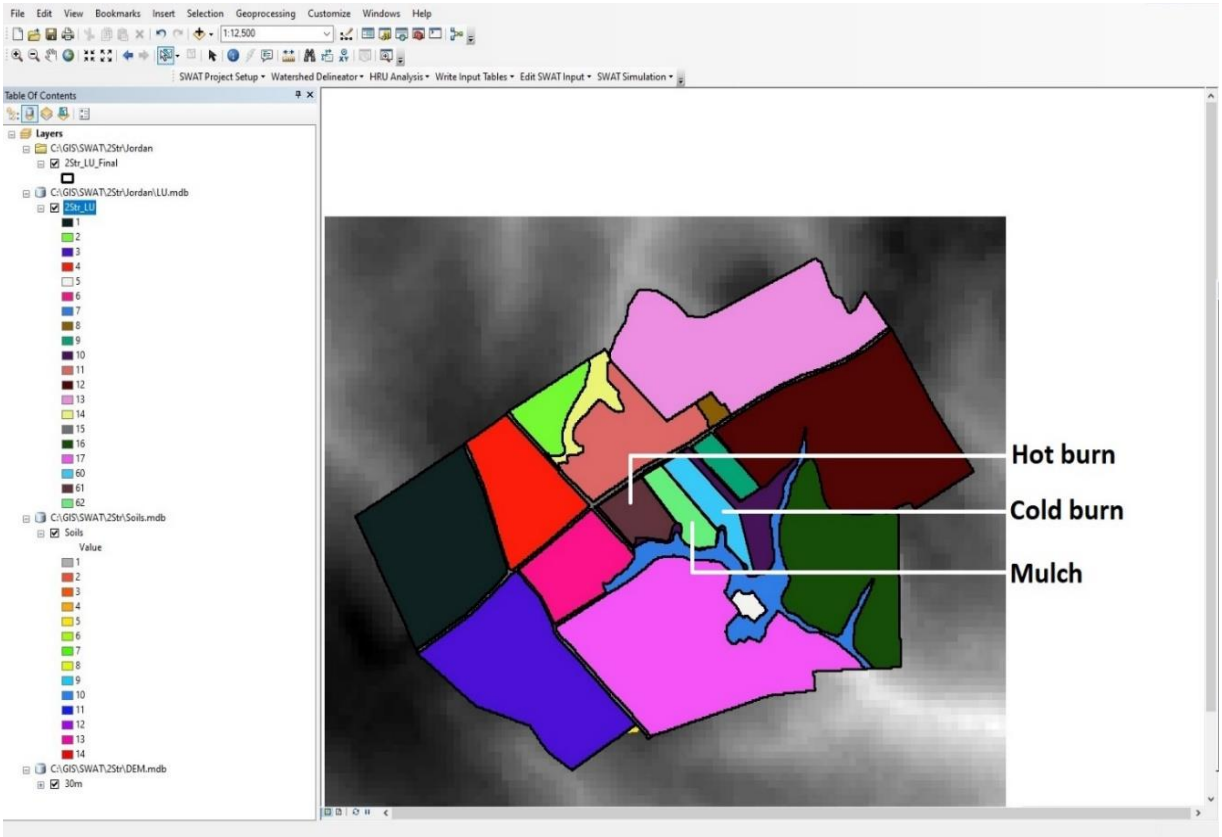

Figure 3.3: Arc-SWAT project containing land-uses, soil data, and a DEM for the study site.

The watershed delineation procedure for the research location can be found below (*Figure 3.4* & *Figure 3.5*). Under the 'Watershed Delineator' tab, 'Automatic Watershed Delineation' was selected, and the DEM was opened in raster format from the map itself, and the current 30 m resolution DEM was selected. In the DEM projection setup (1), the 'Z Unit' was set to 'meters'. Following this the 'Stream definition' was set to 'DEM-based' (2), the 'Flow direction and accumulation' was then selected (3), and calculated, and then the 'Create streams and outlets' was selected (4), under the 'Stream network' field. The catchment outlet was then added manually by selecting 'ADD' (5) in the 'outlet and Inlet Definition' tab. The outlet was then added to the stream network at the catchment outlet (*Figure 3.5*). Under the 'Watershed Outlet(s) Selection and Definition' tab, 'Whole watershed outlets' (6) was selected, the previously defined outlet was then selected, and 'Delineate watershed' was selected (7). Lastly, the subbasin parameters were calculated by selecting 'Calculate subbasin parameters' (8), in the 'Calculation of Subbasin Parameters' tab.

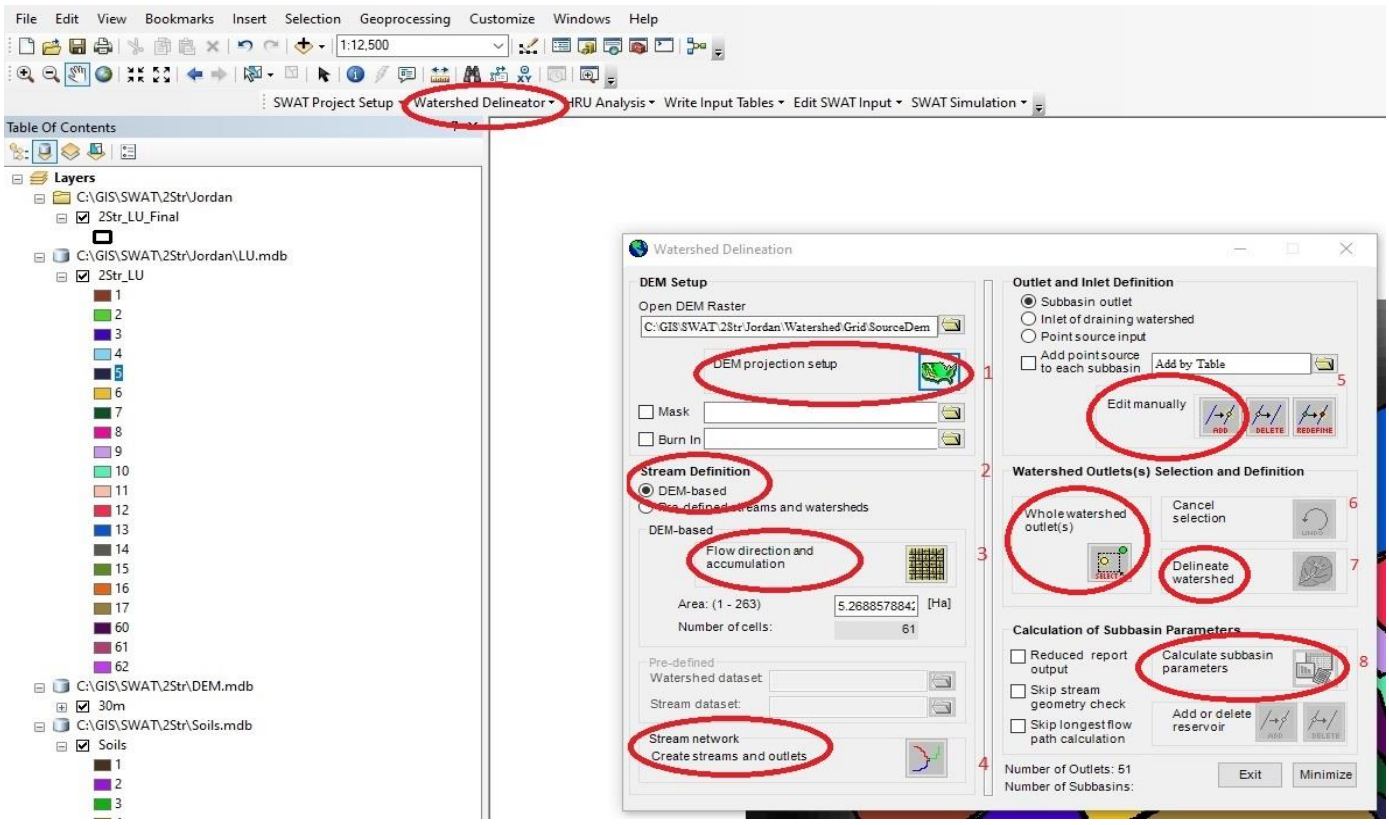

Figure 3.4: Watershed delineation procedure for the study site.

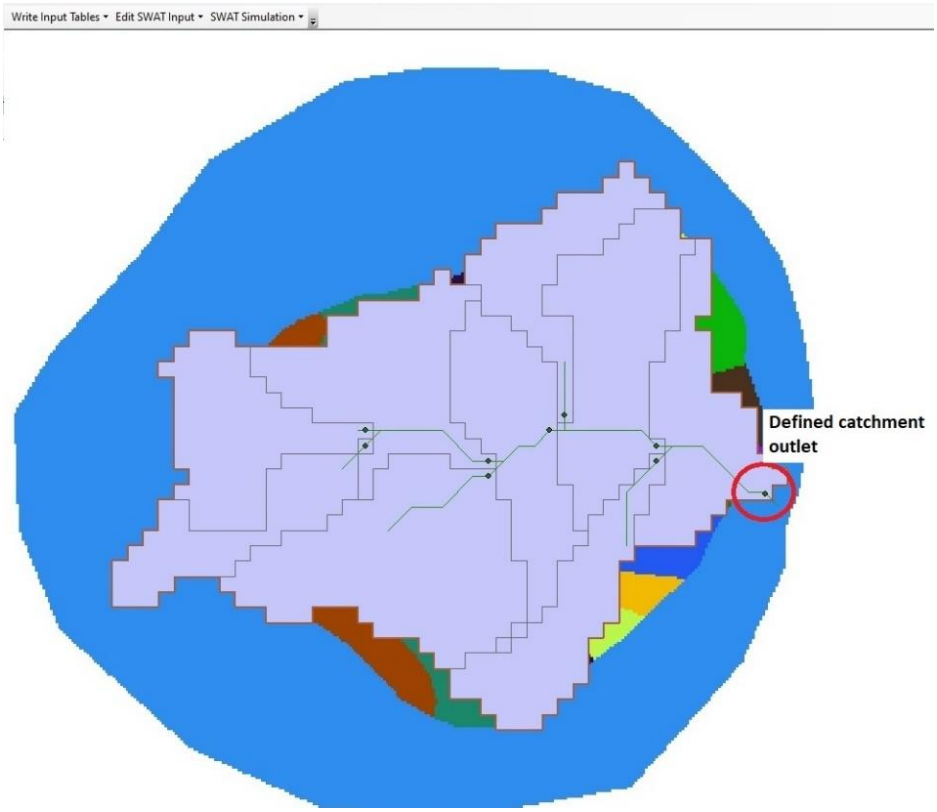

Figure 3.5: Defining the catchment outlet location.

In the 'HRU Analysis' tab, 'Land Use/Soils/Slope Definition' was selected, and the 'Land Use Grid' layer (1) was loaded from the map (2), where the land-use shape file was selected (3), and the grid code values were set to 'SID' (4) (*Figure 3.6*). The 'Choose Grid Value' field was set to 'VALUE' (5), and 'LookUp Table' (6) was selected, 'User Table' was then toggled, and a text file which identifies each Hydrological Research Unit and its specific land-use was chosen. Lastly, 'Reclassify' (7) was selected (*Figure 3.6*).

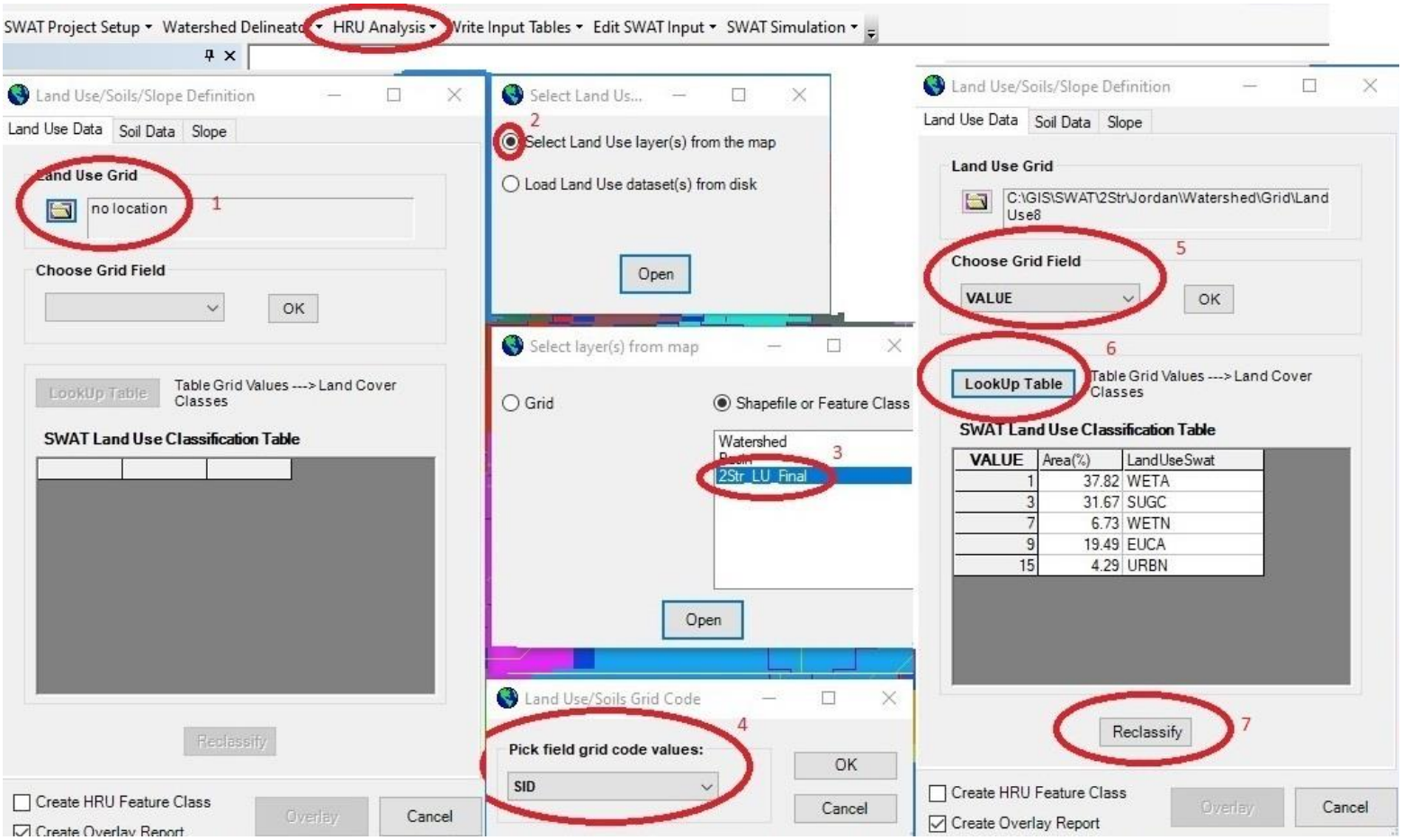

Figure 3.6: Land-use data setup procedure.

Under the 'Soil Data' tab within the 'Land Use/Soils/Slope Definition' window, 'Soils Grid' (1) was selected, and Soil layers from the map was then toggled (2), and lastly 'Soils' was selected (3) and opened (*Figure 3.7*). The 'Choose Grid Value' field was set to 'VALUE' (4), and 'UserSoil' (5) was selected, followed by 'LookUp Table' being selected (6), and a text file which identifies each Hydrological Research Unit and its specific soil type was selected. Lastly, 'Reclassify' (7) was selected (*Figure 3.7*).

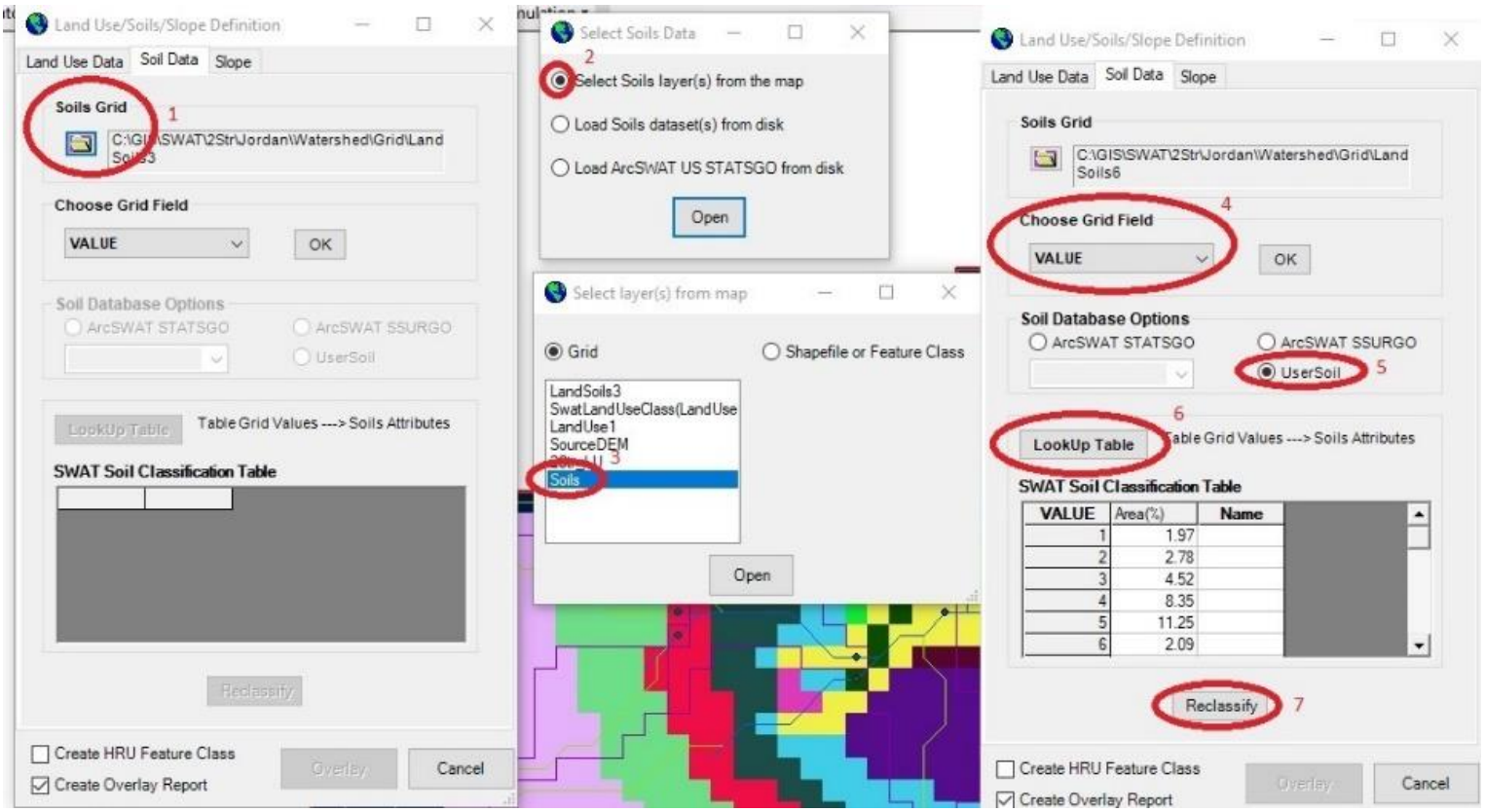

Figure 3.7: Soil data setup procedure.

310

Under the 'Slope' tab within the 'Land Use/Soils/Slope Definition' window, 'Multiple Slope' (1) was selected (*Figure 3.8*). The 'Number of Slope Classes' was set to 5 (2), and each slope class was prescribed an upper and lower limit (3). 'Reclassify' (4) was selected, and then 'Create HRU Feature Class' was toggled (5), and 'Overlay' was selected (6).

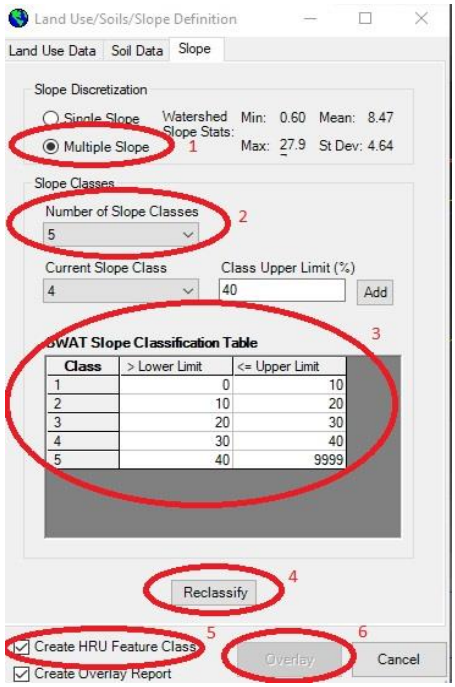

Figure 3.8: Slope data setup procedure.

315

Within the 'HRU Analysis' tab 'HRU Definition' was selected, and 'Create HRUs' was selected in the 'HRU Thresholds' tab – the predetermined SWAT HRU thresholds properties were used (*Figure 3.9*).

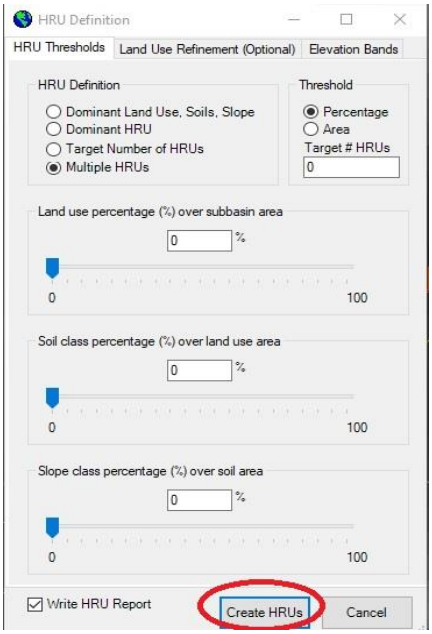

Figure 3.9: HRU thresholds creation.

Within the ‘Write Input Tables’ tab, ‘Weather Stations’ was selected, bringing up the ‘Weather Data Definition’ selection field (*Figure 3.10*). In the ‘Weather Generator Data’ tab (1), the ‘Locations Table’ was set to ‘WGEN_user’ (2) and ‘OK’ was selected (3) (*Figure 3.10*).

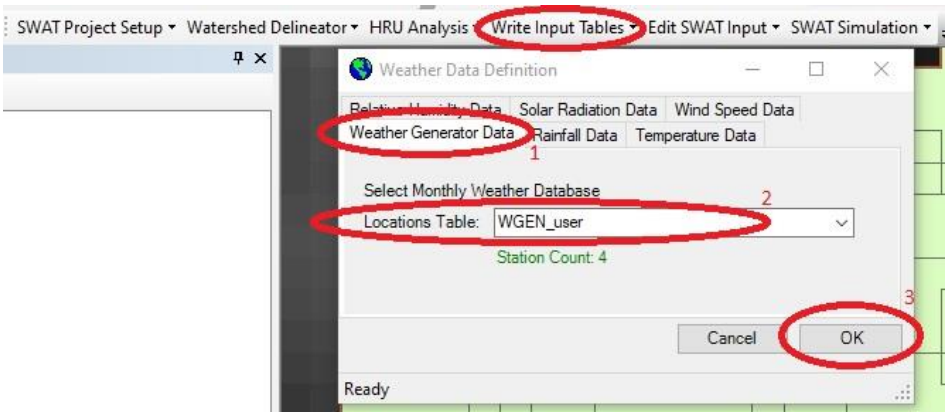

Figure 3.10: Weather data definition procedure.

Within the ‘Weather Data Definition’ selection field, the data parameters: ‘Rainfall Data’ (A), and ‘Temperature Data’ (B), were set to use *in situ* measurements (Raingauges and Climate Stations) (*Figure 3.11* A, B). The ‘Location Tables’ were set to the location table of the dataset which corresponds to that weather data parameter. Due to limited observed data beyond 2017 for ‘Wind Speed Data’ (C), ‘Solar Radiation Data’ (D), and ‘Relative Humidity Data’ (E), these parameters were set to use simulation data (*Figure 3.11* C, D, E).

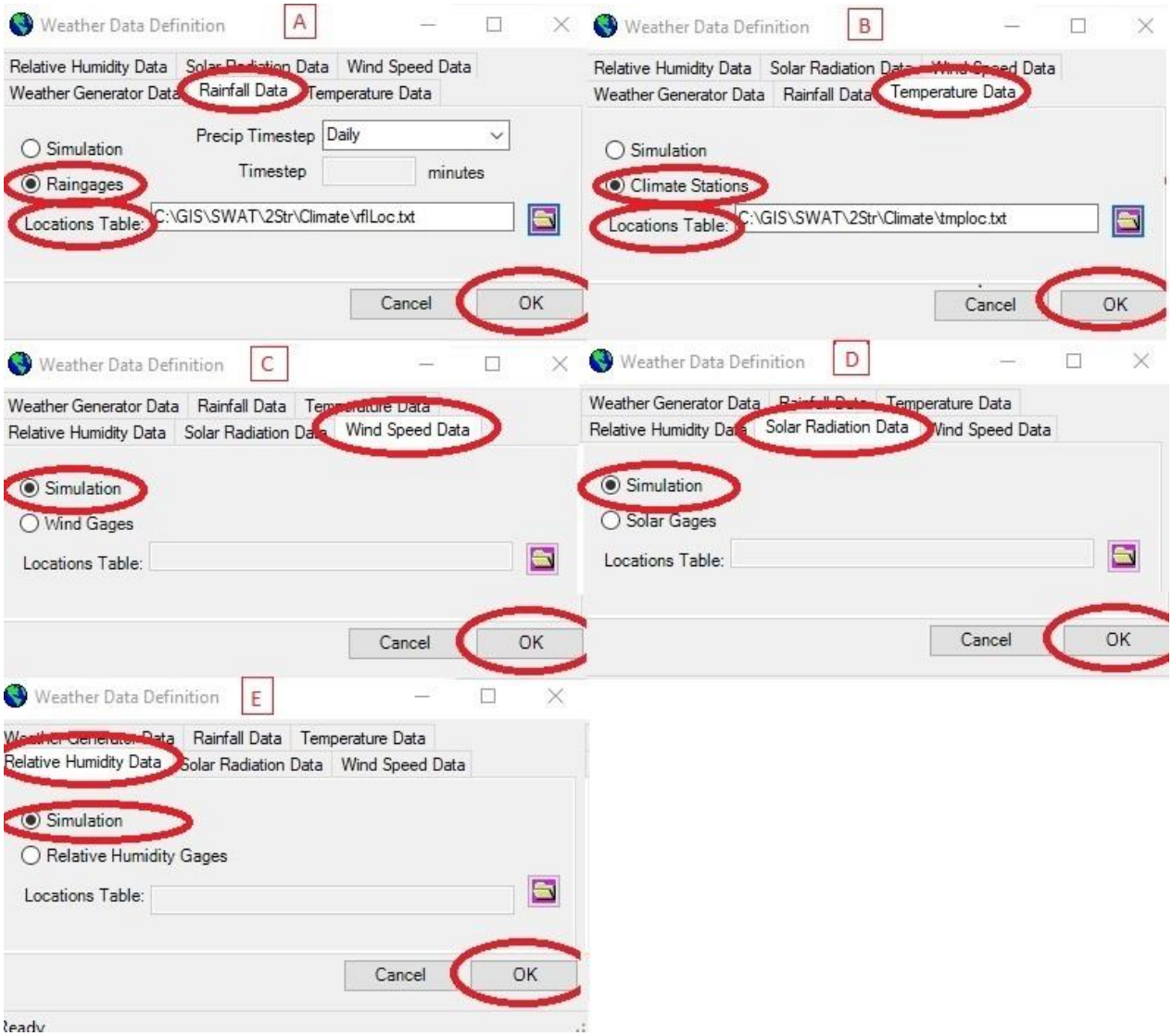

Figure 3.11: Weather data setup of each of the required weather parameters: rainfall (A), temperature (B), wind speed (C), solar radiation (D), relative humidity (E).

335 within the 'Write Input Tables' tab, 'Write SWAT Input Tables' was selected, bringing up the 'Write SWAT Database Tables' selection field (*Figure 3.12*). All of the tables were selected to write (1), 'Create Tables' was then selected (2), and the model was set to not calculate heat units to maturity (3) (*Figure 3.12*).

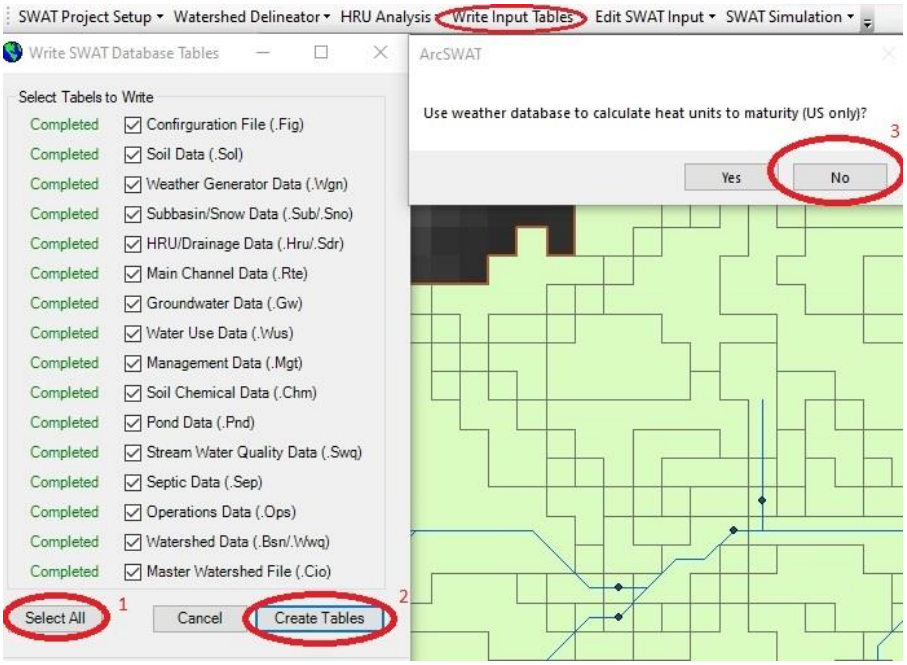

Figure 3.12: Writing SWAT database tables setup procedure.

Management operations were defined for the cold burn management regime by selecting 'Edit SWAT Input' and from the list provided, selecting 'Subbasins Data', which opened the 'Edit Subbasins Inputs' window (*Figure 3.13*). The 'Management' input table (1) was chosen to edit, subbasin '3' was chosen to work on (2), the land use which was edited was the cold burn regime 'COLD' (3), the selected soil type was GLEN (4), and the chosen slope was 0 – 10% (5), and 'ok' was selected (6) (*Figure 3.13*). The operations tab of the second window was opened, and a 7-year Eucalyptus rotation was set up with a burn taking place on the 28th of February of the 1st year, and planting taking place on the 1st of April (7). The burn was set to have consumed 70 % of the biomass on the ground. Management operations were set to be extended (8), and edits were set to be extended to specific HRUs (9). Edits were extended to 'All' subbasins (10), and to the 'COLD' burn land uses (11), on 'All' soils (12) and slopes (13), and lastly the edits were saved (14) (*Figure 3.13).*

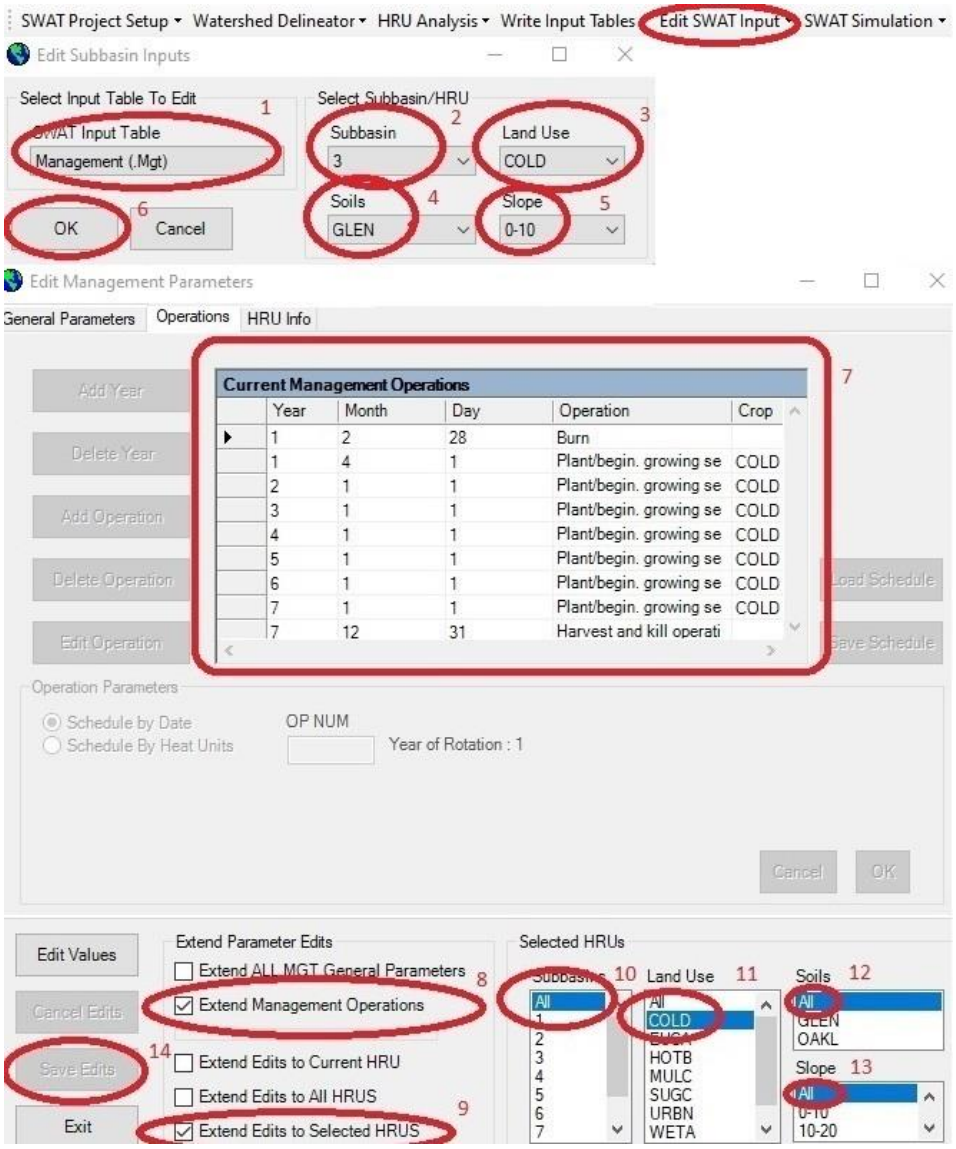

Figure 3.13: Cold burn management operations setup procedure.

Management operations were defined for the hot burn management regime following the same routine, rotation and dates as the cold burn management routine. However, the hot burn was set to have consumed 90 % of the biomass on the ground. Similarly, the mulch management operations were defined using the same dates, and rotation as the hot and cold burn; however, the operations within the mulch treatment were defined to a mulch tillage occurring prior to planting, using a power mulcher.

The setup of the SWAT model was complete at this point, and the model was run. This was done by accessing the 'SWAT Simulation' tab, and selecting 'Run SWAT' option, opening the 'Setup and Run SWAT' window (*Figure 3.14*). The 'Period of Simulation' (1) was set to begin at 1/1/1998 and end at 1/1/2020, 'Setup SWAT Run' (2) was selected, and lastly 'Run SWAT' (3) was selected (*Figure 3.14*).

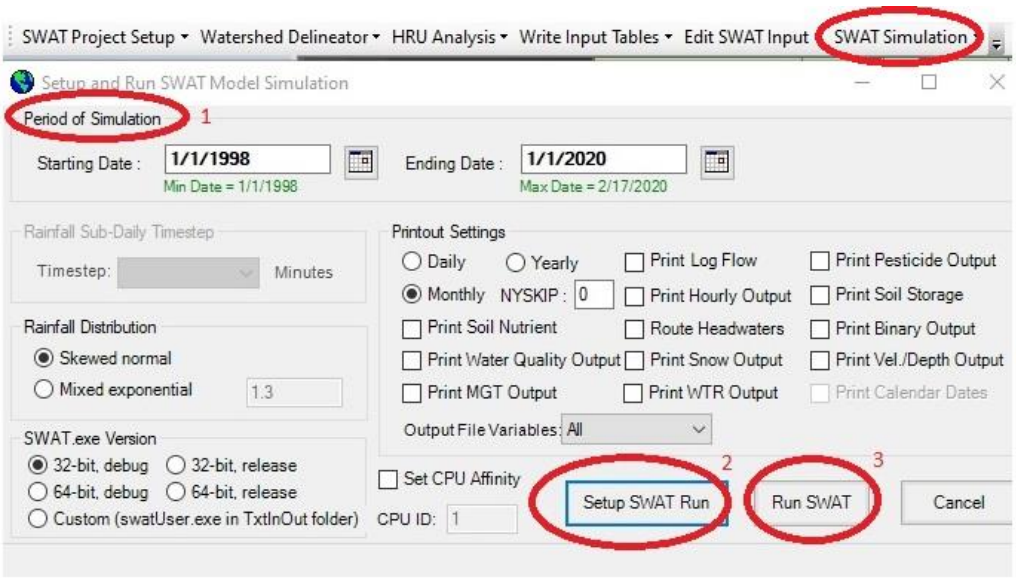

Figure 3.14: SWAT model simulation period setup and model run.

The initial outputs were manually calibrated to best replicate the observed data while remaining within realistic values for the calibrated parameters. The iterative calibration process found the adjustments of the USLE_C (land cover factor), USLE_P (support practice factor) and SUR_LAG (surface runoff lag time) inputs had little effect on consolidating the simulated data with the observed data, and were thus left as their default values. The USLE_K (soil erodibility factor) was adjusted to a value of 0.08 for all treatments, which had a moderate effect on consolidating the simulated with the observed data, and these output values were the values used in this study.

3.10 Statistical Procedures

Several statistical methods were employed in the analysis of the data. To provide a comparison of the different plot sizes and different spatial scales between each treatment, comparative tables, means, and standard deviation were used. Visual comparisons were made through the construction of scatter graphs and bar charts using Excel, and correlation heat maps, notched box and whisker plots, and Principal Component Analysis' using MATLAB version 9.2. The overlap of notches on the notched box and whisker plots indicated that the median of a data set was statistically similar to another, at a 95% confidence interval. The use of the notched box and whisker plot about the median was employed over the use of the mean as the data did not have a normal distribution, which was tested for using the Shapiro-Wilk test. The Principal Component Analysis (PCA) was used to identify the relative impacts the treatments, hillslope positions and erosion types had on the measured variables. All data were normalized before producing the PCAs to account for the large variabilities between events.

A parametric one-way ANOVA was used to indicate whether there were any significant differences in data observed between the different treatment types and at differing hillslopes. For this test, a confidence level of 95% ($P < 0.05$) was used. Several assumptions were made for this test, namely the errors in the data were independent, residuals had a normal distribution, variances in the data were homogenous, and model effects were additive (University of New Hampshire, 2015). Upon finding a significant difference, the data was further analysed using a post-hoc Tukey HSD (Honest Significant Difference) to identify which datasets were statistically significantly different.

3.11 Data Analysis

The recorded data were analysed using the previously mentioned statistical procedures. The water quality of the micro-runoff plots and runoff plots was analysed using a PCA to understand how sediment load, nitrogen, phosphorus, DOC, and POC were affected by differing scales (micro-runoff plot and runoff plot), hill slope positions (steep and gentle), and treatments (CBT, HBT, mulch).

The environmental data were analysed using a parametric one-way ANOVA, which indicated whether there was a significant difference in the slope, rainfall, soil chemical properties, soil infiltrability, and LAI data observed at different hillslope positions of each treatment. If a statistical difference was shown by the ANOVA test, a post-hoc Tukey HSD (Honest Significant Difference), was used to identify where those differences lay.

3.12 Conclusions

The research site is the Two Streams catchment, situated within the Mondi Mistley/Canema estate, in the KwaZulu-Natal Province, South Africa, approximately 70 km north east of the University of KwaZulu-Natal (Pietermaritzburg campus). The catchment area has a MAP which ranges from 659 to 1139 mm, and a mean slope of 16%, with the soils being predominantly comprised of the apedal and plinthic soil forms (Clulow *et al*., 2011; Le Roux *et al*., 2015).

Three site preparation treatments were employed on the new *Eucalyptus dunnii* stand, namely a hot burn treatment, cold burn treatment, and a mulch treatment. Prior to the commencement of the study, several environmental attributes were measured on each treatment, namely LAI, sail water repellency, slope angle, and vegetation abundance (Braun Blanquet classification method). On each treatment six runoff (10 m^2) and micro-runoff (1 m^2) plots were installed, covering two different slopes. Runoff and micro-runoff plots were employed as they are a cost-effective method for measuring soil erosion, while being able to provide valuable data on the spatially explicit scales that different soil erosion processes operate (Hartanto *et al*., 2003; Chaplot and Poesen, 2012). A tipping bucket runoff gauge was installed at each slope of each treatment to provide a time series of the runoff which is produced by each treatment. A manual rain gauge was installed at each slope of each treatment to measure the spatial variation of rainfall, in conjunction with rainfall measurements being recorded on a nearby AWS. Following a rainfall event, runoff volume measurements and water samples were taken and transported to the laboratory for sediment and nutrient analysis. Several constituents of the water samples were measured, namely sediment load, nitrogen, phosphorous, DOC and POC content. Data capturing took place over several summer rainfall months, October 2018 – March 2019. In addition to capturing *in situ* data, runoff and soil

erosion of each treatment was simulated using the SWAT model, and compared against the observed data to validate the model outputs.

An array of statistical approaches were employed to produce numeric and visual analysis of the data measured on each treatment. These consist of means, standard deviations, comparative tables, ANOVA tests, post-hoc Tukey HSD tests, notched box and whisker plots, bar charts, scatter plots, correlation heat maps, and PCA's. The purpose of the methods was to install an experimental design, which was capable of capturing the necessary data to answer the research question.

Chapter Four

Results

4.1 Introduction

The chapter provides an in-depth account of the relationships between the observed rainfall, resultant runoff, sediment yield, and nutrient loss (nitrogen, phosphorous, dissolved organic carbon and particulate organic carbon), at the treatment sites. In addition, the environmental conditions of the study site are described, namely slope, soil characteristics, vegetation, and rainfall patterns. These aspects are important as they impact on erodibility, erosivity, runoff produced, and available nutrients (Blackburn *et al*., 1986; Obi and Salako, 1995; Kort *et al*., 1998; van Oost *et al*., 2000; da Silva, 2004; Chaplot *et al*., 2011).

4.2 Results

4.2.1 Precipitation

A six-month sampling period from October 2018 – March 2019 during the summer season recorded a total of ten precipitation events (*Table 4.1*). Throughout the study, there was little variation between the AWS and the treatments with respect to the measured precipitation depths of each individual event (*Figure 4.1*). The most variation was for an event measured on 13/3/2019, with a standard deviation of 7.4 mm, which was due to the manual rain gauges reaching their maximum capacity.

Table 4.1: Precipitation collection dates and the number of days since the previous collection date.

Date	Days since previous event
16/10/2018	N/A
18/10/2018	2
6/11/2018	19
23/11/2018	17
14/12/2018	21
20/12/2018	6
1/2/2019	50
12/2/2019	11
19/2/2019	7
13/3/2019	23

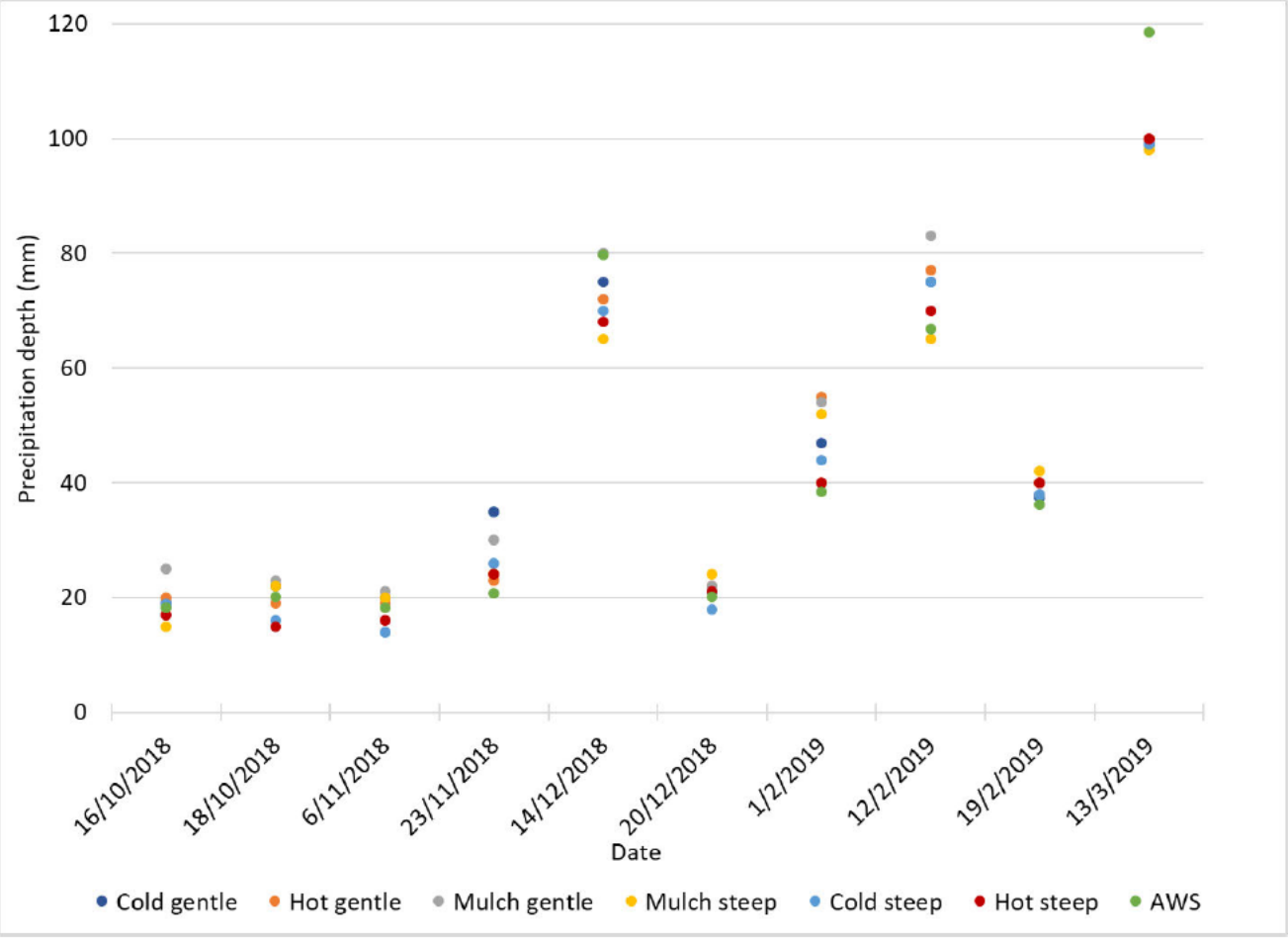

Figure 4.1: Rainfall variation between the steep and gentle slope of each treatment (CBT - Cold, HBT - Hot, mulch - Mulch), and the AWS for each rainfall event.

Using a parametric one-way ANOVA it was determined that the precipitation recorded by the rain gauges on each treatment (CBT, HBT and mulch), and at each hillslope position, and that recorded by the AWS throughout the study period had no statistically significant differences (P = 1) (*Table B-1* Appendix B). Therefore, the precipitation analysed throughout the rest of the study was that acquired from the AWS, since it provides the most accurate data due to its better design and regular hourly and daily recording interval.

The highest rainfall event (118.6 mm) occurred over four days leading up to the collection date on 13/3/2019. The smallest event was recorded on 6/11/2018 (18.2 mm) (*Figure 4.2*). The precipitation event which occurred on 12/2/2019 produced the highest precipitation intensity (4.77 mm hr^{-1}), and the lowest intensity was produced by the event on 6/11/2018 (0.44 mm hr^{-1}) (*Figure 4.2*). The accumulated precipitation was 473.4 mm for the six-month measurement period (*Figure 4.3*).

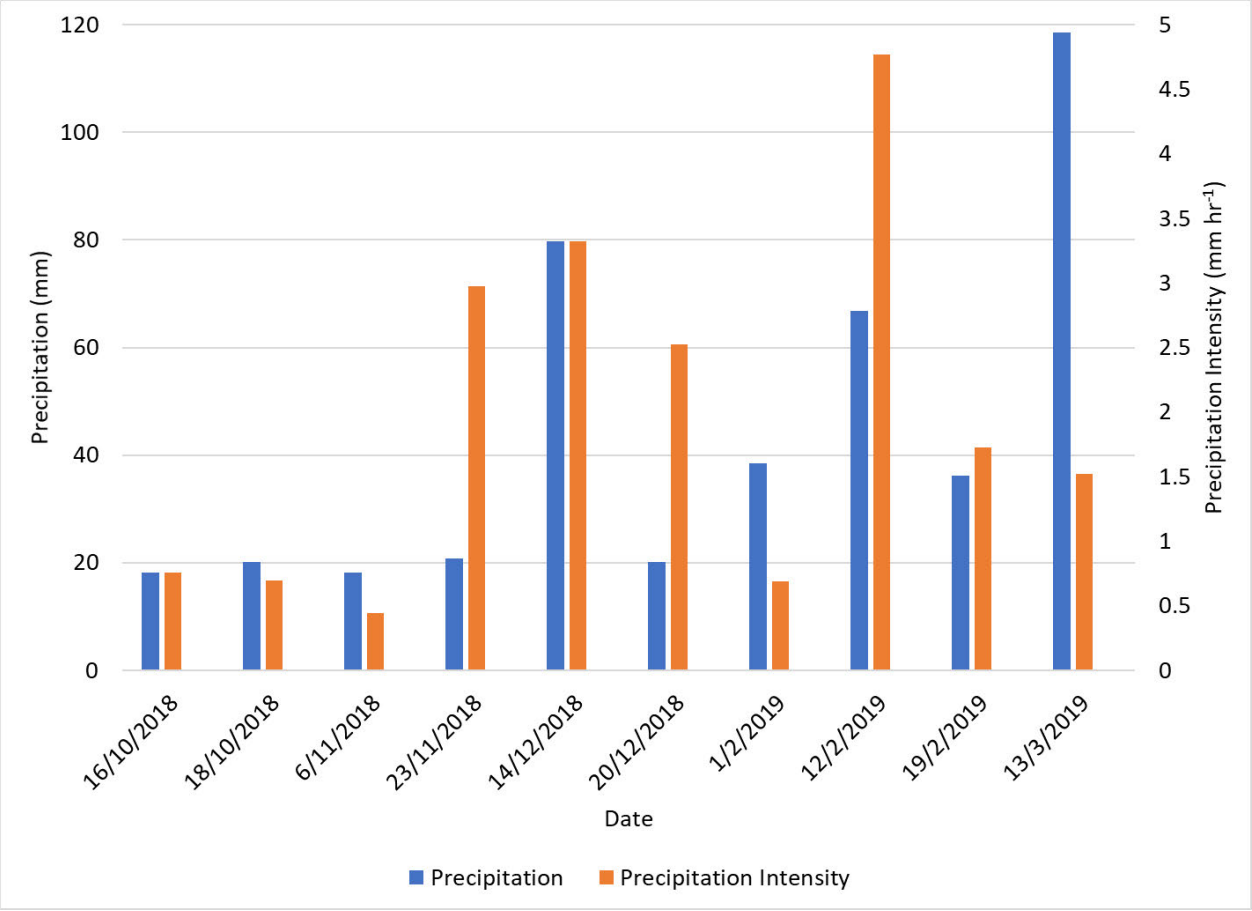

Figure 4.2: Event-based rainfall, and corresponding intensity throughout the study period (October 2018 – March 2019).

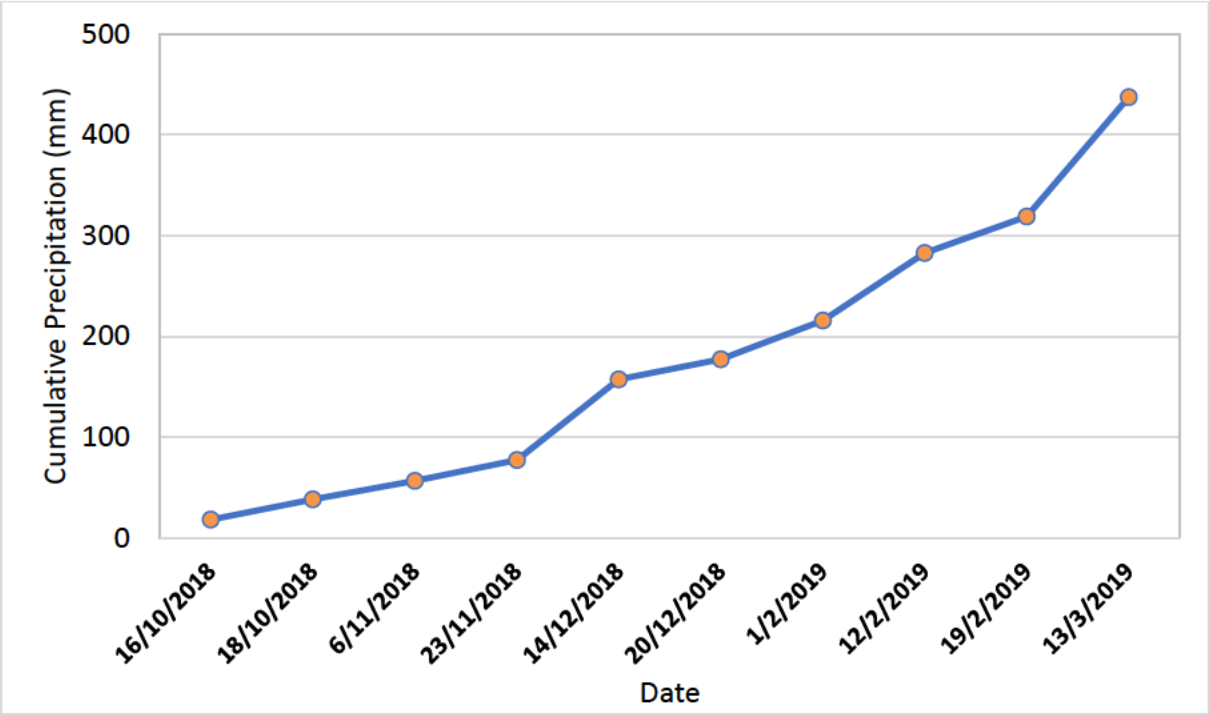

Figure 4.3: Cumulative Precipitation of measured events from 16 October 2018 to 13 March 2019.

4.2.2 Slope characteristics

Runoff and micro-runoff plots placed on the gentle slopes had similar average slopes between all treatments, whereas the steep slopes had greater variation (*Table 4.2*). Plots placed on the steep slopes were shown by a parametric one-way ANOVA to be significantly steeper than those on the gentle slopes ($P = 0.0006$). There was no statistical difference in slope between plots on the gentle slopes ($P = 0.07$) (*Table B-2* Appendix B). However, there was a statistically significant difference between plots on the steep slopes ($P = 0.01$) (*Table B-3* Appendix B).

Table 4.2: Measured slope steepness (%) for each treatment at each hillslope position.

Slope	Treatment	Slope (%)	Mean Slope (%)
Gentle	CBT	8	8.7
		9	
		9	
	Mulch	9	9.7
		9	
		11	
	HBT	9	9.7
		10	
		10	
Steep	CBT	20	19.3
		19	
		19	
	Mulch	9	13
		16	
		14	
	HBT	12	12.3
		13	
		12	

The post-hoc Tukey HSD showed that on the steep slope, the slope of the CBT was significantly steeper than both the mulch and the HBT (*Table 4.3*). However, the slopes of the mulch and HBT were not significantly different (*Table 4.3*).

Table 4.3: Post-hoc Tukey HSD test, comparing the difference in mean slope to the critical range, and indicating the statistical significance of the difference across each treatment, at a 95% confidence level (✔ = significant; ✘ = not significant).

Treatment Comparison	Difference in Means	Critical Range	Significance
CBT Vs Mulch	6.33	4.38	✔
CBT Vs HBT	7.00	4.38	✔
Mulch Vs HBT	0.67	4.38	✘

4.2.3 Soil properties

Soil samples of the research site were analysed by the Department of Agriculture and Rural Development, Soil Science Analytical Services laboratory, Cedara, who conducted a soil texture test of the study site (*Table 4.4*). It was found that the HBT had a clay loam soil type on both slopes. The soils of the mulch treatment were classified as clay soils on the gentle slope and a clay loam on the steep slope. The soils of the CBT were classified as clay loam soils on the gentle slope and a clay on the steep slope.

Table 4.4: Soil classification of each treatment at each slope class.

Slope	Treatment	Soil type
Gentle	CBT	Clay loam
	Mulch	Clay
	HBT	Clay loam
Steep	CBT	Clay
	Mulch	Clay loam
	HBT	Clay loam

Soil samples of the research site were analysed by the Department of Agriculture and Rural Development, Soil Science Analytical Services laboratory, Cedara, who conducted a soil fertility test of the soils (*Table 4.5*). Using a parametric one-way ANOVA, all three treatment sites were analysed at both slope positions for all of the aforementioned soil properties (*Table B-4 – Table B-15* Appendix B). It was determined that there were no statistically significant differences across all three treatments at both slope positions for all of the tested soil properties ($P > 0.05$), except for the potassium found in the soil ($P = 0.04$) (*Table 4.6*).

Table 4.5: Mean values of analysed soil properties.

Slope	Treatment	Soil Density ($g\ mL^{-1}$)	P ($mg\ L^{-1}$)	K ($mg\ L^{-1}$)	Ca ($mg\ L^{-1}$)	Mg ($mg\ L^{-1}$)	Exch. acidity ($cmol\ L^{-1}$)	Total cations ($cmol\ L^{-1}$)	Acid sat. %	pH (KCl)	Zn ($mg\ L^{-1}$)	Mn ($mg\ L^{-1}$)	Cu ($mg\ L^{-1}$)
Gentle	CBT	0.6	24.7	216.7	375.7	92.3	2.2	5.4	42.0	3.8	1.0	47.3	1.4
	Mulch	0.7	19.3	124.3	381.7	53.3	2.7	5.3	51.7	3.8	0.7	36.0	1.2
	HBT	0.6	22.0	132.0	498.7	70.7	1.9	5.3	34.7	4.0	0.8	54.3	1.2
Steep	CBT	0.7	24.3	62.0	247.0	50.0	2.8	4.6	66.3	3.6	1.0	19.7	1.2
	Mulch	0.7	23.0	101.3	473.0	81.3	2.9	6.2	50.7	3.8	1.0	27.3	1.4
	HBT	0.7	13.7	105.3	258.3	61.0	2.8	4.9	58.7	3.9	0.6	28.3	1.1

Table 4.6: Parametric one-way ANOVA of the soil properties of the study site, indicating whether there is a significant difference at a 95% confidence level (✔ = significant; ✘ = not significant).

Variable Measured	Alpha Value	P-Value	Significance
Sample Density ($g\ mL^{-1}$)	0.05	0.78	✘
P ($mg\ L^{-1}$)	0.05	0.08	✘
K ($mg\ L^{-1}$)	0.05	0.04	✔
Ca ($mg\ L^{-1}$)	0.05	0.74	✘
Mg ($mg\ L^{-1}$)	0.05	0.80	✘
Exch. acidity ($cmol\ L^{-1}$)	0.05	0.65	✘
Total cations ($cmol\ L^{-1}$)	0.05	0.79	✘
Acid sat. %	0.05	0.37	✘
pH (KCl)	0.05	0.30	✘
Zn ($mg\ L^{-1}$)	0.05	0.46	✘
Mn ($mg\ L^{-1}$)	0.05	0.26	✘
Cu ($mg\ L^{-1}$)	0.05	0.31	✘

It was shown by the post-hoc Tukey HSD that the potassium found in the soil of the CBT on the gentle slope was significantly greater than the mulch (gentle), CBT (steep), mulch (steep), and HBT (steep) (*Table 4.7*). There were no significant differences found in the potassium concentrations between any other treatment sites (*Table 4.7*).

Table 4.7: Post-hoc Tukey HSD outputs for the soil potassium content of each treatment site, and an indication of which sites were significantly different at a 95% confidence level (✔ = significant; ✘ = not significant).

Treatment Comparison	Difference in Means	Critical Range	Significance
Cold burn (gentle) vs Mulch (gentle)	92.33	89.35	✔
Cold burn (gentle) vs Hot burn (gentle)	84.67	89.35	✘
Cold burn (gentle) vs Cold burn (steep)	154.67	89.35	✔
Cold burn (gentle) vs Mulch (steep)	115.33	89.35	✔
Cold burn (gentle) vs Hot burn (steep)	111.33	89.35	✔
Mulch (gentle) vs Hot burn (gentle)	7.67	89.35	✘
Mulch (gentle) vs Cold burn (steep)	62.33	89.35	✘
Mulch (gentle) vs Mulch (steep)	23.00	89.35	✘
Mulch (gentle) vs Hot burn (steep)	19.00	89.35	✘
Hot burn (gentle) vs Cold burn (steep)	70.00	89.35	✘
Hot burn (gentle) vs Mulch (steep)	30.67	89.35	✘
Hot burn (gentle) vs Hot burn (steep)	26.67	89.35	✘
Cold burn (steep) vs Mulch (steep)	39.33	89.35	✘
Cold burn (steep) vs Hot burn (steep)	43.33	89.35	✘
Mulch (steep) vs Hot burn (steep)	4.00	89.35	✘

For soil organic carbon (%) and nitrogen (%) soil samples were analysed at the Department of Agriculture and Rural Development, Soil Science Analytical Services laboratory, Cedara (*Table 4.8*). Across all three treatments the ANOVA test (*Table B-16* – *Table B-18* Appendix B) indicated that there were no statistically significant difference for each of the tested soil attributes ($P < 0.05$) (*Table 4.9*).

Table 4.8: Mean values of analysed soil properties cont.

Slope	Treatment	Organic Carbon (%)	Nitrogen (%)
Gentle	CBT	6.00	0.37
	Mulch	5.83	0.51
	HBT	5.87	0.47
Steep	CBT	5.10	0.37
	Mulch	5.30	0.32
	HBT	5.97	0.47

Table 4.9: Parametric one-way ANOVA of the soil properties of the study site, indicating whether there were significant differences at a 95% confidence level (✔ = significant; ✘ = not significant).

Variable Measured	Alpha Value	P-Value	Significance
Organic Carbon (%)	0.05	0.17	✘
Nitrogen (%)	0.05	0.10	✘

4.2.4 Vegetation

The vegetation aerial cover and abundance of each treatment at each slope position was determined using the Braun-Blanquet classification method (*Table 4.10*). Within the young plantation, the litter cover was only that of the applied mulch. The area had a relatively low species richness in terms of grass cover; *Eragrostis teff* being the dominant grass species.

Table 4.10: Vegetation abundance on each treatment at each slope position as described by the Braun-Blanquet method (r = rare occurrence; + = cover < 1%; 1 = 1-5% cover, 2 = 5-25% cover; 3 = 25-50% cover; 4 = 50-75% cover; and 5 = cover > 75%), where "cover" is the estimated above-ground space covered by sample category when projected vertically (Poore, 1995).

		10 m^2					1 m^2		
Slope	Treatment	Individual trees	Average tree diameter at breast height (dbh) (mm)	Aerial tree cover	Litter cover	Grass cover	Aerial tree cover	Litter cover	Grass cover
Gentle	CBT	2	0	1	r	2	r	r	2
	Mulch	2	0	1	5	r	r	5	r
	HBT	2	0	1	r	2	r	r	2
Steep	CBT	2	0	1	r	2	r	r	2
	Mulch	2	0	1	5	r	r	5	r
	HBT	2	0	1	r	2	r	r	2

4.3 In-field Measurements

4.3.1 Vegetation and soil characteristics

The Leaf Area Index (LAI) was monitored from October 2018 – March 2019 (*Figure 4.4*). Due to minor variability between each treatment and hillslope position for each measurement, a single monthly mean LAI value was used to represent the study area for each month throughout the investigation. Significant increases across all treatments in mean LAI were observed from January 2019 – February 2019, before beginning to plateau from February 2019 – March 2019.

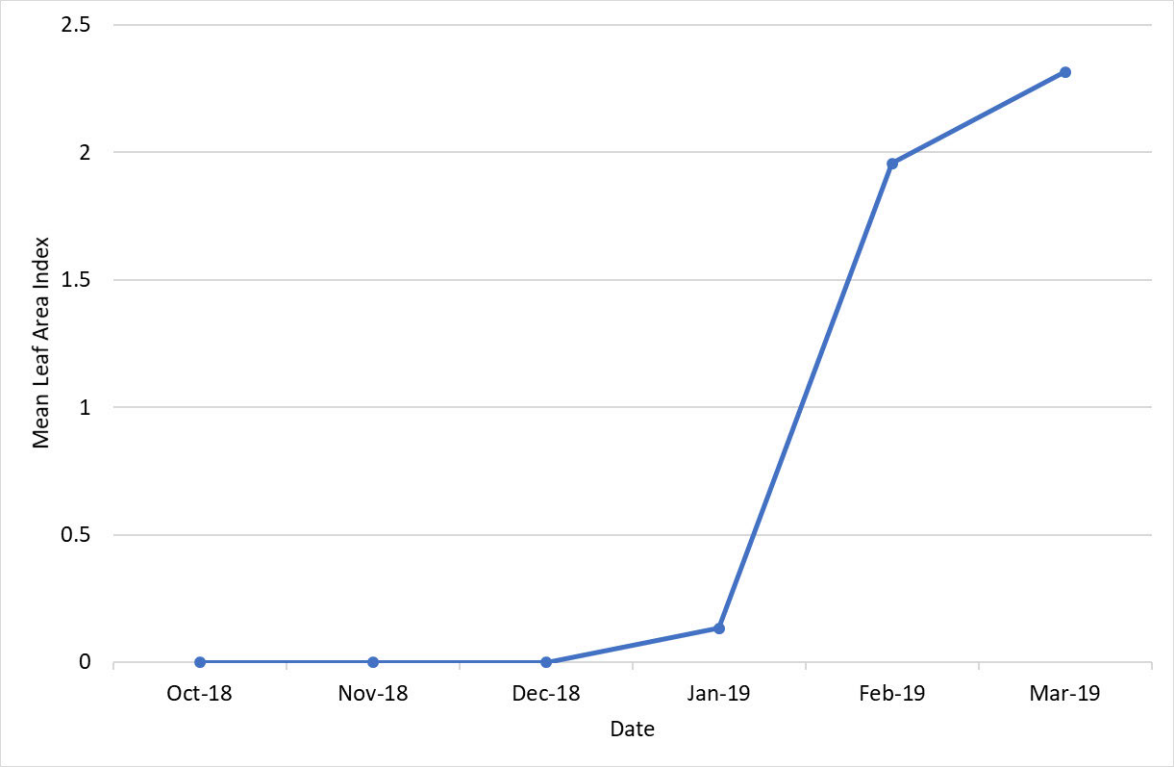

Figure 4.4: Mean Leaf Area Index for the study site throughout the research period (October 2018 – March 2019).

Soil water repellency was monitored on each treatment at each slope. There was a high level of soil water repellecy - a water drop taking greater than 5 minutes to infiltrate the soil. This behaviour was observed consistently throughout the study duration and repeatedly across all treatments at each slope. The high level of repellency is indicative of hydrophobic soils at the study site.

4.3.2 Runoff volume

The CBT produced statistically similar median runoff volume on the 1 m^2 plots (3.19 L m^{-2}) and 10 m^2 plots (1.53 L m^{-2}) (*Figure 4.5*). The 1 m^2 plots exhibited a greater variation of runoff volume generation than the 10 m^2 plots and produced no extreme values. The 10 m^2 plots generated a single extreme runoff volume value of 21.44 L m^{-2} recorded on 12/2/2019.

The HBT produced statistically similar median runoff volume on the 1 m^2 plots (3.36 L m^{-2}) and 10 m^2 plots (1.85 L m^{-2}) (*Figure 4.5*). The 10 m^2 plots exhibited a greater variation and extreme runoff volume values than the 1 m^2 plots, recorded on (in descending order of magnitude) 12/2/2018 (16.66 L m^{-2}) and the 14/12/2018 (14.63 L m^{-2}). The 1 m^2 plots generated two extreme runoff volume values recorded on 14/12/2018 (14.64 L m^{-2}) and the 12/2/2019 (11.87 L m^{-2}).

The mulch treatment produced statistically similar median runoff volume on the 1 m^2 plots (1.44 L m^{-2}) and 10 m^2 plots (0.64 L m^{-2}) (*Figure 4.5*). The 1 m^2 plots exhibited a greater variation of runoff volume than the 10 m^2 plots. The 1 m^2 plots witnessed extreme runoff volume values recorded on (in descending order of magnitude) 12/2/2019 (16.40 L m^{-2}) and the 13/3/2019 (14.31 L m^{-2}), while the 10 m^2 plots generated extreme values on 12/2/2019 (21.94 L m^{-2}); 14/12/2018 (10.53 L m^{-2}) and 13/3/2019 (10.34 L m^{-2}).

The median runoff volume across all three treatments on the 1 m^2 plots were statistically similar. The CBT produced the largest variation of runoff volume, while the mulch treatment had a similar degree of variation to the HBT. The median runoff volume on the 10 m^2 plots across all three treatments were statistically similar. The largest degree of variability in runoff volume on the 10 m^2 plots was produced by the HBT, while the mulch treatment produced the lowest. The 10 m^2 plots on each treatment were more prone to producing extreme runoff volume values than their 1 m^2 counterparts. The extreme runoff volume values were produced by three rainfall events which occurred on 14/12/2018; 12/2/2019 and 13/3/2019.

The following sections consisting of the notched box and whisker plots utilize the median value. In addition, the extreme values are also expressed for each notched box and whisker plot. Since the data were not normally indicated, it was more appropriate to use the notch about the median rather than the mean.

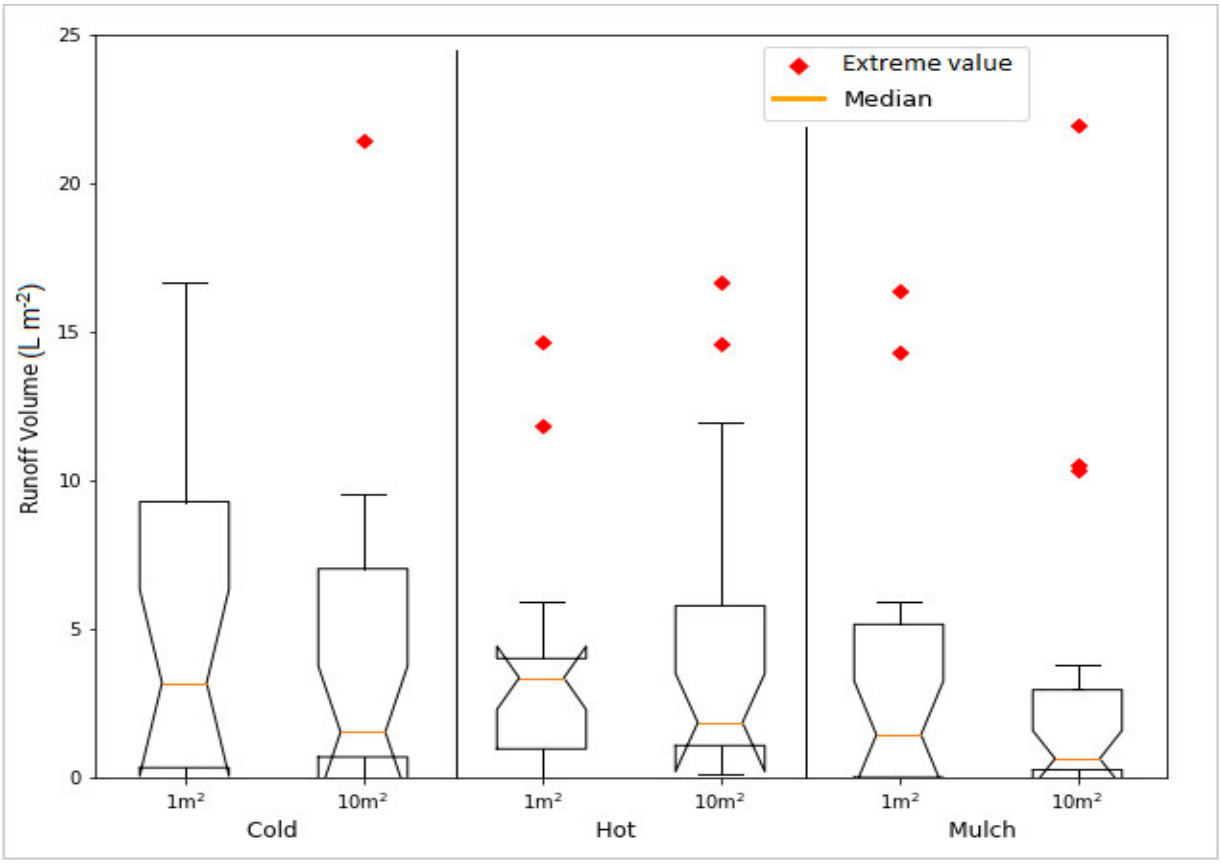

Figure 4.5: Notched Box and whisker plot representing the runoff volume data observed on the "Cold" burn, "Hot" burn, and "Mulch" treatments at the 1 m^2 and 10 m^2 scales.

4.3.3 Sediment load

The CBT produced statistically similar median sediment loads on the 1 m^2 plots (19.56 g m^{-2}) and 10 m^2 plots (10.62 g m^{-2}) (*Figure 4.6*). The 1 m^2 plots exhibited a greater variation of sediment load generation than the 10 m^2 plots and produced a single extreme sediment load value of 177.39 g m^{-2} recorded on 14/12/2018. The 10 m^2 plots generated several extreme sediment load values which were greater than those produced by the 1 m^2 plots, that were recorded on (in descending order of magnitude) 12/2/2019 (814.01 g m^{-2}); 14/12/2018 (226.65 g m^{-2}); 20/12/2018 (215.49 g m^{-2}) and 23/11/2018 (190.02 g m^{-2}).

The HBT produced statistically similar median sediment loads on the 1 m^2 plots (8.71 g m^{-2}) and 10 m^2 plots (20.43 g m^{-2}) (*Figure 4.6*). The 10 m^2 plots witnessed greater variability in sediment

load generation and produced larger extreme values than the 1 m^2 plots, which were recorded on (in descending order of magnitude) 12/2/2019 (966.86 g m^{-2}); 14/12/2018 (225.711 g m^{-2}) and 14/12/2018 (223.72 g m^{-2}). The 1 m^2 plots produced two extreme values on 14/12/2018 (107.16 g m^{-2}) and the 13/3/2019 (72.10 g m^{-2}).

The mulch treatment generated statistically similar median sediment loads on the 1 m^2 plots (3.37 g m^{-2}) and 10 m^2 plots (3.12 g m^{-2}) (*Figure 4.6*). The 1 m^2 plots had greater variation in the generation of sediment load than the 10 m^2 plots; however, the 10 m^2 plots produced larger extreme values than the 1 m^2 plots, which were recorded on (in descending order of magnitude) 12/2/2019 (97.77 g m^{-2}); 14/12/2018 (63.64 g m^{-2}) and 13/3/2019 (43.10 g m^{-2}). The 1 m^2 plots produced a single extreme value of 32.99 g m^{-2} on 12/2/2019.

The median sediment load generation on the 1 m^2 plots across all three treatments were statistically similar. The CBT displayed the greatest variability of sediment load generation on the 1 m^2 plots, while the mulch treatment displayed the lowest variability. The median sediment load generation on the 10 m^2 plots of the CBT were statistically similar to both other treatments; however, the mulch treatment produced a median sediment load which was statistically less than the HBT. The sediment load variability of the CBT and HBT on the 10 m^2 plots were similar, while the mulch had a reduced variability. On each treatment, the 10 m^2 plots were more prone to generating larger extreme sediment load values than their 1 m^2 counterparts. All three treatments saw extreme sediment load values being generated from five rainfall events, occurring on 23/11/2018; 14/12/2018; 20/12/2018; 12/2/2019 and 13/3/2019.

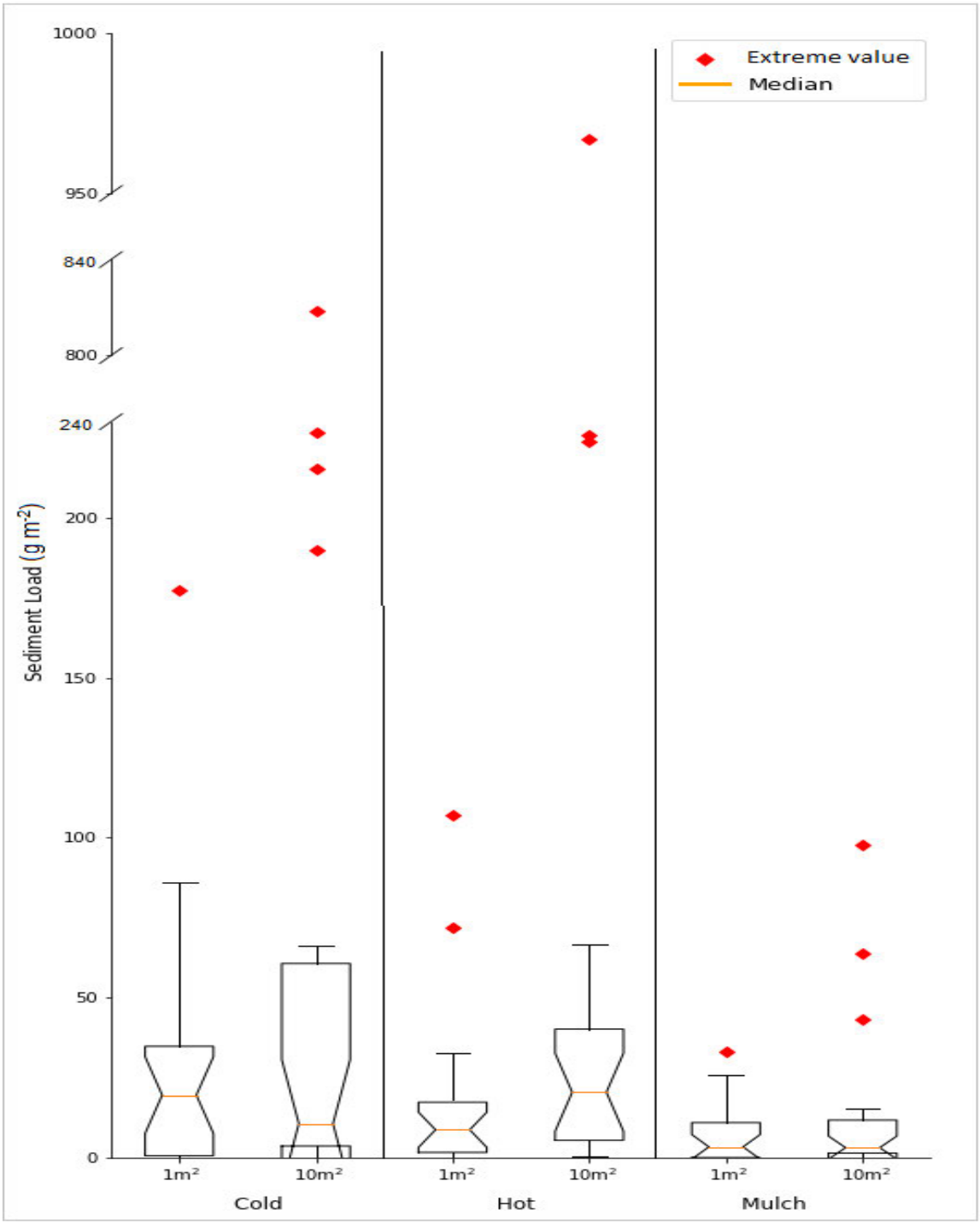

Figure 4.6: Notched Box and whisker plot representing the sediment load data observed on the "Cold" burn, "Hot" burn, and "Mulch" treatments at the 1 m^2 and 10 m^2 scales.

215

4.3.4 Nitrogen loss

The CBT produced statistically similar median nitrogen loss on the 1 m^2 plots (51.10 mg m^{-2}) and 10 m^2 plots (22.78 mg m^{-2}) (*Figure 4.7*). The 10 m^2 plots exhibited a greater variation of nitrogen loss than the 1 m^2 plots, and produced a single extreme value of 321.73 mg m^{-2}, recorded on 23/11/2018, while the 1 m^2 plots generated no extreme values.

The HBT produced statistically similar median nitrogen loss on the 1 m^2 plots (25.71 mg m^{-2}) and 10 m^2 plots (41.64 mg m^{-2}) (*Figure 4.7*). The 10 m^2 plots exhibited a greater variation of nitrogen loss than the 1 m^2 plots, and produced a single extreme value of 257.41 mg m^{-2} recorded on 12/2/2019. The 1 m^2 plots generated two extreme nitrogen loss values recorded on (in descending order of magnitude) 14/12/2018 (363.23 mg m^{-2}) and the 12/2/2019 (136.69 mg m^{-2}).

The mulch treatment produced statistically similar median nitrogen loss on the 1 m^2 plots (19.80 mg m^{-2}) and 10 m^2 plots (11.26 mg m^{-2}) (*Figure 4.7*). There were no extreme nitrogen loss values produced by the 1 m^2 plots; however, there was a greater variation of nitrogen loss than the 10 m^2 plots. The 10 m^2 plots produced two extreme nitrogen loss values of 136.10 mg m^{-2} and 93.92 mg m^{-2}, which were both recorded on 12/2/2019.

The median nitrogen loss on the 1 m^2 plots across all three treatments were statistically similar; however, the mulch treatment displayed the greatest variability of nitrogen loss of all three treatments, while HBT had the lowest variability. The median nitrogen loss on the 10 m^2 plots across all three treatments were statistically similar. The greatest variability in nitrogen losses on the 10 m^2 plots were observed on the CBT, and the lowest on the mulch treatment. The CBT and HBT witnessed a larger variability in nitrogen loss on the 10 m^2 plots, while the 1 m^2 plots produced a larger variability on the mulch treatment. The events which produced extreme nitrogen loss values occurred on 23/11/2018; 14/12/2018 and 12/2/2019.

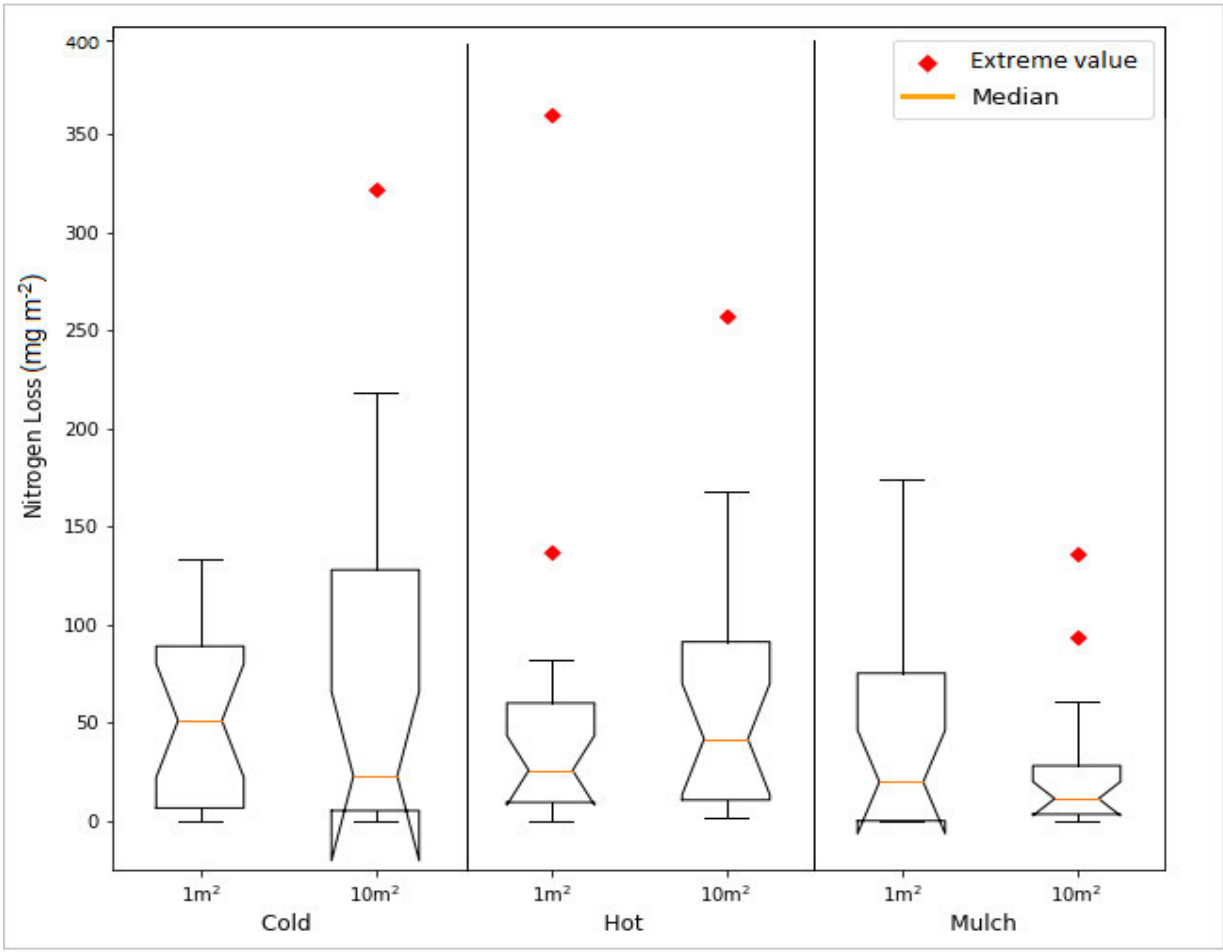

Figure 4.7: Notched Box and whisker plot representing the nitrogen loss data observed on the "Cold" burn, "Hot" burn, and "Mulch" treatments at the 1 m^2 and 10 m^2 scales.

4.3.5 Phosphorous loss

The CBT produced statistically similar median phosphorous losses on the 1 m^2 plots (0.24 mg m^{-2}) and 10 m^2 plots (0.13 mg m^{-2}) (*Figure 4.8*). The 1 m^2 plots exhibited a greater variation of phosphorous loss than the 10 m^2 plots and produced several extreme phosphorous loss values which were recorded on (in descending order of magnitude) 13/3/2019 (29.62 mg m^{-2}); 13/3/2019 (11.40 mg m^{-2}); 12/2/2019 (6.93 mg m^{-2}) and 12/2/2019 (3.00 mg m^{-2}). The 10 m^2 plots produced multiple extreme phosphorous loss values which were recorded on 1/2/2019 (2.19 mg m^{-2}); 12/2/2019 (1.24

mg m^{-2}) and 12/2/2019 (0.64 mg m^{-2}); however, these values were not as extreme as those observed on the 1 m^2 plots.

The HBT produced statistically similar median phosphorous losses on the 1 m^2 plots (0.12 mg m^{-2}) and 10 m^2 plots (0.26 mg m^{-2}) (*Figure 4.8*). Both plot sizes had similar variability of phosphorous loss, while the 1 m^2 plots showed two extreme phosphorous loss values recorded on (in descending order of magnitude) 13/3/2019 (8.60 mg m^{-2}) and the 6/11/2018 (1.68 mg m^{-2}). The 10 m^2 plots produced multiple extreme phosphorous loss values which were recorded on 12/2/2019 (3.10 mg m^{-2}); 13/3/2019 (2.92 mg m^{-2}) and 6/11/2018 (1.85 mg m^{-2}).

The mulch treatment produced statistically similar median phosphorous losses on the 1 m^2 plots (0.10 mg m^{-2}) and 10 m^2 plots (0.07 mg m^{-2}) (*Figure 4.8*). The 1 m^2 plots exhibited a greater variation of phosphorous loss than the 10 m^2 plots. The 1 m^2 plots witnessed multiple extreme phosphorous loss values recorded on (in descending order of magnitude) 1/2/2019 (6.10 mg m^{-2}); 12/2/2019 (3.94 mg m^{-2}) and 14/12/2018 (2.10 mg m^{-2}), while the 10 m^2 plots generated extreme values on 12/2/2019 (2.19 mg m^{-2}); 20/12/2018 (1.10 mg m^{-2}); 12/2/2019 (0.95 mg m^{-2}) and 14/12/2018 (0.74 mg m^{-2}).

The median phosphorous loss on the 1 m^2 plots across all three treatments were statistically similar. The CBT displayed the greatest variability of phosphorous loss on the 1 m^2 plots, with the mulch treatment having the lowest variability. The median phosphorous loss on the 10 m^2 plots across all three treatments were statistically similar; however, the HBT had the largest variability. The mulch and CBT had similar variation of phosphorous loss on the 10 m^2 plots. The greatest extreme phosphorous loss values were all observed on the 1 m^2 plots across all treatments, with the CBT having the largest extreme values. All three treatments saw extreme phosphorous loss values being generated from six rainfall events, occurring on 13/3/2019; 12/2/2019; 1/2/2019. 14/12/2018; 20/12/2018 and 6/11/2018.

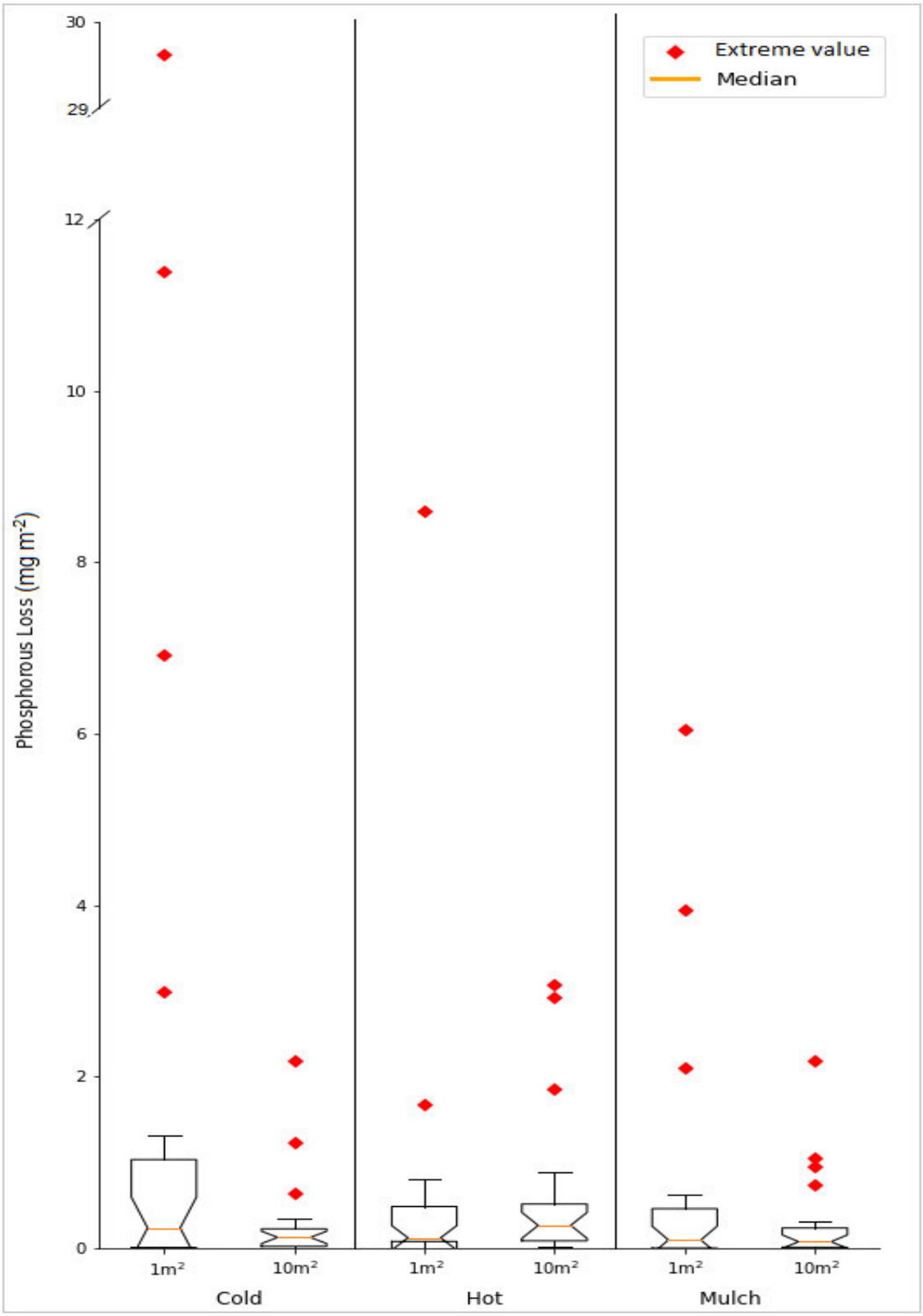

Figure 4.8: Notched Box and whisker plot representing the phosphorous loss data observed on the "Cold" burn, "Hot" burn, and "Mulch" treatments at the 1 m^2 and 10 m^2 scales.

4.3.6 Dissolved organic carbon loss

The CBT produced statistically similar median DOC losses on the 1 m^2 plots (54.55 mg m^{-2}) and 10 m^2 plots (28.42 mg m^{-2}) (*Figure 4.9*). The 10 m^2 plots had a greater variation of DOC loss than the 1 m^2 plots. The 10 m^2 plots were the only plots which generated an extreme DOC loss value of 302.83 mg m^{-2}, which was recorded on 12/2/2019.

The HBT produced statistically similar median DOC losses on the 1 m^2 plots (36.64 mg m^{-2}) and 10 m^2 plots (29.23 mg m^{-2}) (*Figure 4.9*). Both the 1 m^2 and 10 m^2 plots had similar degrees of DOC loss variability. The 1 m^2 plots produced two extreme DOC loss values which were recorded on (in descending order of magnitude) 14/12/2018 (313.33 mg m^{-2}) and the 23/11/2018 (246.32 mg m^{-2}). However, the 10 m^2 plots produced more extreme values and at greater extremes, recorded on 12/2/2019 (564.87 mg m^{-2}); 14/12/2018 (477.52 mg m^{-2}) and 14/12/2018 (238.41 mg m^{-2}).

The mulch treatment produced statistically similar median DOC loss values on the 1 m^2 plots (27.40 mg m^{-2}) and 10 m^2 plots (16.40 mg m^{-2}) (*Figure 4.9*). The 1 m^2 plots on the mulch treatment had a larger variation of DOC loss than the 10 m^2 plots, and produced a single extreme value of 360.50 mg m^{-2} recorded on 23/11/2018. The 10 m^2 plots saw two extreme DOC loss values which were recorded on (in descending order of magnitude) 12/2/2019 (298.35 mg m^{-2}) and the 14/12/2018 (227.33 mg m^{-2}).

The median DOC loss on the 1 m^2 plots across all three treatments were statistically similar; however, the mulch treatment displayed the greatest variability, while the HBT and CBT had similar DOC loss variabilities. The median DOC loss on the 10 m^2 plots across all three treatments were statistically similar; however, the mulch treatment had the lowest variability. The CBT witnessed the highest variability on the 10 m^2 plots of all three treatments; although, the HBT had larger extreme values, and more extreme values. All three treatments saw extreme DOC loss values being produced from the same three rainfall events, occurring on 23/11/2018; 14/12/2018 and 12/2/2019.

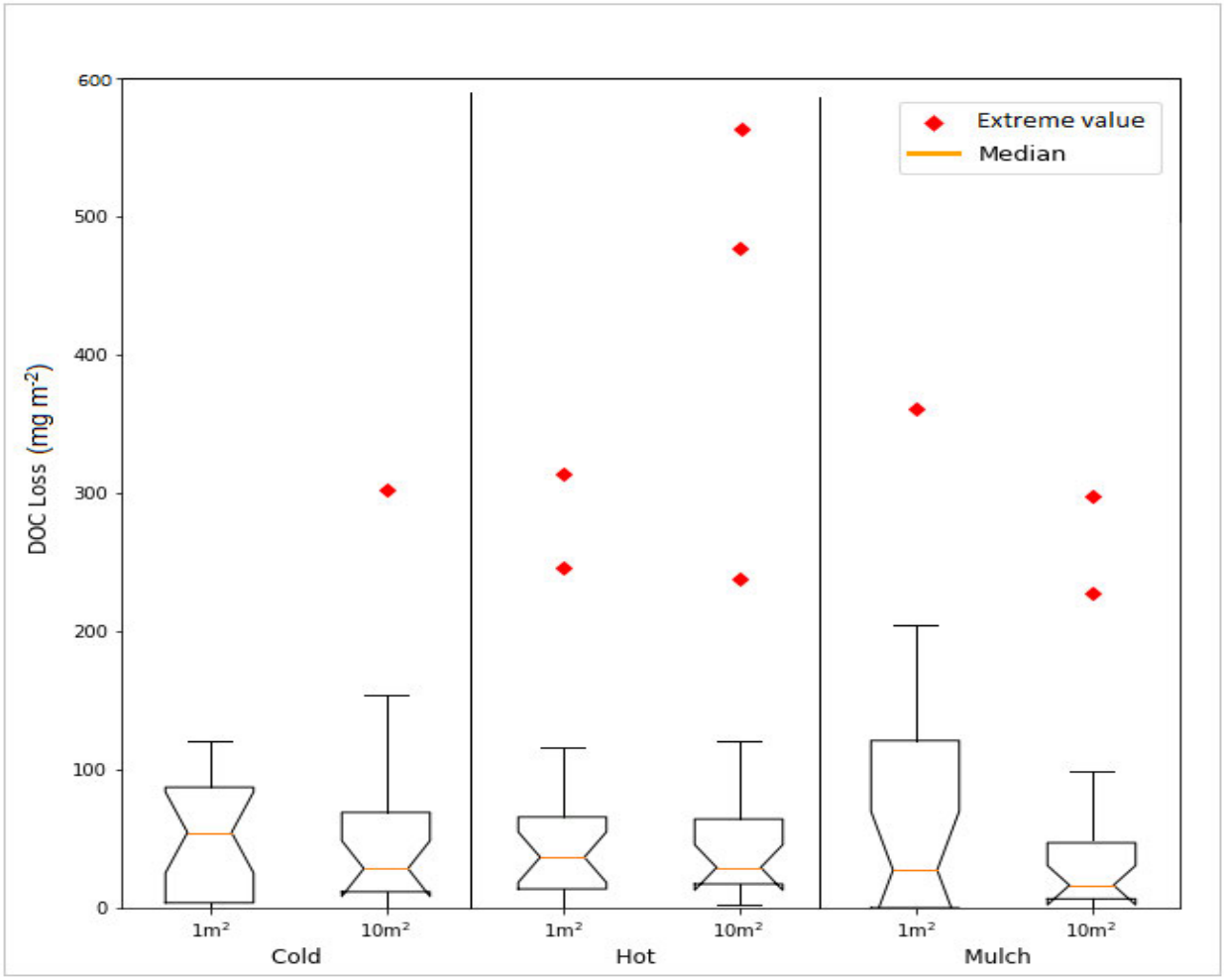

Figure 4.9: Notched Box and whisker plot representing the DOC loss data observed on the "Cold" burn, "Hot" burn, and "Mulch" treatments at the 1 m^2 and 10 m^2 scales.

310

4.3.7 Particulate organic carbon loss

The CBT produced statistically similar median POC losses on the 1 m^2 plots (2.34 g m^{-2}) and 10 m^2 plots (2.03 g m^{-2}) (*Figure 4.10*). The 1 m^2 plots of the CBT had a larger variation of POC loss
315 compared to the 10 m^2 plots. The 10 m^2 plots had several large POC loss values, which were recorded on (in descending order of magnitude) 12/2/2019 (151.42 g m^{-2}); 20/12/2018 (56.18 g m^{-2}); 14/12/2018 (35.76 g m^{-2}) and 23/11/2018 (26.64 g m^{-2}). The 1 m^2 plots had fewer large values which were recorded on 23/11/2018 (28.75 g m^{-2}) and the 14/12/2018 (27.18 g m^{-2}).

The HBT generated statistically similar median values on the 1 m^2 plots (1.03 g m^{-2}) and 10 m^2 plots (2.71 g m^{-2}) (*Figure 4.10*). The 10 m^2 plots had the greatest variation of POC loss on the HBT. The treatment had of a small number of large POC loss values, recorded on (in descending order of magnitude) 12/2/2019 (325.02 g m^{-2}) and the 14/12/2018 (66.63 g m^{-2} and 40.18 g m^{-2}). The 1 m^2 plots had the same number of large values; however, these values were not as large as that found on the 10 m^2 plots. These values were recorded on 13/3/2019 (26.73 g m^{-2}); 14/12/2018 (23.94 g m^{-2}) and 23/11/2018 (11.73 g m^{-2}).

The mulch treatment produced statistically similar median POC loss values on the 1 m^2 plots (0.35 g m^{-2}) and 10 m^2 plots (0.43 g m^{-2}) (*Figure 4.10*). The 1 m^2 plots on the mulch treatment had a larger variation of POC loss compared to the 10 m^2 plots. Despite having a lesser variation, the 10 m^2 plots witnessed several large POC loss values, recorded on (in descending order of magnitude) 12/2/2019 (17.58 g m^{-2}); 14/12/2018 (14.16 g m^{-2}); 13/3/2019 (5.75 g m^{-2}) and 20/12/2018 (3.00 g m^{-2}). The 1 m^2 plots had multiple large POC loss values which resided above the upper limit of the box and whisker plot, which were recorded on 14/12/2018 (8.10 g m^{-2}); 12/2/2019 (5.19 g m^{-2}) and 23/11/2018 (3.93 g m^{-2}).

The median POC loss on the 1 m^2 plots across all three treatments were statistically similar; however, the mulch treatment displayed the lowest variability, and the CBT displayed the greatest. The median values on the 10 m^2 plots across all treatments were statistically similar, with the mulch treatment having the lowest variability, and the HBT having the greatest. All three treatments saw extreme POC loss values being produced from the same five rainfall events, occurring on 23/11/2018; 14/12/2018; 20/12/2018; 12/2/2019 and 13/3/2019.

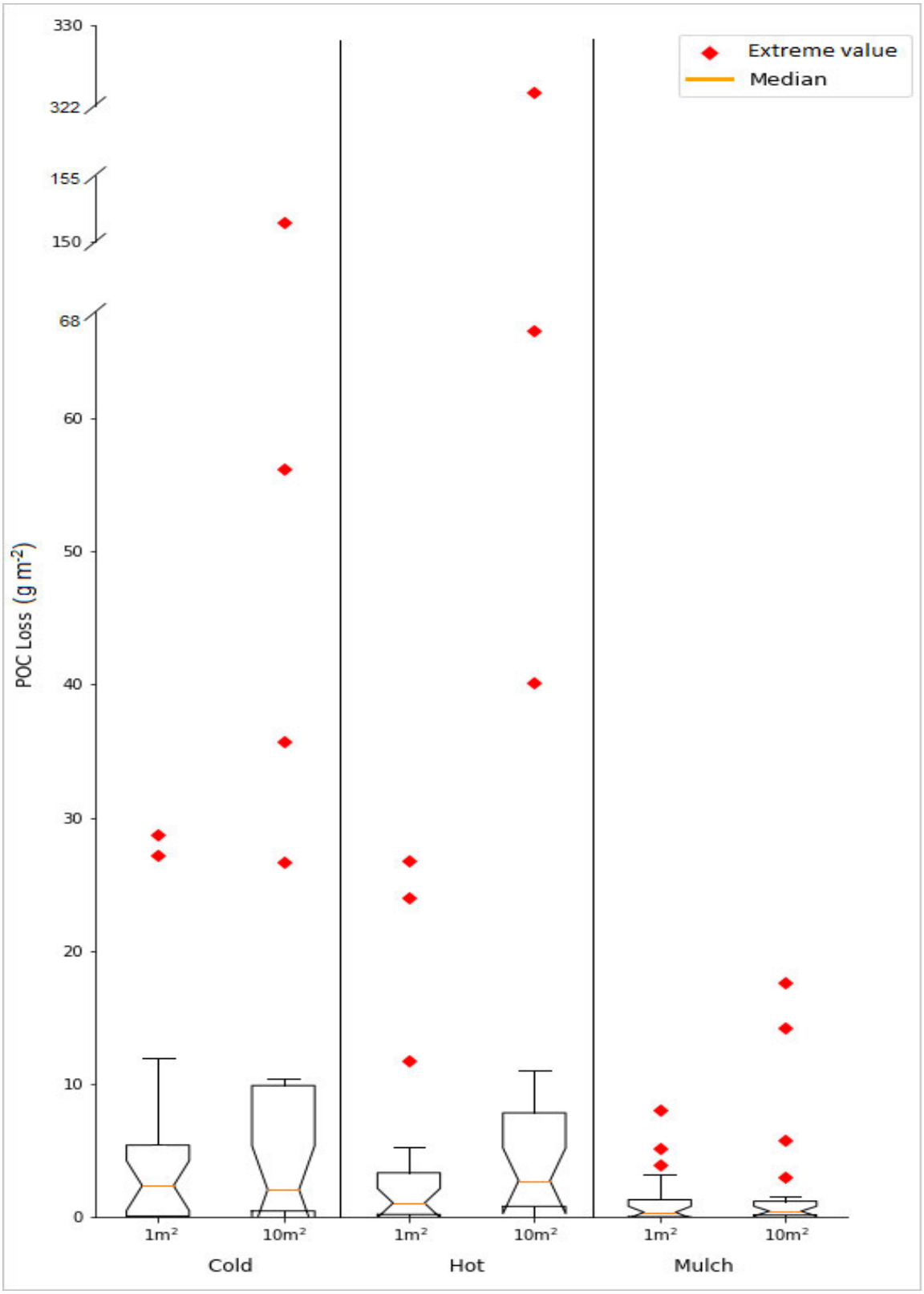

340

Figure 4.10: Notched Box and whisker plot representing the POC loss data observed on the "Cold" burn, "Hot" burn, and "Mulch" treatments at the 1 m^2 and 10 m^2 scales.

4.3.8 Treatment summary

The mulch treatment generated the lowest runoff and erosion of all treatments on both the 1 m^2 plots and 10 m^2 plots, barring DOC and nitrogen loss, where it generated the most on the 1 m^2 plots (*Table 4.11*). The CBT produced the most runoff and erosion (baring DOC and nitrogen loss) on the 1 m^2 plots of all treatments and generated the most nitrogen and DOC loss on the 10 m^2 plots, and the second most on the 1 m^2 plots (*Table 4.11*). The HBT generated the most runoff and erosion on the 10 m^2 plots, and the second most on the 1 m^2 plots of all treatments, barring nitrogen and DOC loss, where it generated the second most on the 10 m^2 plots and the least on the 1 m^2 plots (*Table 4.11*).

Table 4.11: Representation of the order of magnitude of each treatment with respect to each measured variable and the relative plot size. "Hot" = hot burn treatment (orange); "Cold" = cold burn treatment (blue); "Mulch" = mulch treatment (green). Treatment colours are used to aid in the visual identification of each treatment in this table and hold no other meaning.

Variable	Plot size	Treatment with the largest measured values	Treatment with medial measured values	Treatment with the lowest measured values
Runoff volume	1 m^2	Cold	Hot	Mulch
	10 m^2	Hot	Cold	Mulch
Sediment load	1 m^2	Cold	Hot	Mulch
	10 m^2	Hot	Cold	Mulch
Phosphorous loss	1 m^2	Cold	Hot	Mulch
	10 m^2	Hot	Cold	Mulch
POC loss	1 m^2	Cold	Hot	Mulch
	10 m^2	Hot	Cold	Mulch
DOC loss	1 m^2	Mulch	Cold	Hot
	10 m^2	Cold	Hot	Mulch
Nitrogen loss	1 m^2	Mulch	Cold	Hot
	10 m^2	Cold	Hot	Mulch

The tipping bucket runoff plots provide a timeseries of individual rainfall events. A single event was used to produce a runoff hydrograph demonstrating the runoff characteristics observed on each treatment on different slopes. The chosen event was recorded on 12/2/2019, as it was one of the largest rainfall events, with the highest intensities, and generated runoff on all three treatments (*Figure 4.11*).

The steep slope of the CBT had a slightly delayed peak discharge of 0.4 L s^{-1} and a steep rising limb; however, this treatment saw runoff being produced for a significantly longer period than any other treatment, demonstrated by the significantly prolonged recession limb (*Figure 4.11 A*). There was no runoff produced on the gentle slope on the CBT for this event (*Figure 4.11 A*).

The HBT on the steep slope witnessed the earliest peak discharge of 0.4 L s^{-1} with a steep rising limb and prolonged recession limb (*Figure 4.11 B*). The HBT on the gentle slope had a delayed peak discharge of 0.4 L s^{-1} with a steep ascending and descending limb (*Figure 4.11 B*).

The mulch treatment on the steep slope saw a marked reduction in peak discharge of 0.27 L s^{-1} and an increased lag time with the most gradual observed rising limb of all treatments, and a gentle recession limb (*Figure 4.11 C*). In addition, the gentle slope saw no generation of runoff for this event (*Figure 4.11 C*).

The CBT had the quickest runoff response to rainfall, commencing runoff before all other treatments. The mulch treatment had the slowest runoff response to rainfall, commencing runoff significantly later than the other treatments. The HBT had a delayed runoff response to the commencement of rainfall, this was more prevalent on the steep slope.

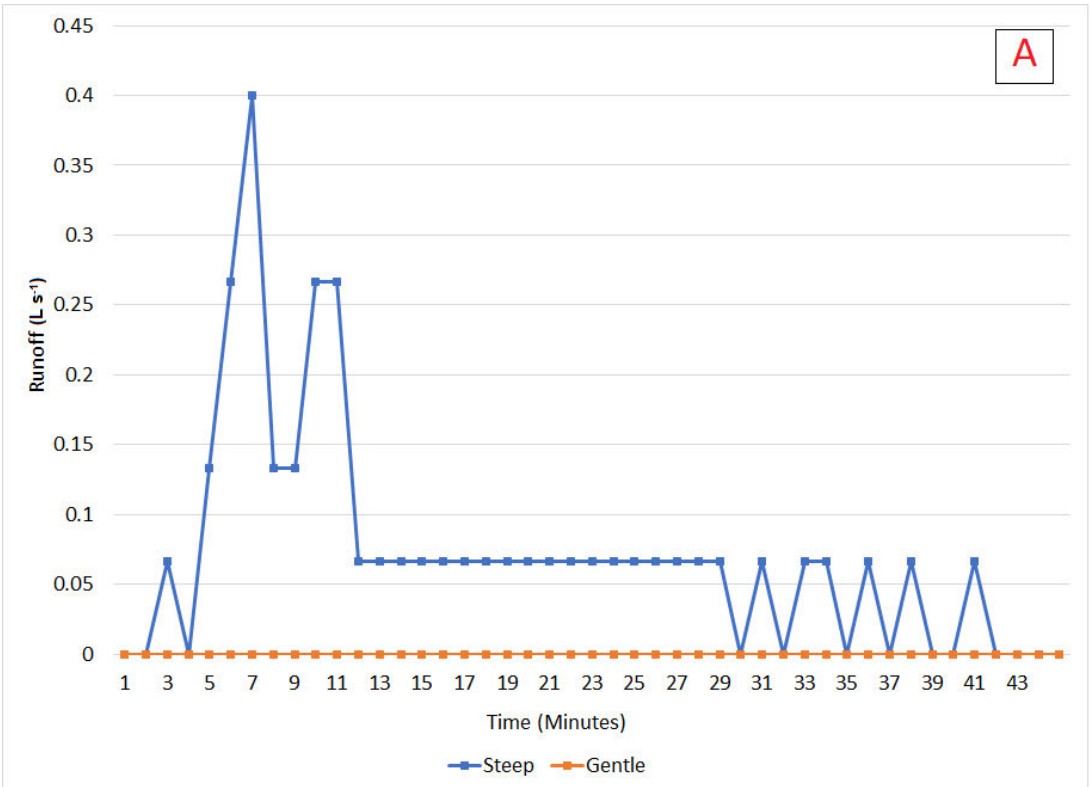
A
0.45
0.4
0.35
0.3
0.25
0.2
0.15
0.1
0.05
0
Runoff (L s⁻¹)
1 3 5 7 9 11 13 15 17 19 21 23 25 27 29 31 33 35 37 39 41 43
Time (Minutes)
Steep
Gentle

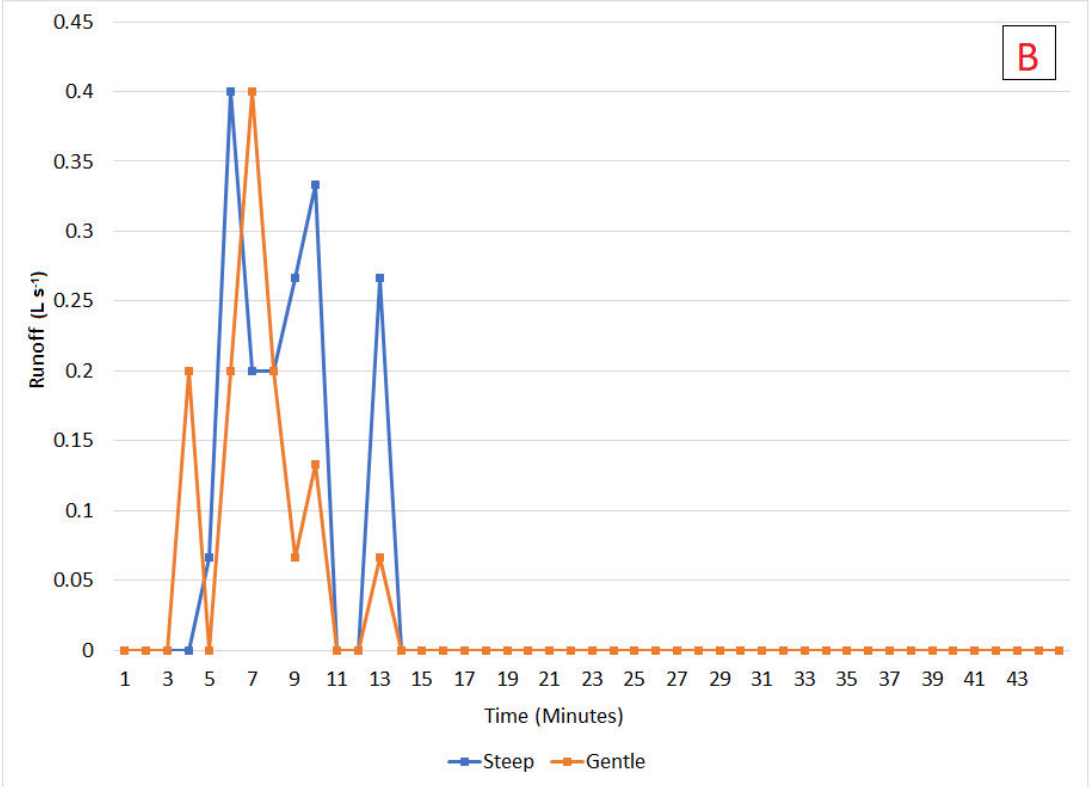
B
0.45
0.4
0.35
0.3
0.25
0.2
0.15
0.1
0.05
0
Runoff (L s⁻¹)
1 3 5 7 9 11 13 15 17 19 21 23 25 27 29 31 33 35 37 39 41 43
Time (Minutes)
Steep
Gentle

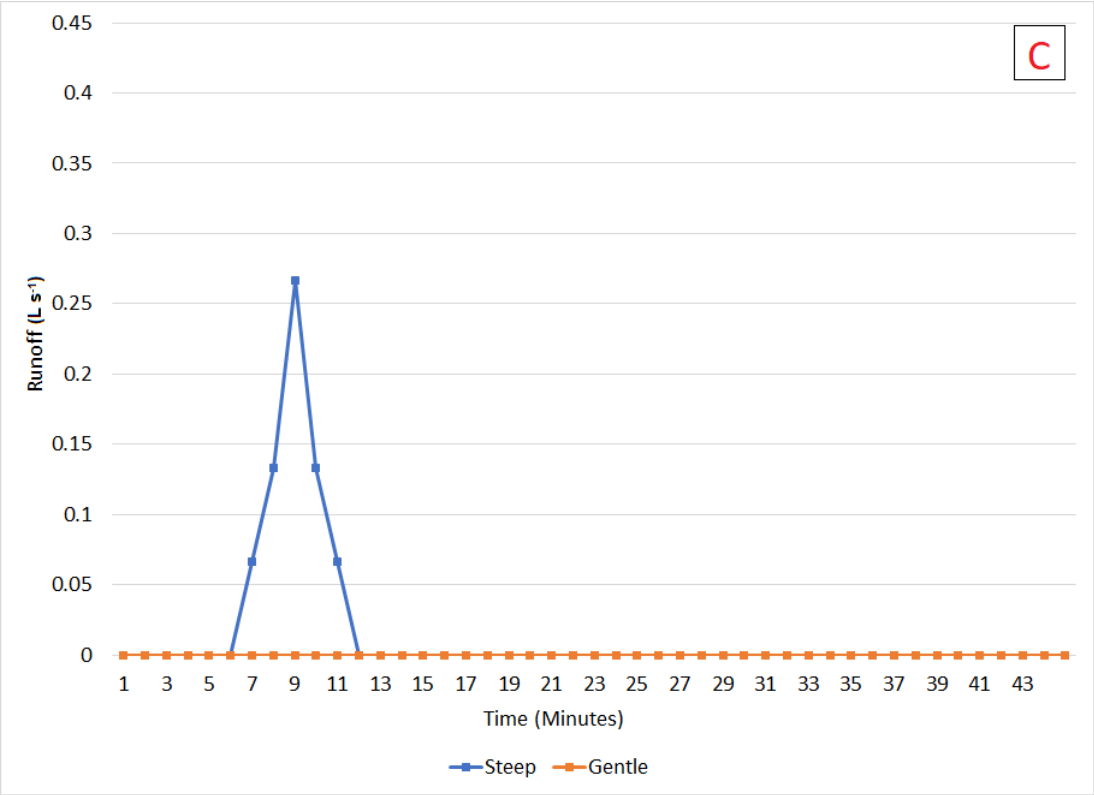

Figure 4.11: Runoff hydrograph measured by the tipping buckets from the 10 m^2 plots at each slope for the cold burn treatment (A), hot burn treatment (B), and mulch treatment (C).

385 The CBT's dataset exhibited clear grouping of observations when categorized by slope (*Figure 4.12 A*). This was evidenced by the observed spatial separation of the colour-coded markers in the PC (Principal Component) coordinate system shown in the biplot. Collectively, the three PC axes shown account for ~93% of the total information content of the original data. The amount of variance accounted for by each PC is given in the axis labels. The variables runoff generation 390 (runoff), phosphorous loss (P), sediment load, POC loss (POC) and DOC loss (DOC), indicated on the biplot by the blue arrows, were all strongly positively associated with the 'steep' slope. Nitrogen loss (N) shared a moderate positive association with the 'steep' slope.

The plot sizes of the CBT associations with individual variables were less evident, where markers were colour coded by plot area (*Figure 4.12 B*). (NB: the principal component scores were not 395 calculated using the categorical 'plot size' or 'slope' information, and so remain the same). Plot size did not display strong associations with any individual variable. There was a moderate positive

association between both the 1 m^2 and 10 m^2 plots with runoff generation, phosphorous loss, nitrogen loss, sediment load, POC loss and DOC loss.

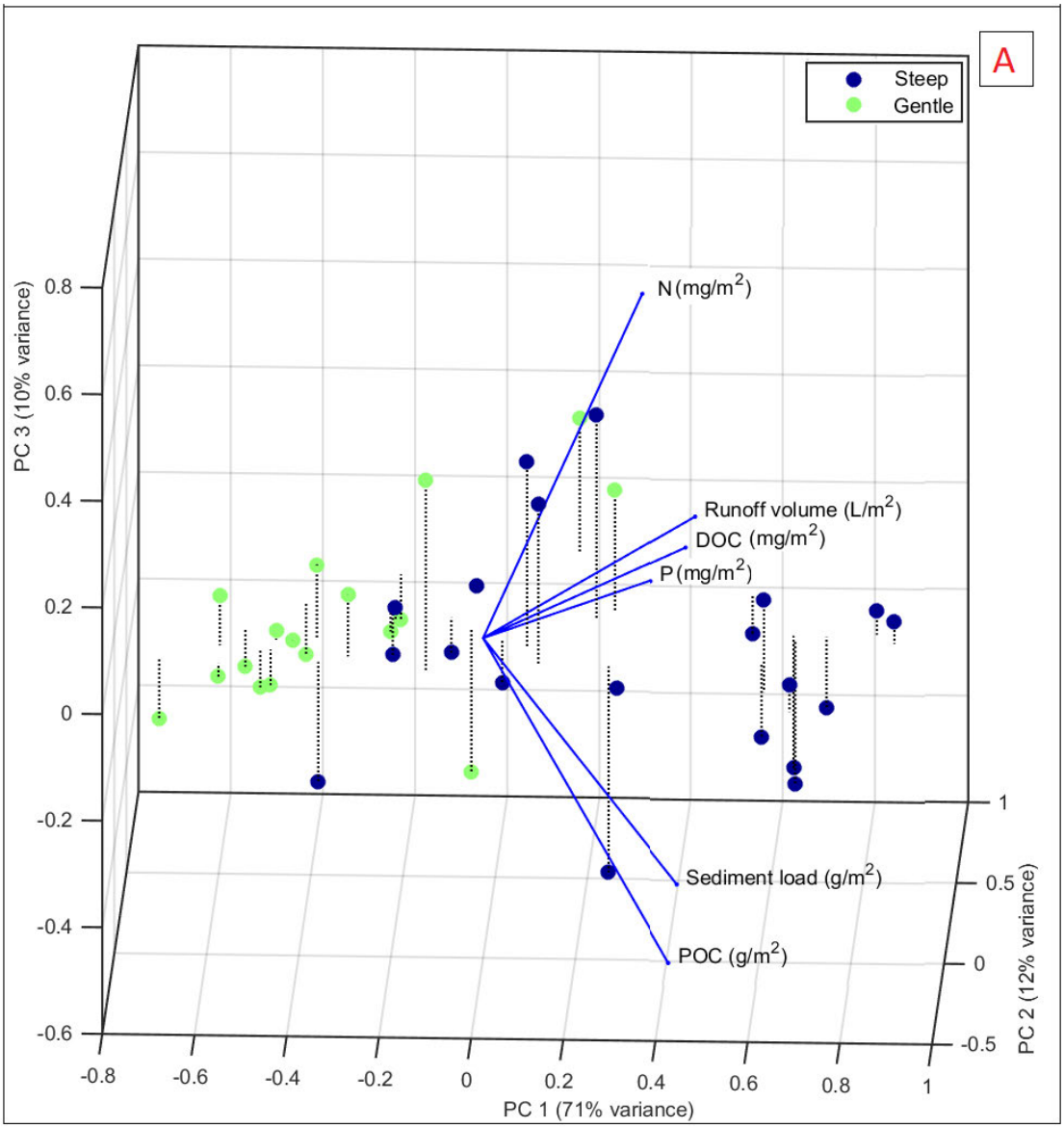

400

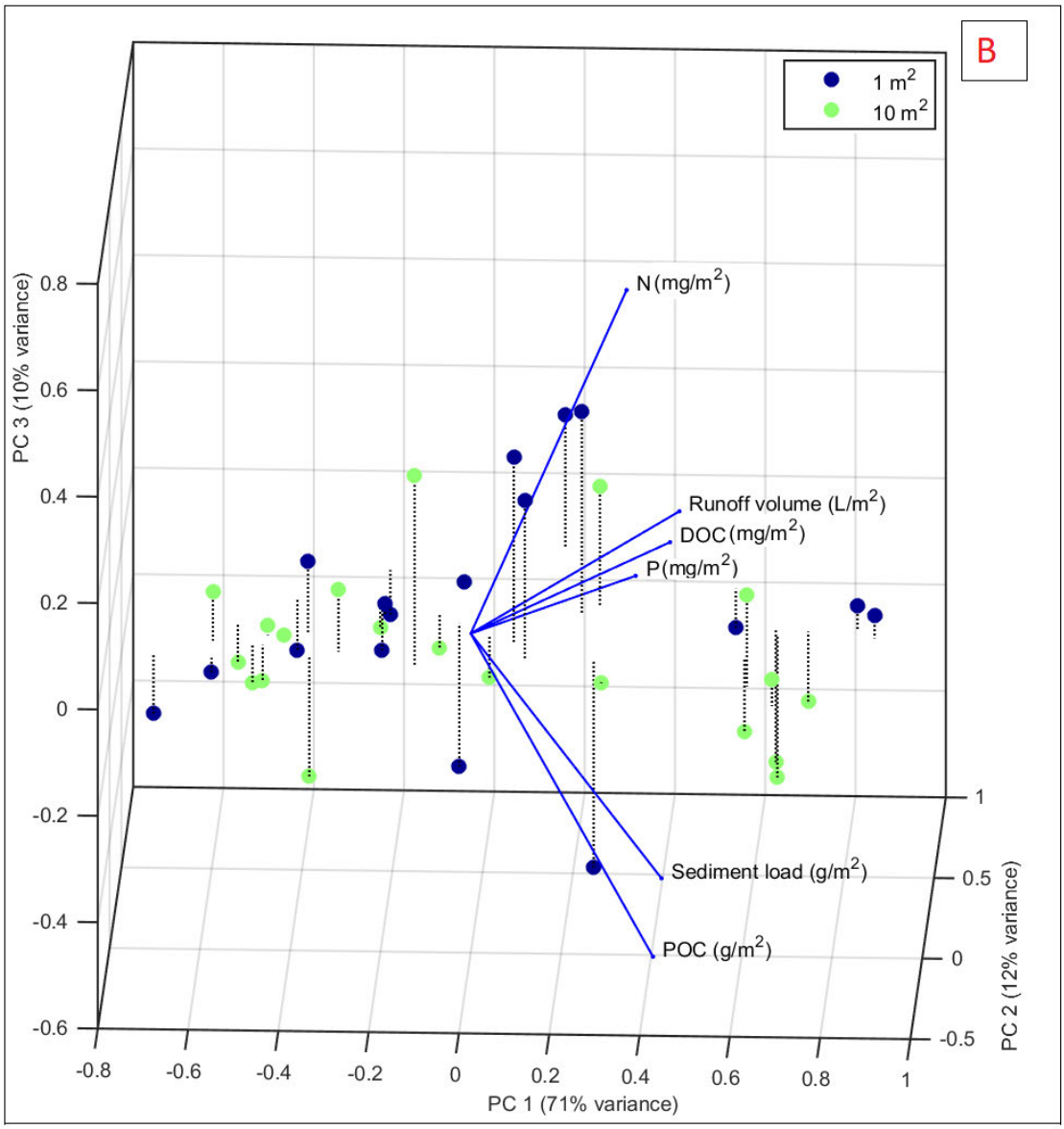

Figure 4.12: PCA biplot showing the first 3 principal components for slope (A) and plot size (B) of the cold burn treatment. PC scores, which represent original observations plotted in PC space, are represented by coloured markers. PC loading weights for each original variable are indicated by the blue arrows.

The CBT showed several notable correlations between the measured variables (*Figure 4.13*). Sediment load was strongly positively correlated to DOC loss (DOC) (correlation coefficient = 0.91) and POC loss (POC) (0.99). While DOC loss was strongly positively correlated to POC loss (0.91). Moderate positive correlations were found between runoff volume and rainfall depth (0.55),

DOC loss (0.57), POC loss (0.62), rainfall intensity (RFL intensity) (0.61), sediment load (0.69), and nitrogen loss (N) (0.70). LAI shared a moderate positive correlation with rainfall depth (0.66). Note that phosphorous loss (P) was weakly negatively correlated to sediment load (− 0.01) and POC loss (− 0.03). Phosphorous had a weak positive correlation with rainfall intensity (0.05), and shared no correlation with DOC loss (0).

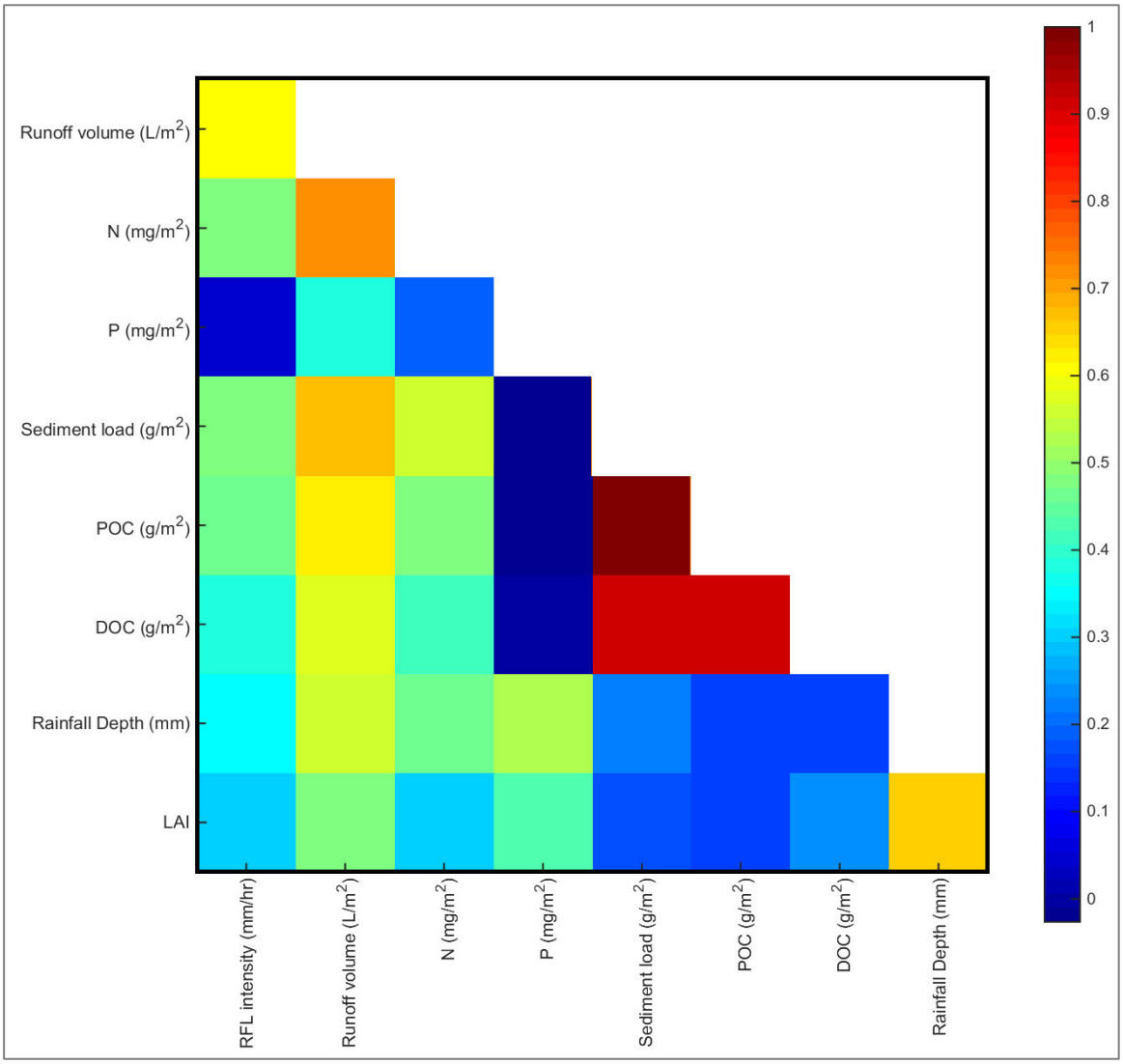

Figure 4.13: Correlation heat map of observed variables on the cold burn treatment.

The HBT's dataset exhibited no clear grouping of observations by slope (*Figure 4.14 A*). This was evidenced by the spatial separation of the colour-coded markers in the PC coordinate system shown

in the biplot. Collectively, the three PC axes shown account for ~90% of the total information content of the original data. The level of variance accounted for by each PC is provided in the axis' labels. Associations with individual variables were not clear. There was a moderate positive association between both slope classes and runoff generation (runoff), phosphorous loss (P), nitrogen loss (N), sediment load, POC loss (POC) and DOC loss (DOC).

The HBTs plot sizes exhibited a similar trend to that of the slope class; associations with individual variables were not clearly observed, where markers were colour coded by plot area (*Figure 4.14 B*). (NB: the principal component scores were not calculated using the categorical 'plot size' or 'slope' information, and so remain the same). There was a moderate positive association between the 1 m^2 and 10 m^2 plots with runoff generation, phosphorous loss, nitrogen loss, sediment load, POC and DOC loss; however, the 10 m^2 plots have a marginally stronger association with runoff and erosion than the 1 m^2 plots.

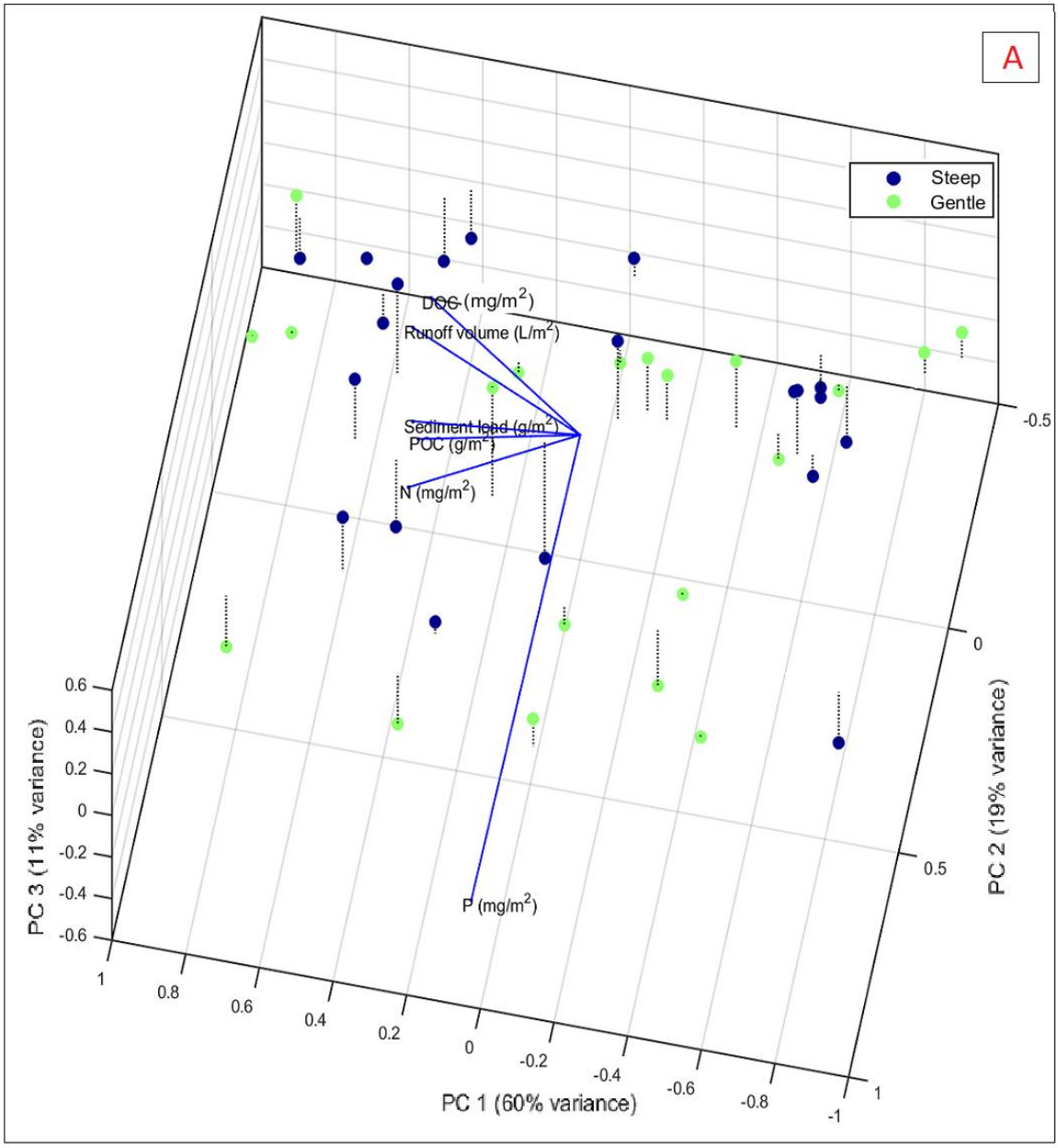
A
Steep
Gentle
DOC (mg/m2)
Runoff volume (L/m2)
Sediment load (g/m2)
POC (g/m2)
N (mg/m2)
P (mg/m2)
PC 3 (11% variance)
PC 1 (60% variance)
PC 2 (19% variance)

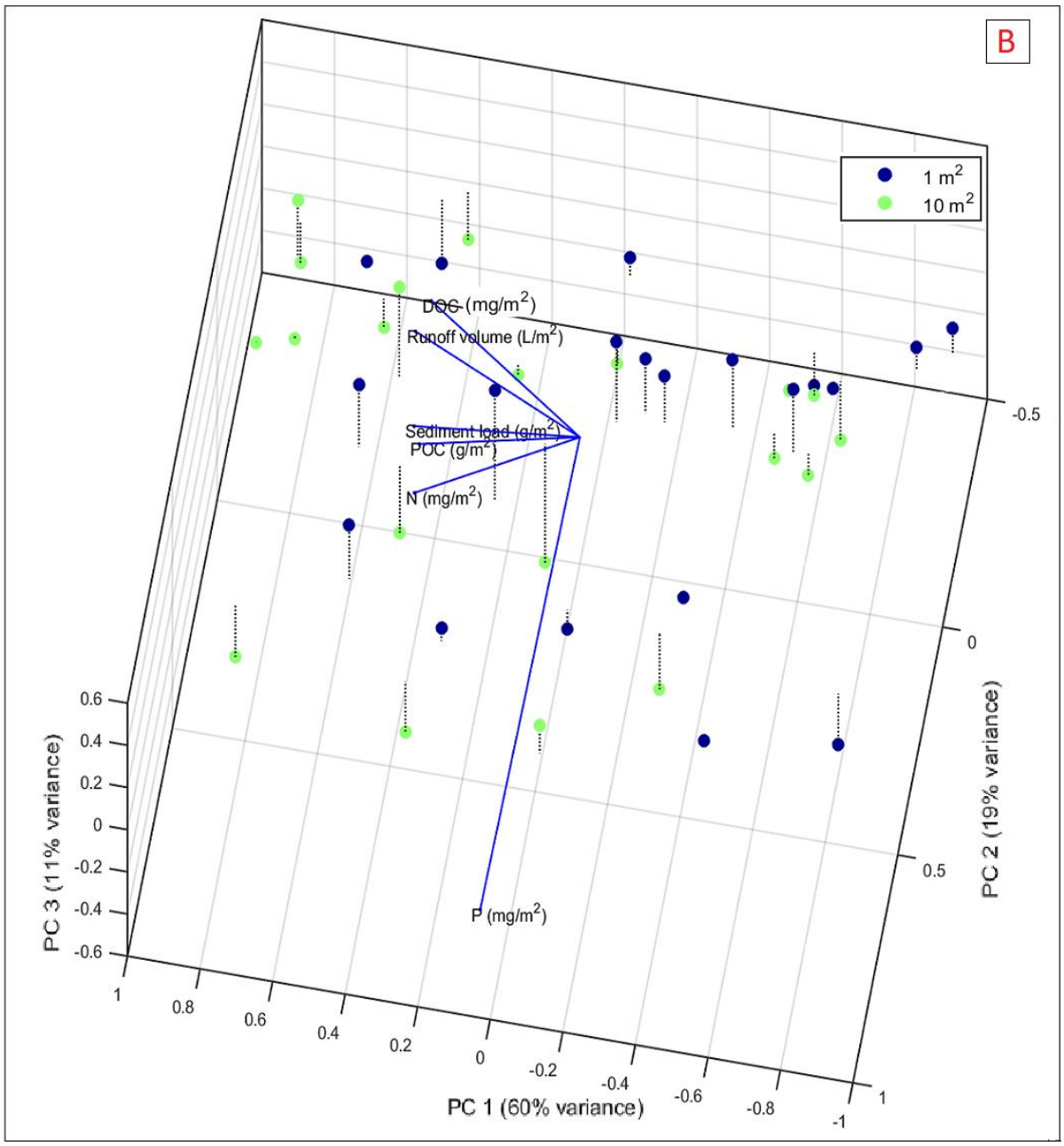

Figure 4.14: PCA biplot showing the first 3 principal components for slope (A) and plot size (B) of the hot burn treatment. PC scores, which represent original observations plotted in PC space, are represented by coloured markers. PC loading weights for each original variable are indicated by the blue arrows.

The HBT exhibited several notable correlations of varying strengths between the measured variables (*Figure 4.15*). Sediment load shared strong positive correlations with DOC loss (correlation coefficient = 0.82) and POC loss (0.99). DOC loss had a strong positive correlation

with POC loss (0.8). Positive correlations varying in strength were found between runoff volume rainfall depth (0.65), DOC loss (0.78), POC loss (0.6), rainfall intensity (0.66), sediment load (0.68), and nitrogen loss (0.8). Nitrogen loss was moderately positively correlated to rainfall intensity (0.6), rainfall depth (0.58), and DOC loss (0.6). In addition, moderate positive correlations were observed between rainfall intensity and DOC loss (0.6), and between LAI and rainfall depth (0.68). Note that phosphorous loss had a weak positive correlation with rainfall intensity (0.02), and a weak negative correlation with sediment load (− 0.03), POC loss (− 0.04), and DOC loss (− 0.05),

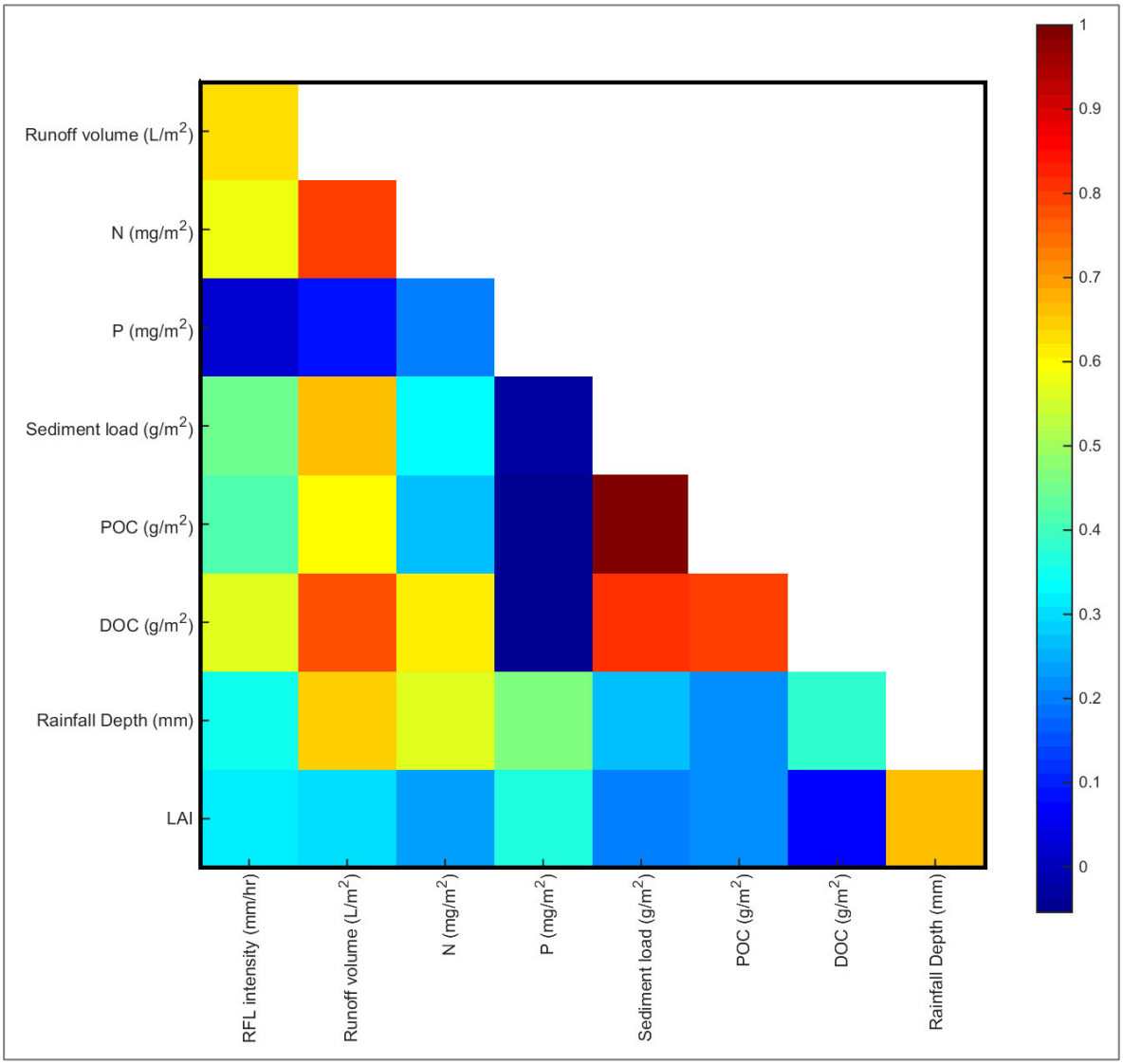

Figure 4.15: Correlation heat map of observed variables on the hot burn treatment.

For the mulch treatment dataset, there was clear grouping of the observations by slope class. This was evidenced by the spatial separation of the colour-coded markers in the PC coordinate system shown in the biplot (*Figure 4.16 A*). Collectively, the three PC axes shown account for ~99% of the total information content of the original data. The level of variance accounted for by each PC is provided in the axis' labels. The variables runoff, nitrogen and DOC loss, indicated on the biplot by the blue arrows, were strongly positively associated with the 'steep' slope, and strongly negatively associated with the 'gentle' slope. Sediment load was positively associated with POC loss, but not with slope. Phosphorous loss was not associated with any other variable or with slope class.

A comparison of the influence of differing plot sizes in which the markers were colour-coded by runoff plot area (*Figure 4.16 B*), associations with individual variables were less clear. (NB: the principal component scores were not calculated using the categorical 'plot size' or 'slope' information, and so remain the same). There was a moderate negative association between the 10 m^2 plots and the generation of nitrogen, runoff and DOC and a moderate positive association with sediment load production, POC and phosphorous loss. There was a moderate positive association between the 1 m^2 plots and the generation of nitrogen, runoff and DOC, POC, sediment load and phosphorous loss.

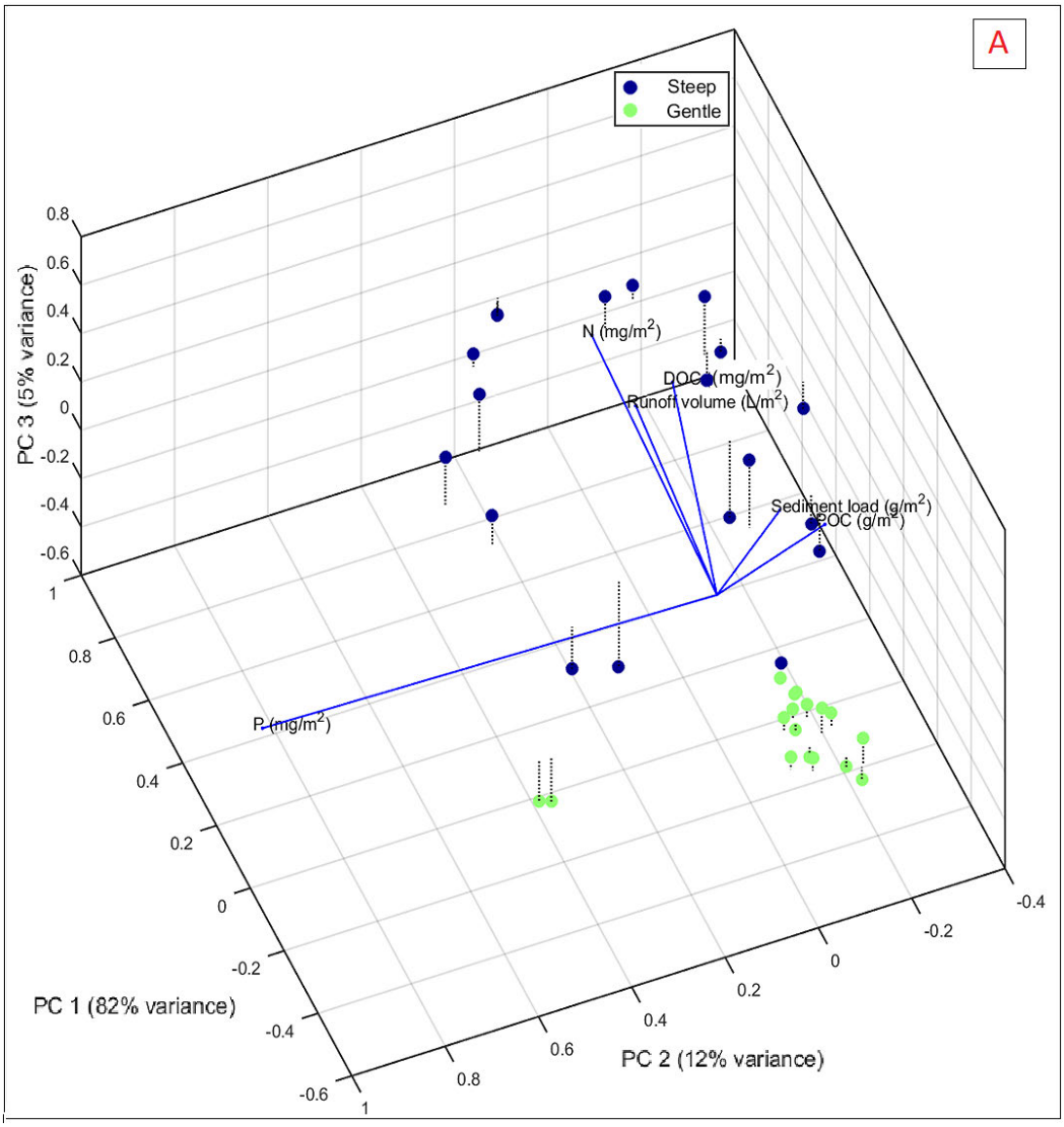
A
Steep
Gentle
N (mg/m2)
DOC (mg/m2)
Runoff volume (L/m2)
Sediment load (g/m2)
POC (g/m2)
P (mg/m2)
PC 3 (5% variance)
PC 1 (82% variance)
PC 2 (12% variance)

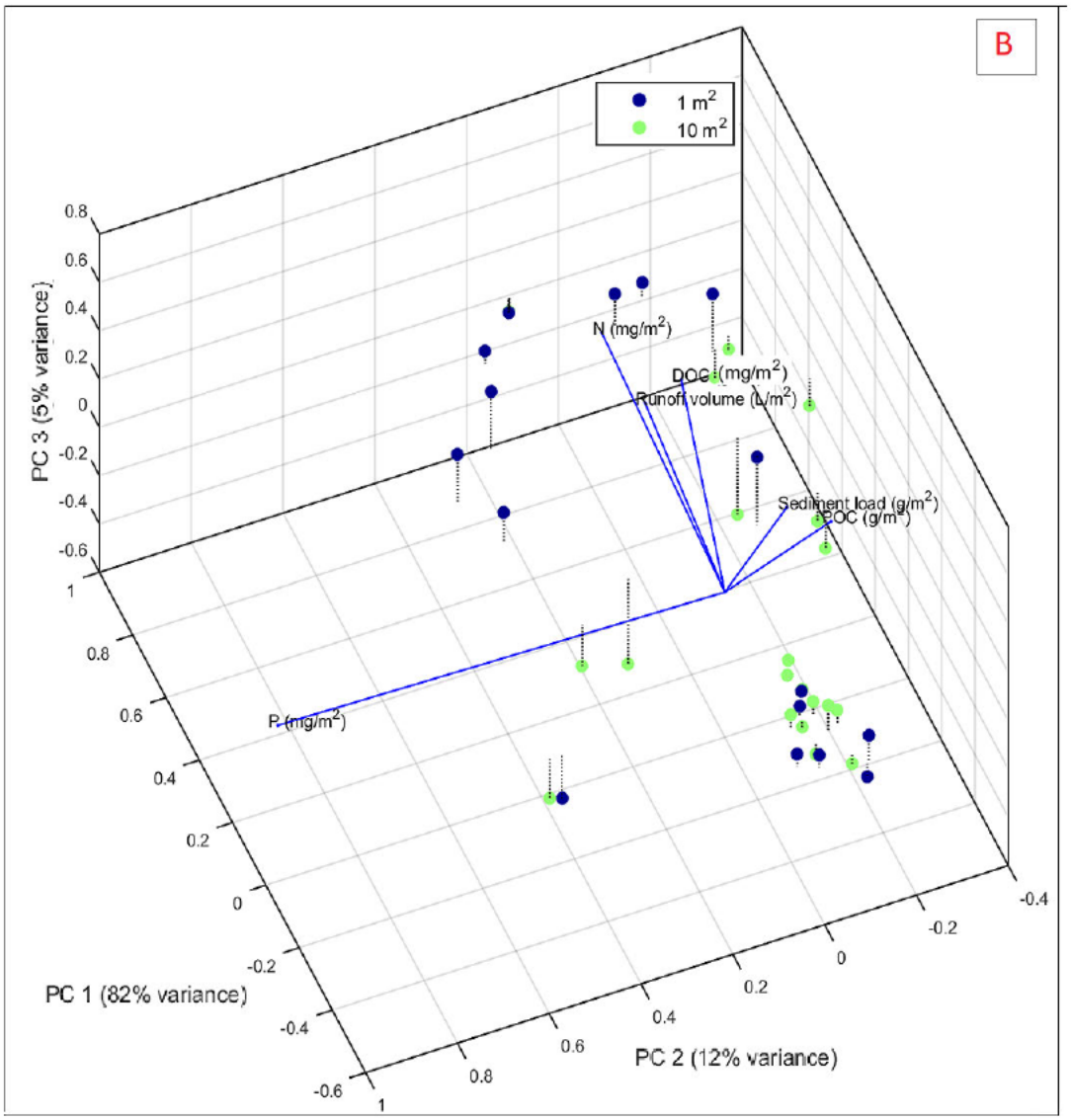

Figure 4.16: PCA biplot showing the first 3 principal components for slope (A) and plot size (B) of the mulch treatment. PC scores, which represent original observations plotted in PC space, are represented by coloured markers. PC loading weights for each original variable are indicated by the blue arrows.

The mulch treatment exhibited correlations of varying strengths between the measured variables (*Figure 4.17*). Sediment load was strongly positively correlated to DOC (0.75) and POC loss (0.92), and moderately positively correlated to nitrogen loss (correlation coefficient = 0.65). POC loss had a strong positive correlation with DOC loss (0.8), and a moderate positive correlation with nitrogen loss (0.59). There were positive correlations varying in strength observed between runoff volume

and rainfall depth (0.56), DOC loss (0.79), POC loss (0.77), rainfall intensity (0.56), sediment load (0.9), and nitrogen loss (0.84). Nitrogen loss was moderately positively correlated to rainfall intensity (0.53), POC loss (0.56), phosphorous loss (0.56), and strongly positively correlated to DOC loss (0.86). Sediment load was moderately positively correlated with nitrogen loss (0.65) and strongly positively correlated to DOC loss (0.75) and POC loss (0.92). POC loss had a positive strong correlation with DOC loss (0.77). LAI had a moderate positive correlation with rainfall depth (0.66), and a weak positive correlation with phosphorous loss (0.13), POC loss (0.14), and DOC loss (0.13). Furthermore, phosphorous loss was weakly correlated to rainfall depth (0.18).

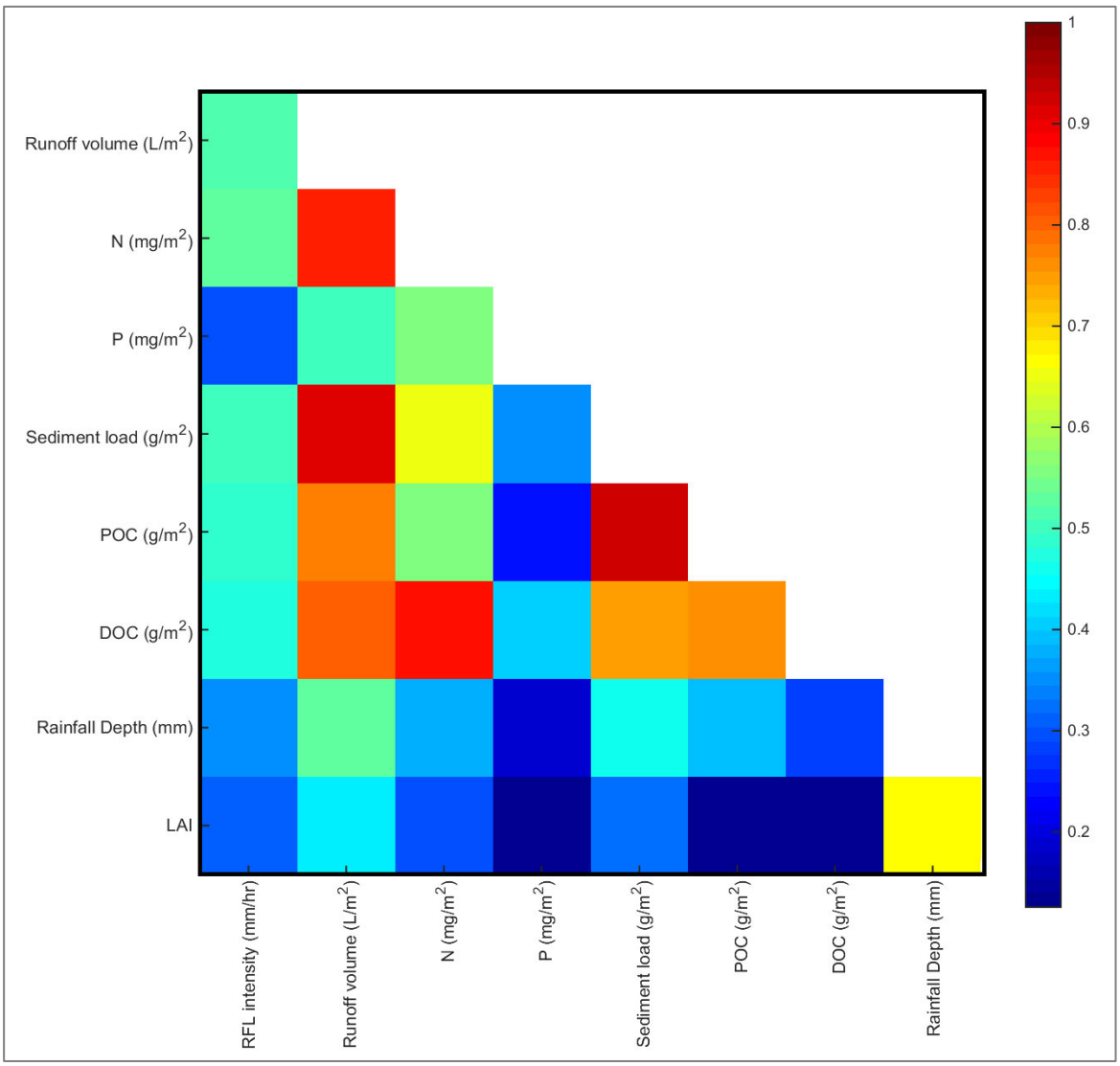

Figure 4.17: Correlation heat map of observed variables on the mulch treatment.

4.4 Arc-SWAT Simulation

4.4.1 Runoff

The median runoff volume of the simulated data (0.48 m^3 ha^{-1}) was statistically similar to the observed (22.66 m^3 ha^{-1}) runoff volume on the CBT (*Figure 4.18*). The observed runoff volume was more variable than the simulated, and produced an extreme value, where the simulated data did not. The simulated data was skewed towards zero, as many zero values were simulated, and fewer large values.

The median runoff volume of the observed data (28.01 m^3 ha^{-1}) was statistically greater than the simulated (0.39 m^3 ha^{-1}) runoff volume on the HBT (*Figure 4.18*). The simulated runoff volume was more variable than the observed; however, no extreme values were produced, while the observed witnessed several extreme runoff volume values. The simulated data was skewed towards zero, producing many values of zero than the observed data, and fewer large values.

The median runoff volume of the observed data (9.01 m^3 ha^{-1}) was statistically similar to the simulated (0.48 m^3 ha^{-1}) runoff volume on the mulch treatment (*Figure 4.18*). The simulated runoff volume was more variable than the observed; however, no extreme values were produced, while the observed witnessed several extreme runoff volume values. The simulated data was skewed towards zero and contained a moderate proportion of larger values.

Each of the simulated treatments had a similar degree of variation. The CBT witnessed an under-simulation of the high and low runoff volume values, while the HBT and mulch treatment witnessed an under-simulation of the low values, and an over-simulation of the high values. None of the simulated treatments produced extreme values as seen in the observed data.

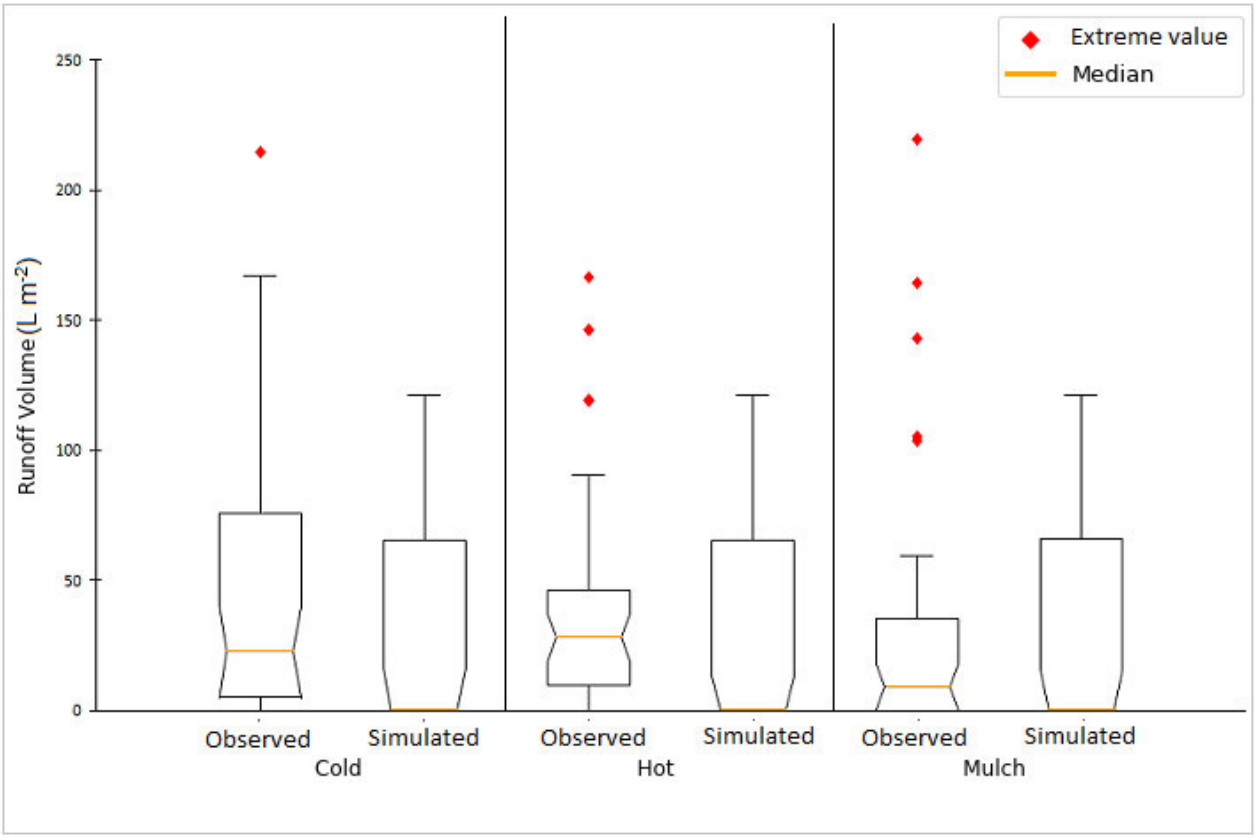

505 *Figure 4.18: Notched Box and whisker plot representing the simulated versus the observed runoff volume data on the "Cold" burn, "Hot" burn, and "Mulch" treatments.*

4.4.2 Sediment load

510 The CBT witnessed a statistically similar median sediment load produced by the simulation (0.03 kg ha^{-1}) to the observed (0.13 kg ha^{-1}) (*Figure 4.19*). The simulated sediment load had a greater variation than the observed and generated extreme values which were greater in magnitude and quantity than the observed. The simulated data had many zero values, and fewer large and extreme sediment load values.

515 The HBT produced a statistically similar simulated (0.03 kg ha^{-1}) median sediment load as the observed (0.10 kg ha^{-1}) (*Figure 4.19*). The simulated sediment load had a greater variability than the observed, with a larger number of extreme values as the observed and at greater magnitudes. The simulated data had many zero values, and many large and extreme sediment load values.

The mulch treatment produced a statistically similar simulated (0.03 kg ha^{-1}) median sediment load as the observed (0.03 kg ha^{-1}) (*Figure 4.19*). The simulated sediment load had a greater variability than the observed, with the same number of extreme values as the observed, but at greater magnitudes. The simulated data generated many zero values, and fewer large nitrogen loss values.

The simulated mulch treatment had the largest variation and nitrogen loss, while the CBT had the lowest. The HBT simulation produced the greatest number of extreme values of all treatments, while the simulated mulch generated the lowest. The mulch treatment was the only treatment to have the same number of simulated and observed extreme sediment load values, with the other two treatments simulating a greater number of extreme values. The model under-simulated the low sediment load values and over-simulated the large and extreme values on all treatments.

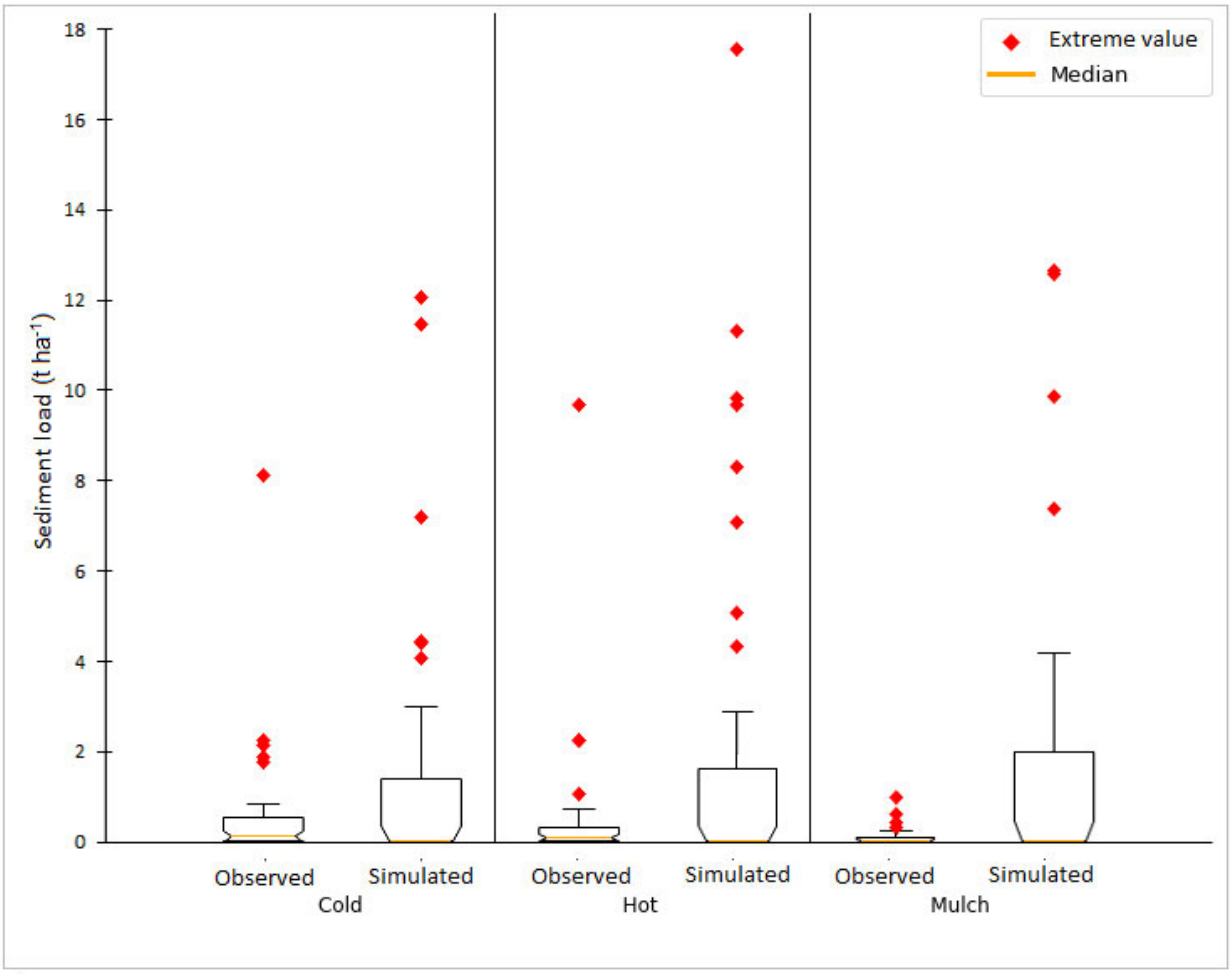

Figure 4.19: Notched Box and whisker plot representing the simulated versus the observed sediment load data on the "Cold" burn, "Hot" burn, and "Mulch" treatments.

4.4.3 Phosphorous loss

The CBT witnessed a statistically similar median phosphorous loss produced by the simulation (0.004 kg ha^{-1}) to the observed (0.002 kg ha^{-1}) (*Figure 4.20*). The simulated data had a larger variation of phosphorous loss with fewer extreme values, and a many low phosphorous loss values and fewer high values.

The HBT had a statistically similar median phosphorous loss produced by the simulation (0.004 kg ha^{-1}) to the observed (0.002 kg ha^{-1}) (*Figure 4.20*). There was a larger variation of phosphorous loss produced by the simulated data than the observed. The simulated data had more extreme values than the observed data, and many low phosphorous loss values and many high values.

The mulch treatment witnessed a statistically similar median phosphorous loss produced by the simulation (0.005 kg ha^{-1}) to the observed (0.001 kg ha^{-1}) (*Figure 4.20*). The simulated data had a greater variation of phosphorous loss with fewer extreme values, and a many low phosphorous loss values and a moderate number of high values.

The simulated mulch treatment had the largest variation of phosphorous loss, and the CBT had the lowest. The simulated HBT produced the most extreme values and was the only treatment to witness more extreme values than the observed data. The model under-simulated the low phosphorous loss values and over-simulated the high values on all treatments.

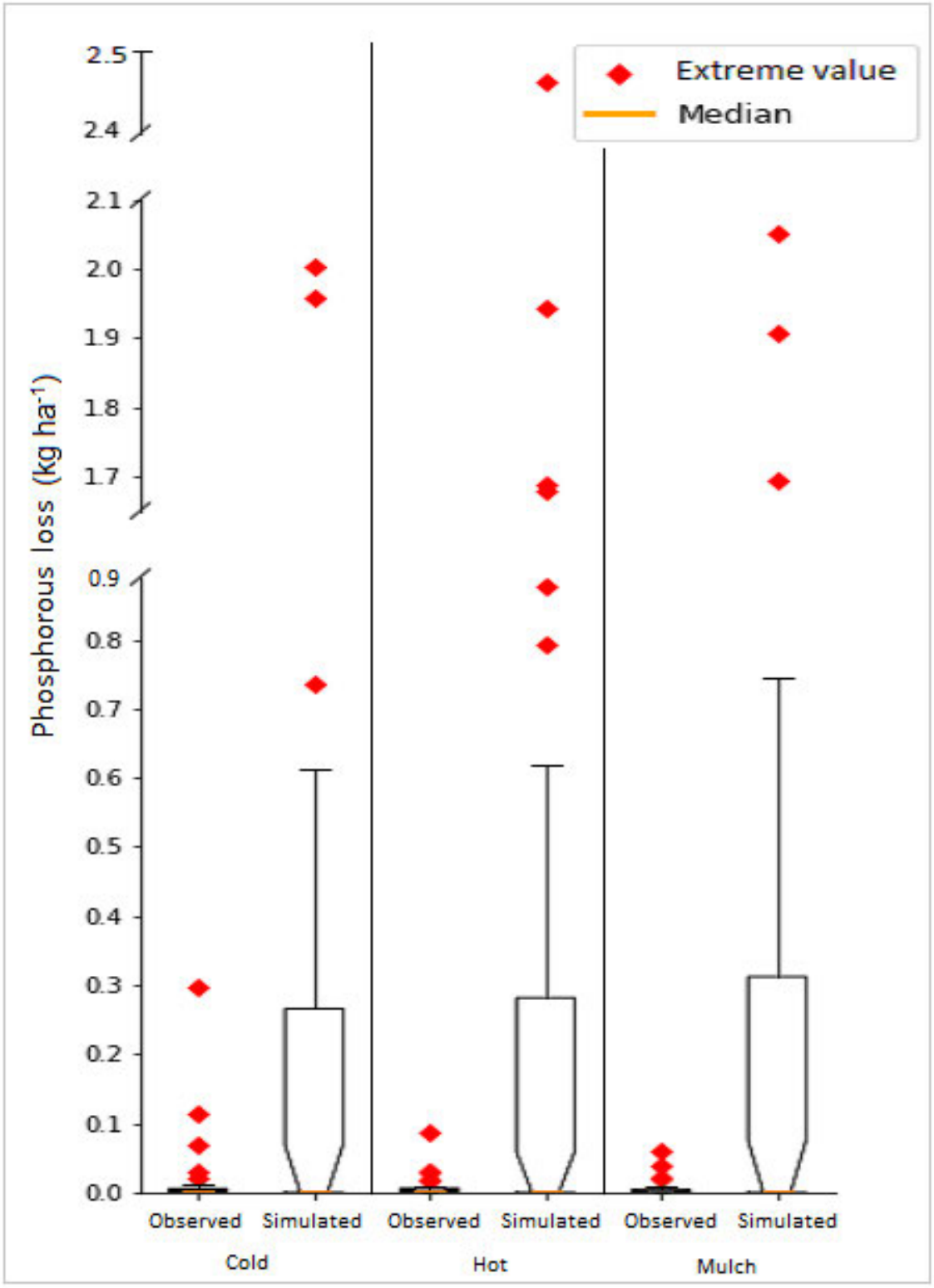

Figure 4.20: Notched Box and whisker plot representing the simulated versus the observed phosphorous loss data on the "Cold" burn, "Hot" burn, and "Mulch" treatments.

4.4.4 Nitrogen loss

The CBT produced a median simulated (0.035 kg ha^{-1}) nitrogen loss which was statistically similar to the observed (0.31 kg ha^{-1}) (*Figure 4.21*). The simulated nitrogen loss had a greater variation of values and produced extreme values which were greater in magnitude and quantity than the observed. The simulated data had many zero values, and a moderate number of large nitrogen loss values.

The HBT generated a simulated (0.036 kg ha^{-1}) median nitrogen loss which was statistically similar to the observed (0.35 kg ha^{-1}) (*Figure 4.21*). The simulated nitrogen loss had a greater variation than the observed and generated extreme values which were greater in magnitude and quantity than the observed. The simulated nitrogen loss consisted of many zero values, and a moderate number of large and extreme values.

The mulch treatment produced a simulated (0.039 kg ha^{-1}) median nitrogen loss which was statistically similar to the observed (0.13 kg ha^{-1}) (*Figure 4.21*). The simulated nitrogen loss was more variable than the observed and had the same number of extreme values as the observed, but at greater magnitudes. The simulated data had many zero values, and a moderate number of large nitrogen loss values.

The simulated mulch treatment had the largest variation in nitrogen loss, while the CBT had the lowest. The simulated HBT generated the greatest number of extreme values of all treatments, while the simulated mulch and CBT generated the same number of extreme values. The mulch treatment was the only treatment to have the same number of simulated and observed extreme nitrogen loss values, with the other two treatments simulating a greater number of extreme values. The model under-simulated the low nitrogen loss values and over-simulated the large and extreme values on all treatments.

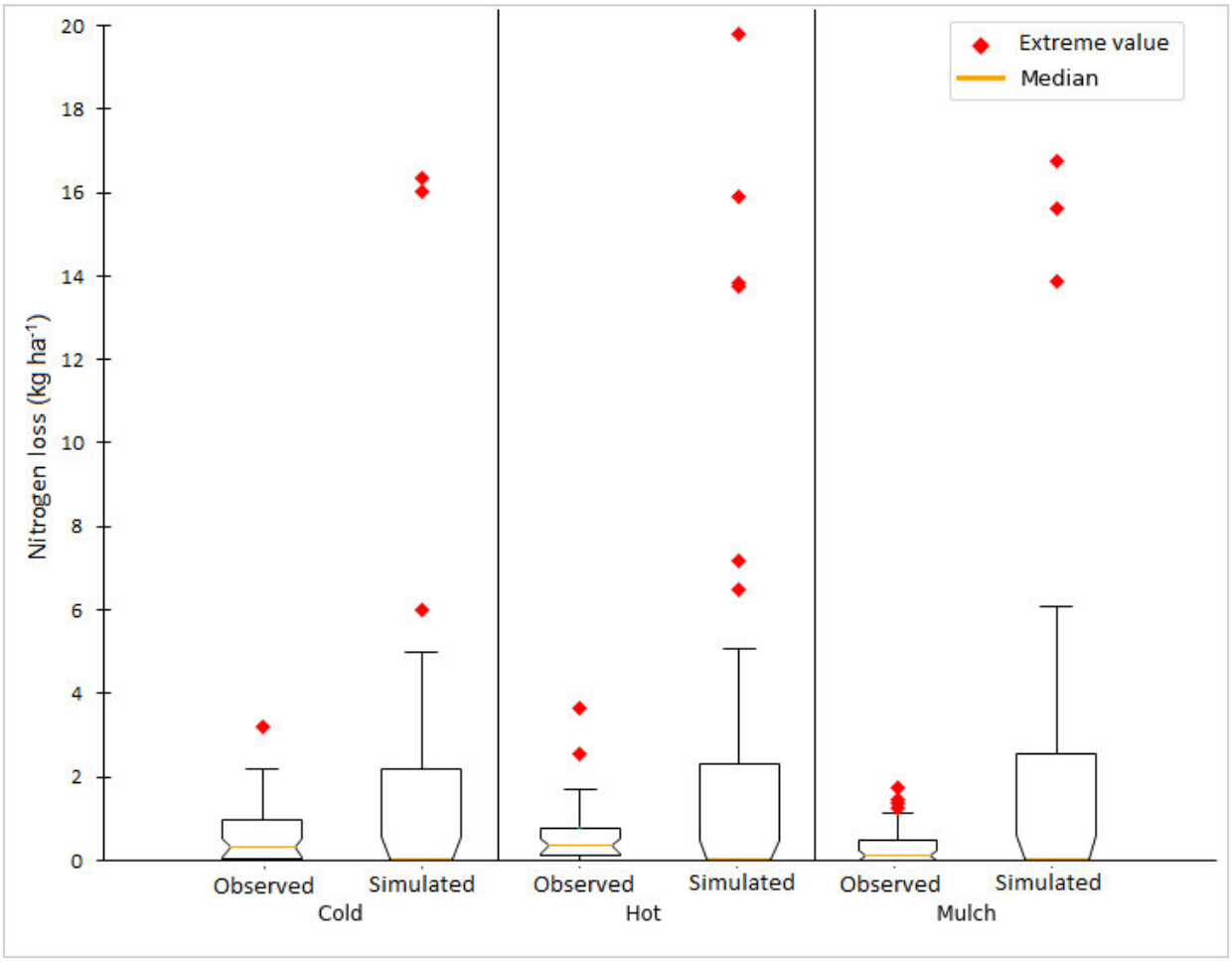

Figure 4.21: Notched Box and whisker plot representing the simulated versus the observed nitrogen loss data on the "Cold" burn, "Hot" burn, and "Mulch" treatments.

4.5 Conclusions

The study site had consistent soil properties, ranging from soil chemical properties to soil water repellency. Although, there was varying soil type, slopes, and concentrations of soil potassium these attributes were not widespread and were only found on a few of the data capturing sites. There was no interception loss measured, indicated by the manual rain gauges in the plantation having no statistical difference to the readings of the AWS.

The measured variables, excluding nitrogen and DOC loss, shared a similar trend, whereby the mulch treatment generated the least runoff and erosion on both the micro-runoff and runoff plots,

while the CBT generated the greatest runoff and erosion on the 1 m^2 micro-runoff plots, and the HBT generated the most on the 10 m^2 runoff plots. Nitrogen and DOC loss share the same trend, whereby the mulch treatment generated the greatest nutrient loss of all treatments on the micro-runoff plots, while the HBT generated the least on these plots. On the runoff plots, the CBT witnessed the greatest nitrogen and DOC loss of all treatments, while the mulch treatment produced the lowest. The high runoff and erosion values of all treatments were driven by a select few rainfall events which shared attributes of being high intensity and having a shorter duration since the previous event. Phosphorous loss, however, differs in that the high values favoured events of high rainfall depths.

On the CBT, runoff volume shared a positive moderate (0.35 – 0.7 CC) to strong (0.71 – 1 CC) correlation with a number of variables, namely DOC loss, POC loss, nitrogen loss, and sediment load. Sediment load was strongly correlated to POC loss and DOC loss. While POC loss had a strong positive correlation with DOC loss. These correlations demonstrated that the primary driver of erosion of the aforementioned variables was runoff volume which was driven by rainfall intensity followed by rainfall depth. Runoff volume drove the generation of sediment load, resulting in a loss of POC, which was accompanied by DOC loss. However, phosphorous loss was primarily driven by rainfall depth. The CBT displayed an early peak discharge regarding the runoff hydrograph with a steep rising limb, and an extended recession limb; however, runoff was only produced on the steep slope of the observed event depicted in the hydrograph. Slope class was influential in the generation of runoff and erosion on the CBT. The SWAT model under-simulated runoff volume; however, there was a significant over-simulation of phosphorus loss, nitrogen loss and sediment load.

On the HBT runoff volume shared a positive moderate (0.35 – 0.7 CC) to strong (0.71 – 1 CC) correlation with DOC loss, POC loss, nitrogen loss, and sediment load. While sediment load was strongly positively correlated to DOC and POC loss. While DOC loss was positively correlated with POC loss. These interconnected correlations suggest that the primary driver of the loss of these variables from the soil via erosion was runoff volume (which was driven by rainfall depth and intensity). This led to the generation of sediment load, resulting in a loss of POC, which was accompanied by DOC loss. Phosphorous loss was driven by rainfall depth and not runoff volume, indicated by their moderate positive correlation, and phosphorous' weak positive correlation (0 – 0.34 CC) with all other variables. The HBT witnessed a large peak discharge, and a steep rising

limb of the hydrograph on both slopes. Slope was influential in the production of runoff and erosion on the HBT. This was the only treatment to produce runoff hydrographs on both slopes. The SWAT model over-simulated runoff volume on the HBT, while over-simulating phosphorus, nitrogen and sediment loss.

Runoff volume on the mulch treatment had a strong positive correlation (0.71 – 1 CC) with DOC loss, POC loss, nitrogen loss, and sediment load. Sediment load was strongly positively correlated to POC and DOC loss. POC and DOC loss shared a strong positive correlation with each other. These interconnected correlations demonstrated that the primary driver of erosion was runoff volume, which was driven by rainfall depth and intensity. Runoff volume drove the generation of sediment load, resulting in a loss of POC, which was accompanied by DOC loss. The mulch treatment led to a reduction in runoff generation as seen by a delayed and reduced peak discharge on the runoff hydrograph of the steep slope; however, runoff was not generated on the gentle slope of the graphed event. Slope was influential in the production of runoff and erosion on the mulch treatment. The SWAT model over-simulated runoff volume, phosphorous loss, nitrogen loss, and sediment load on the mulch treatment.

The results demonstrated the mulch treatments ability to generate the lowest runoff and erosion, despite the isolated increases in DOC and nitrogen loss on the micro-runoff plots, while the burn treatments exacerbated soil erosion. The different burn treatments generated greater soil erosion and runoff at different scales, where the HBT was the primary contributor to soil erosion at the runoff plot scale, and the CBT was the primary contributor at the micro-runoff plot scale. However, these trends differ for DOC and nitrogen loss, where the HBT produced less erosion on both the micro-runoff and runoff plot scale compared to the CBT. The varied response of runoff and soil erosion in these results illustrated the effect that different burning regimes have on natural soil erosion processes, compared to that of a mulch treatment.

Chapter Five

Discussion

5.1 Introduction

It is critical that commercial forestry utilize management practices which are conducive to soil conservation, due to the potential of commercial plantations to exacerbate soil erosion coupled with their global coverage and annual growth (Blackburn *et al.*, 1986; Jewitt, 2005; Geißler *et al.*, 2012). The well-used site preparation technique of burning has the potential to reduce soil infiltrability, promoting runoff and exacerbating erosion (Neary *et al.*, 1999; Martin and Moody, 2001). The focus of this research was on different available site preparation techniques and their potential to accelerate natural soil erosion, having *in situ* and *ex situ* consequences, or to protect against soil erosion and land degradation, and the SWAT model's ability to simulate these interactions.

This chapter provides a detailed discussion of how the measured variables interacted with each treatment and offers insights as to the reasoning behind these processes, integrating recent literature, and determining what it means for commercial plantation management. Precipitation patterns throughout the study and interception loss on the study site are presented in the section 'Rainfall'. The individual variables affected by soil erosion at its different operational spatial scales (i.e. rain splash & rill erosion) are discussed in relation to each treatment type and the different scalar erosion processes acting upon them are provided in the section entitled 'Treatments'. The outputs of the SWAT model in relation to the observed results will be discussed in 'SWAT Simulated Runoff and Erosion'. An inter-treatment comparison of the dominant erosion processes and the ability of each treatment to either accelerate or curb runoff generation and soil erosion is provided in the section 'Synthesis'.

5.2 Rainfall

Total observed rainfall was less than the MAP of the region (659 to 1139 mm) (Clulow *et al.*, 2011); however, the investigation took place over six months, encapsulating most of the summer rainfall season. The remaining six months contained the end of the rainfall season leading into the drier winter months. Rainfall continued to occur during the dry months and thus the MAP of the year of investigation was likely to fall into the normal range for the region.

The spatial variation of rainfall across the study site was negligible, with all treatments and the AWS producing statistically similar rainfall measurements for all individual events measured. The similarities of the treatments to the AWS values were indicative of the absence of interception loss due to the young age and growth form of the newly planted *Eucalyptus dunnii* stand. These characteristics continued into the late rainfall season where, despite an increase in the LAI at the research site, no interception loss was observed. This demonstrated that canopy does not close in the first year of growth, which leaves the rain gauges (and soil) uncovered. This suggested that interception loss within the first year of growth of the *Eucalyptus dunnii* stand was low, offering marginal reductions to the kinetic energy of raindrops through the provision of little protective cover (Pimentel *et al*., 1995).

5.3 Treatments

No statistically significant differences were found for most of the soil characteristics and it was concluded that the soil properties of the study site were predominantly uniform. This implied that soil erodibility at each treatment was comparable (Lal, 2001; Buttafuoco *et al.*, 2012). The only soil property which was significantly different was the potassium concentrations across the CBT. The CBT and mulch treatments consisted of clay and clay loam soils, while the HBT consisted of clay loam soils. The small degree of variability was not observed to skew the generation of runoff on the mulch and CBT. These instances of dissimilitude of soil characteristics between treatments is to be expected in field studies, as the spatial variation of soils is natural, and demonstrates the reliability of the results of this research over a lab-based experiment. Soil properties were assumed to be constant over the study period, and thus the analysis of soil properties was only conducted

upon the commencement of the research, and not throughout, nor were soil infiltration rate tests or cost/benefit analyses conducted, limiting land-use management guidance. However, Soil water repellency was regularly measured, and was unaffected by treatment types, remaining uniform throughout the study. There was a high degree of water repellency, which has been noted as a frequent occurrence on *Eucalyptus* plantations in South Africa (Scott, 2000). The slope characteristics of each treatment shared similar trends, whereby the gentle and steep slopes were uniform in gradient across treatments. The exception was the steep slope of the CBT, which was significantly steeper than the HBT by 7 % and the mulch treatment by 6.3 %.

5.3.1 Cold burn treatment

The CBT demonstrated a susceptibility to splash erosion over rill erosion for several variables, namely, runoff volume, sediment load, phosphorous loss and POC loss. This susceptibility to splash erosion was attributed to the cold burn leaving burnt and unburnt debris littered across the treatment area (Chapter 3.2 Study Site, *Plate 3.2 A*), exposing a significant area of the soils to raindrop impact, leading to a breakdown of soil aggregates, sealing of soil pores, reducing infiltrability, increasing the potential for runoff and erosion (Morin and Benyamini, 1977; Podwojewski *et al.*, 2011). The large sparsely situated debris on the treatment aided in reducing runoff velocity by increasing the friction on runoff, slowing the velocity and allowing more time for infiltration to occur, resulting in less runoff generation on the runoff plots and thus less rill erosion of the aforementioned variables (Podwojewski *et al*., 2011).

The CBT was vulnerable to DOC and nitrogen loss via rill erosion, demonstrated by the elevated loss of these variables on the runoff plots. This was the result of the unburnt debris decomposing and depositing additional nitrogen and carbon into the soils, coupled with the high degree of observed runoff and sediment yield on these plots removing the recently deposited and pre-existing DOC and nitrogen (Youkhana and Idol, 2009). The decomposition of the unburnt debris released nitrogen and organic carbon, which resided on the debris and in the surrounding soils which was transported via overland flow and rill erosion (Youkhana and Idol, 2009). The runoff plots on the CBT producing higher levels of nitrogen and DOC loss than the micro-runoff plots was attributed to the previously discussed greater volume of runoff coming into contact with the debris for a longer

duration due to the increased friction to overland flow (Youkhana and Idol, 2009). The longer contact time with the debris allowed for a greater amount of nitrogen and DOC to dissolve into the runoff and be transported downslope.

The CBT was strongly influenced by slope steepness, as indicated by the runoff hydrographs (Chapter 4.3.8 Treatment summary, *Figure 4.11 A*). The steeper slope of the CBT produced a large quantity of runoff volume, while the gentle slope was unresponsive to the rainfall event. The increased runoff was a result of the steeper slope upon which the runoff volume was measured (Ziadat and Taimeh, 2013). The increased runoff, coupled with the increased rainfall erosivity due to the increased slope angle, resulted in increased soil erosion on the steeper slopes (Obi and Salako, 1995; Le Bissonnais *et al.*, 1998). This was illustrated in the positive relationships depicted by the PCA (Chapter 4.3.8 Treatment summary *Figure 4.12*) between steep slopes and the generation of soil loss and runoff, indicating that on the CBT, steeper slopes were more inclined to produced runoff and soil erosion than the gentle slopes (Obi and Salako, 1995; Le Bissonnais *et al.*, 1998). In addition, the PCA demonstrated that the micro-runoff and runoff plots were both prone to runoff and soil erosion on the CBT, and this treatment was not dominated by a single erosion process.

The correlation heat map (Chapter 4.3.8 Treatment summary *Figure 4.13*) indicated that on the CBT, runoff volume was primarily driven by rainfall intensity, and then rainfall depth, which led to erosion and the removal of soil nitrogen and sediment load (Carpenter *et al.*, 1998; Le Bissonnais *et al.*, 1998). The runoff and sediment load eroded from the soil transported with it POC and DOC. Phosphorous loss was driven by rainfall depth followed by rainfall volume, and shared no link to sediment load, which was demonstrated by the high phosphorous loss values observed due to splash erosion, yet lower sediment loss values resulting from splash erosion. The strong positive association observed between LAI and rainfall depth was the result of increasing rainfall depths later into the rain season, supplying the stand with additional plant available water, facilitating plant growth, increasing LAI.

5.3.2 Hot burn treatment

The HBT was more vulnerable to rill erosion than splash erosion for all the measured variables, demonstrated by the increased runoff and soil erosion on the runoff plots compared to the micro-

runoff plots. The resistance to splash erosion on the HBT was attributed to the hot burn producing a fine ash across the treatment site (Chapter 3.2 Study Site, *Plate 3.2 B*), which behaved as a thin mulch, covering the soil and effectively dissipating raindrop kinetic energy, reducing runoff velocity and erosion, and promoting infiltration (Podwojewski *et al*., 2011), agreeing with the findings of Bautista et al. (1996) and Prats et al. (2012). The fine ash layer was not as effective in reducing overland flow which had the potential to remove most of the ash, leaving large soil pores blocked by remaining fine ash, and exposing the bare soils to raindrop impact, which sealed the pores and destroys soil aggregates, all of which reduced the infiltrability of the soils (Morin and Benyamini, 1977; Martin and Moody, 2001). An early flush event was observed on 14/12/2019, which was the first rainfall event of the season with a high rainfall intensity and depth (Chapter 4.2.1 Precipitation, *Figure 4.2*), producing high runoff values (Chapter 4.3.2 Runoff volume, *Figure 4.5*), flushing the fine ash layer from the soil of the runoff plots, generating a significant spike in observed sediment load due to rill erosion, which was predominantly comprised of ash that had been removed from the soil surface. The micro-runoff plots generated less than half the sediment load (107.16 g m^{-2}) during this flush event than observed on the runoff plots (225.71 g m^{-2}) (Chapter 4.3.3 Sediment load, *Figure 4.6*), resulting in ash remaining on the micro-plots continuing to protect the soil from splash erosion, where the runoff plots were left exposed to rill erosion.

The runoff hydrographs (Chapter 4.3.8 Treatment summary, *Figure 4.11 B*) produced on the HBT demonstrated the treatments vulnerability to rill erosion. The runoff hydrograph showed that the steeper slope reached its peak discharge of overland flow earlier than the gentle slope; however, the gentle slope witnessed a peak discharge of the same magnitude and produced runoff for a similar duration. This demonstrated the susceptibility of the HBT to generate overland flow regardless of slope, resulting in wide-spread rill erosion (Le Bissonnais *et al.*, 1998). This behavior was observed in the PCA (Chapter 4.3.8 Treatment summary *Figure 4.14*) of the HBT, whereby the slope class produced no observable difference on the generation of runoff and erosion; however, there was a stronger positive association between the 10 m^2 plots and generated runoff and erosion, than the 1 m^2 plots. This relationship demonstrated the propensity of the HBT to generate overland flow and its increased vulnerability to rill erosion over splash erosion (Le Bissonnais *et al*., 1998; Cantón *et al.,* 2011; Chaplot and Poesen, 2012).

The correlation heat map (Chapter 4.3.8 Treatment summary *Figure 4.15*) of the HBT illustrated that the primary driver of runoff volume on this treatment was rainfall depth, while rainfall intensity was a secondary driver. Runoff volume was the primary driver of nitrogen loss, sediment load and DOC loss (Carpenter *et al*., 1998; Le Bissonnais *et al*., 1998). The runoff volume and sediment load drove POC and DOC loss, as indicated by the strong positive associations of DOC and POC loss with runoff volume and sediment load. Phosphorous loss was driven by rainfall depth and, despite no associations of phosphorous loss with other variables, the high levels of phosphorous loss observed on this treatment was attributed to the high burn severity, agreeing with the findings of Saá et al. (1994). Similar to the CBT, the strong positive association observed between LAI and rainfall depth was due to increasing rainfall depths over time, providing the stand with increased plant available water, facilitating plant growth and increasing LAI.

5.3.3 Mulch treatment

The mulch treatment exhibited a greater vulnerability to splash erosion over rill erosion for all measured variables. This trend was the result of the plot sizes, whereby the shorter plot lengths of the micro-runoff plots rendered the mulch less effective than that of the larger runoff plots, resulting in increased runoff and erosion observed on the micro-runoff plots, agreeing with the findings of Smets et al. (2008). The ability of the mulch treatment to reduce runoff and subsequent erosion was observed in the small peak discharge observed in the hydrograph, the short duration of the runoff event, and the lack of runoff produced on the gentle slope (Chapter 4.3.8 Treatment summary, *Figure 4.11 C*) (Le Bissonnais *et al.*, 1998; Ziadat and Taimeh, 2013). This behavior was observed in the outputs of the PCA (Chapter 4.3.8 Treatment summary *Figure 4.16*), whereby the steep slope was prone to the generation of runoff and soil erosion, and the gentle slope witnessed a reduction in the generation of runoff and soil erosion (Ziadat and Taimeh, 2013). Similarly, the micro-runoff plots had a stronger positive association with runoff and erosion (nitrogen and DOC loss in particular) than the runoff plots, demonstrating the reduced effectiveness of the mulch when measured on smaller plot sizes (Smets *et al.*, (2008). However, the mulch treatment provided an effective soil cover (Chapter 3.2 Study Site, *Plate 3.2 C*) dissipating the erosive energy of water on

the treatment, reducing runoff and soil erosion (Lal, 2001; Mohammad and Adam, 2010; Prats *et al*., 2012).

The correlation heat map (Chapter 4.3.8 Treatment summary *Figure 4.17*) of the mulch treatment indicated that the runoff volume was primarily driven by rainfall depth and rainfall intensity. Runoff volume was the primary driver of sediment load, DOC, POC, and nitrogen loss (Carpenter *et al*., 1998; Le Bissonnais *et al*., 1998). The strong positive association between DOC and nitrogen loss, and both of these variables with runoff volume was attributed to the decaying mulch which released both these nutrients onto the debris and into the soils, allowing for their transportation downslope via runoff (Youkhana and Idol, 2009). Sediment load was the driver of POC and DOC loss. Similar to the other treatments, the strong positive association observed between LAI and rainfall depth was due to rising rainfall depths as the rain season progressed supplying more plant available water, encouraging plant growth and increasing LAI.

5.4 SWAT Simulated Runoff and Erosion

The simulated runoff generated by the SWAT model was unable to capture the differences in observed runoff between each treatment. This was shown by the simulated runoff of each treatment being nearly identical, while the observed runoff was notably different between treatments. The under-simulated runoff of the CBT agrees with the findings of Scott-Shaw et al. (2020), who observed that the SWAT model under-simulated streamflow, requiring calibration to better simulate the observed streamflow. These findings suggested that the SWAT-simulated runoff in this study required calibration, like that of Scott-Shaw et al. (2020). Runoff on the HBT and mulch treatment were both over-simulated, with identical simulated values, while being under-simulated on the CBT, displaying the model's inability to differentiate the volume of runoff generated on each land management type.

The SWAT model over-simulated sediment load, nitrogen and phosphorous loss, across all treatments, with the CBT and HBT having similar values, while the highest values were simulated on the mulch treatment. These simulations did not follow the trends of the observed data where the mulch treatment generated the lowest sediment and nutrient loss, suggesting the model's inability to simulate the effects of mulch on sediment and nutrient loss. The over-simulations of sediment

and nutrient loss were several orders of magnitude greater than the over-simulated runoff (in the case of the mulch and HBT), indicating that the erosion process within the model had a sensitivity to runoff which was not observed in nature. This sensitivity was particularly apparent on the CBT, which under-simulated runoff volume, yet over-estimated soil and nutrient loss to the same degree as the HBT.

Phosphorous loss had the highest over-simulation, followed by sediment load, with nitrogen loss having the lowest degree of over-simulation. This suggested that within the model, phosphorous loss had the highest sensitivity to runoff, while nitrogen loss had the lowest. These over-simulations were likely due to the land-use management tools within the model not being refined, or inaccurate land-use management input variables, which resulted in unrealistic simulations at the catchment scale. These findings suggested that the SWAT-simulated sediment and nutrient loss in this study also required calibration.

Modelling has been proven to be a beneficial spatial tool for land-use management and the SWAT model is effective at simulating streamflow and sediment yield under certain land-use management practices (Oeurng *et al.,* 2011; Scott-Shaw *et al.,* 2020). However, the model was unable to accurately simulate runoff and erosion on the assessed land-use treatments without calibration, providing valuable insight on the limitations of the model and consequently demonstrating that without calibration the model outputs are not realistic, rendering the model ineffective. Moreover, the model did not only over-simulate the measured variables, it was also unable to capture the observed trends in relation to each treatment (e.g. the mulch treatment had the lowest observed nitrogen loss, but the greatest simulated nitrogen loss), making the uncalibrated model ineffective with regards to advising management decisions. It is possible that this poor correlation between observed and simulated data is the result of USA-specific constants hardwired into the model due to its location of development, which are affecting the outputs for each modelled treatment (Oeurng *et al.,* 2011). However, the model is gaining traction in South Africa, and has been used to produce accurate simulations for other land-use types (Govender and Everson, 2005; Gyamfi *et al.,* 2016; Scott-Shaw *et al.,* 2020). Importantly, there is a necessity to set up SA-specific defaults for land-use types, ensuring that they are better representing within the model, which is what the results of this thesis will facilitate. Furthermore, it is recommended that the land management tools within the SWAT model be refined to improve the model's ability to capture natural runoff and soil

erosion on a wider range of land-use treatments, with particular regards to different tree species and commercial forestry site preparation techniques.

5.5 Synthesis

There were observable trends across treatments with regards to the treatment with the lowest, medial and highest measured runoff and erosion on each plot size. Runoff volume, sediment yield, phosphorous and POC loss followed a similar pattern, whereby the 1 m^2 plots (splash erosion) of the CBT produced the most of all treatments and the mulch treatment produced the least. On the 10 m^2 plots (rill erosion), the HBT produced the most runoff and erosion, while the mulch treatment produced the least, with regards to the above-mentioned variables. The HBT producing less runoff and erosion of the aforementioned variables, than the CBT on the 1 m^2 plots, was attributed to the fine ash layer on the HBT that protected the soil against splash erosion, where the sparsely littered debris on the CBT was not conducive to reducing splash erosion (Podwojewski *et al*., 2011). The fine ash layer residing on the micro-runoff plots of the HBT protected against soil erosion, maintaining soil nutrients for emerging plants, encouraging plant growth, leading to an increase in the soil cover (*Plate A-5* Appendix A), further reducing splash erosion (Blackburn *et al*., 1986; Podwojewski *et al*., 2011). The HBT generated the most runoff and erosion of the above-mentioned variables on the 10 m^2 plots which can be attributed to the flushing of the fine ash layer, which left the soil exposed to rill erosion, while the CBT had more coarse debris littered throughout, which helped resist overland flow, promoting soil infiltration, reducing runoff and thus erosion (Le Bissonnais *et al.*, 1998). The mulch treatment generating the lowest runoff, splash and rill erosion attributed to the mulch providing a protective soil layer which did not disrupt the natural erosion process (Bautista *et al*., 1996; Prats *et al*., 2012: Robichaud *et al*., 2013).

Nitrogen and DOC loss shared the same trend in terms of the treatment with the lowest, medial and highest measured values on each plot size. The 1 m^2 plots of the mulch treatment generated the most nitrogen and DOC loss of all treatments, with the HBT producing the least. The high DOC and nitrogen loss due to splash erosion on the mulch treatment was attributed to the decomposition of the mulch, releasing DOC and nitrogen into the soils, coupled with a reduction in the effectiveness of the mulch to reduce runoff and erosion on the smaller 1 m^2 plots, resulting in high

levels of nutrient loss (Smets *et al.*, 2008; Youkhana and Idol, 2009). The HBT generating the least nitrogen and DOC loss via splash erosion was attributed to the discussed soil cover provided by the fine ash and plant cover, protecting against splash erosion (*Plate A-5* Appendix A) (Blackburn *et al*., 1986; Podwojewski *et al*., 2011). The CBT generated the highest levels of nitrogen and DOC loss on the 10 m^2 plots, while the mulch treatment generated the least. The increased effectiveness of the mulch to reduce erosion at larger scales was evident on the 10 m^2 plots, where despite nitrogen and DOC loading in the soils due to decomposing mulch, the mulch was effective at protecting nutrient rich soils from erosion compared to the other treatments (Smets *et al.*, 2008; Youkhana and Idol, 2009). The CBT generating the most nitrogen and DOC loss on the 10 m^2 plots and the second most on the 1 m^2 plots was attributed to the previously discussed decomposition of the unburnt debris, which was transported by splash and rill erosion coupled with the large amounts of sediment loss, contributing to the removal of pre-existing soil nitrogen and DOC (Youkhana and Idol, 2009).

The high nitrogen and DOC loss measured on the mulch treatment was primarily due to the decomposing mulch releasing nitrogen and carbon coupled with the reduced effectiveness of the mulch on the smaller plots, rather than these nutrients being eroded from the soil, as indicated by the low sediment load measurements (Smets *et al.*, 2008; Youkhana and Idol, 2009). These high measurements on the mulch treatment were not compromising the productivity of the soil prior to mulching, but rather it is likely that the nutrients released from the decomposing mulch were entering the soil and remaining there due to low levels of sediment loss, increasing the productivity of the soils (Blackburn *et al*., 1986; Chaplot *et al*., 2011). The CBT, however, was dissimilar to the mulch as it did not protect the nitrogen and DOC released into the soils from decomposing unburnt debris (Youkhana and Idol, 2009). The elevated sediment loss on the CBT ensured that the nitrogen and DOC released from unburnt debris, was eroded along with the existing soil nitrogen and DOC stores, resulting in a decline in the productivity of the soils of this treatment (Blackburn *et al*., 1986; Chaplot *et al*., 2011). The HBT not producing the most nitrogen or DOC loss; however, it still generated high levels of both, without the decomposition of unburnt debris enriching the soils with nitrogen and DOC (Youkhana and Idol, 2009), and with evidence of these nutrients not significantly increasing in concentration in post-burn runoff (Knoepp and Swank, 1993; Clay *et al*., 2009). This indicated that the high levels of nitrogen and DOC loss on the HBT were products of the increased soil erosion resulting from burning, agreeing with the findings of Fernández *et al*.,

2004, rather than direct products of the burn itself (Knoepp and Swank, 1993; Clay *et al*., 2009). The high levels of nitrogen loss threaten downstream water quality as the introduction of nitrogen to fresh water sources leads to eutrophication (Carpenter *et al*., 1998). The high loss of DOC from the soils of the CBT and HBT is of particular concern as the loss of soil organic carbon will hinder vegetation growth, soil aggregation, and compromises the sequestration of the greenhouse gas carbon dioxide (Le Bissonnais and Arrouays, 1997; Zinn *et al*., 2002; Mohammad and Adam, 2010; Oliveira *et al*., 2013).

High runoff and erosion value trends were shared across all measured variables, barring phosphorous loss, and across all treatments. The generation of high values of these variables was driven primarily by high rainfall intensities, followed by a short duration since the previous event (inferring a greater antecedent soil moisture), and thereafter rainfall depth. The high rainfall intensities coupled with the soil water repellency, promoted the generation of Hortonian overland flow, while the antecedent soil moisture reduced the volume of water necessary for the soil to reach saturation, promoting saturated overland flow (Parsons and Abrahams, 1992). This suggested that the generation of high values of the aforementioned variables was primarily driven by Hortonian overland flow, and then to a lesser extent by saturated overland flow. The compounding effect of these processes resulted in high levels of runoff being produced which were long lasting and began early in the rainfall event, leading to increased runoff and erosion (Le Bissonnais *et al.*, 1998). The trend observed for phosphorous loss differs in that high values were primarily driven by rainfall depth, followed by antecedent soil moisture and rainfall intensity. This suggests that phosphorous loss was driven by saturated overland flow, as the high rainfall depths were able to easily saturate the soil, while the antecedent soil moisture reduced the volume of water necessary for the soil to reach saturation, further promoting saturated overland flow (Parsons and Abrahams, 1992).

The increased slope of the steep slope on the CBT compared to the other treatments had the potential to increase the relative runoff produced by the CBT (Ziadat and Taimeh, 2013). In addition, at the onset of the study the CBT had significantly greater concentrations of soil potassium compared to the other treatments, which has been known to increase runoff (Auerswald *et al*., 1996). Despite these factors which exacerbate the generation of runoff on the CBT, the HBT produced a greater amount of runoff on the 10 m^2 plots, indicating the propensity of the HBT to runoff and erosion once the fine ash layer has been flushed from the site. This is supported by severe burns having been noted for sealing soil pores with fine ash and reducing soil infiltration,

which was evident in the HBT's increased tendency to generate runoff regardless of slope, compared to the CBT, as demonstrated by the runoff hydrographs (Morin and Benyamini, 1977; Strydom, 2013). In addition, although there was a uniform degree of water repellency observed across all treatments, it was possible that the treatments had different infiltration rates, leading to the different magnitudes of runoff and subsequent erosion observed (Rycroft, 1947; Scott and Van Wyk, 1990; Neary *et al.,* 1999). The burning of catchments damages soil aggregates, and seals soil pores, reducing infiltration rates, resulting in the burn treatments being more susceptible to runoff and erosion than the mulch treatment (Neary *et al.,* 1999; Martin and Moody, 2001).

The increased runoff and erosion observed on the burn treatments threatens downstream water quality through the promotion of eutrophication, and the sedimentation of reservoirs (Chaplot *et al*., 2011; Ekholm and Lehtoranta, 2012). The nitrogen measurements on the mulch treatment suggested that it threatens downstream water quality through high levels of nitrogen loss from splash erosion; however this has been attributed to a reduction in the efficiency of the mulch to reduce erosion as a result of the small scale at which the measurements took place, where a truer reflection of the mulch to control erosion was observed on the 10 m^2 plots (Smets *et al*., 2008). The reductions in runoff generation and erosion observed on the mulch treatment compared to the burn treatments agree with the findings of Fernández et al. (2004), and suggest that mulching can aid in ensuring that commercial forestry practices are sustainable and help achieve several United Nations Sustainable Development Goals (United Nations, 2015).

The research suggests that of all treatments, the mulch treatment had the greatest potential to conserve *in situ* soil properties, thus protecting soil productivity, downstream water quality and security. These results are representative of the first year of growth of a *Eucalyptus dunnii* stand and are subject to change as the development of the stand brings about changes to the soil properties and soil cover (canopy and basal), accompanied by changes in interception loss, and thus runoff and erosion (Mohammad and Adam, 2010; Podwojewski *et al*., 2011; Oliveira *et al*., 2013). Hence, the continued call to research institutes and funders alike to develop long-term monitoring sites, such as is being conducted at the present site.

Chapter Six

Conclusions

The importance of conservative management practices in commercial forestry plantations is evident as commercial plantations have been known to exacerbate soil erosion, and are vulnerable to certain site preparation techniques (Blackburn *et al*., 1986; Fernández *et al*., 2004; Geißler *et al.*, 2012). The annual growth and significant area covered by commercial forestry, coupled with the commonly employed site preparation technique of burning (Swift *et al*., 1993; Jewitt, 2005), poses a significant threat to global soil and water quality (Carpenter *et al*., 1998; Chaplot *et al*., 2011). This is of particular concern to South Africa, a country severely affected by soil erosion and land degradation, yet actively relies on commercial forestry plantations, despite the environmental and economic consequences (Le Roux *et al*., 2008; Chaplot *et al*., 2011; Albaugh *et al*., 2013).

The paradoxical nature of commercial forestry in South Africa prompted this research, focusing on different current site preparation techniques and their potential to either accelerate natural soil erosion, having *in situ* and *ex situ* consequences, or to protect against soil erosion and land degradation, and the ability of the SWAT model to simulate these interactions. The findings of this research demonstrated that commercial forestry site preparation techniques influence soil erosion processes, whereby mulching protected the natural erosion process and burning accelerated soil erosion process. These findings concur with several other studies, in that the process of burning resulted in accelerated runoff generation and soil erosion, while the practice of mulching curbed runoff and soil erosion. The results demonstrated the scalar variation of the erosion process, and the different erosion processes that were dominant on each treatment.

Multi-facetted and multi-scale measuring used within this research was induced for the first objective through the necessity to capture soil erosion data at its different functioning scales (Chaplot and Poesen, 2012). This experimental design was suitable for achieving the first objective, and ensured that soil erosion processes could be measured at the different spatial scales at which they operate. The results demonstrated how soil erosion is affected by the spatial scales at which it is measured, the site preparation treatments, and the slope. The success of the second objective in determining runoff generation, sediment yield, and nutrient loss on all treatments at the different operating spatial scales of the erosion processes, ensured that the causes of varying runoff, nutrient

loss and sediment yield generation of different site preparation treatments could be identified. The research demonstrated that the key driver of phosphorous loss was rainfall depth, while the other measured soil erosion variables were driven by rainfall intensity, followed by antecedent soil moisture, regardless of treatment type. Nitrogen and DOC measurements were higher on treatments with unburnt debris able to decompose, which infers that the decomposition of OM led to the deposition of additional DOC and nitrogen within the soils (Youkhana and Idol, 2009). Fine ash deposits protected the HBT from splash erosion, but exacerbated rill erosion through the clogging of soil pores once the ash had been flushed (Blackburn *et al*., 1986; Podwojewski *et al*., 2011). Coarse debris littered throughout the CBT protected the treatment against rill erosion, but due to the sparseness of the debris, left the soil exposed to splash erosion (Le Bissonnais *et al.*, 1998; Salles and Poesen, 2000). The mulch treatment protected against splash and rill erosion, yet appeared to be more susceptible to splash erosion which was the result of a reduction in the effectiveness of the mulch to reduce runoff and erosion on smaller plots (Smets *et al.*, 2008). The final objective sought to use the observed soil erosion to validate modelled soil erosion of the study site using the implemented site preparation techniques. It was shown that the SWAT model was unable to simulate the observed runoff and erosion on each treatment, which was likely caused by land-use management input variables which were unrepresentative of the observed land-uses. This led to processes such as infiltration, and surface runoff mechanisms (e.g., resistance to flow and sediment transportation) deviating from their natural function, resulting in the poor simulations. It was potentially the result of the variables (i.e., support practice factor, soil erodibility, land cover) used within the USLE calculation within the model ineffectively representing the relationships between the observed land-uses and erosional processes. It was also likely that the land-use management tools within the model require refinement, whereby the misrepresentation of the intrinsic characteristics of each treatment (e.g., soil infiltrability, resistance to flow by debris, soil water holding capacity, post-burn debris deposits) led to poor simulations.

The inability of the SWAT model to simulate the interactions and processes between observed soil erosion and land-use management in this research has been recorded. This model may benefit from calibration with regards to the land-use scenarios examined in this research, which may be achieved through the use of calibration tools such as SWAT-CUP. It is however, advised that future efforts are directed towards the refining of the land-use management tools within the SWAT model, to enhance the model's ability to simulate runoff and erosion generated on a diverse set of land-use

treatments relating to different commercial forestry preparation techniques and tree species. These findings of this research will contribute towards increasing the number of data sets of varying land-use management necessary to refine the land-use management tools within the model.

The projections of climate change to increase extreme rainfall events, coupled with the findings of this research, whereby larger rainfall events generate extreme runoff and erosion, threatens the sustainability of soil and water quality as we move into an uncertain climatic future (Mason *et al.*, 1999). Despite prescribed burns having little impact on DOC content in runoff (Knoepp and Swank, 1993), soil erosion increases soil carbon losses as seen in this study by the POC loss being linked to sediment loss on the burn treatments. Therefore, the increased soil erosion and sediment loss from burn treatments, have the potential to exacerbate climate change by contributing to atmospheric carbon dioxide (Lal, 2001). This would result in a positive feedback loop, whereby the increasingly extreme rainfall events generated by climate change would increase soil erosion, increasing atmospheric carbon dioxide, accelerating climate change, leading to a further rise in extreme rainfall events.

This research demonstrates the potential of mulching as a site preparation technique, compared to burning, to control runoff and soil erosion, protecting soil productivity and downstream water quality, and aid in the accomplishment of several United Nations Sustainable Development Goals (United Nations, 2015). In addition, this research has demonstrated the value that would be provided by conducting a cost/benefit analysis, soil chemical and infiltration rate monitoring for the study site over an extended growth period, in terms of delivering more conclusive and definitive land-use management guidance. However, one needs to take cognisance of the increase in field-based resources associated with such endeavours. Monitoring over an extended growth period is critical due to the long rotation period, and the concomitant accumulation of litter and canopy cover has the potential to reduce soil erosion in commercial plantations, which could be positive when compared with other land-use activities (e.g. overgrazing) (Oliveira *et al*., 2013; Gillham, 2016). The proposed monitoring regime is critical in determining the long-term effects of site preparation techniques on subsequent soil productivity, downstream water quality, and the ability of each technique to aid in the mitigation of climate change.

This research provides insights into the effects of different commercial site preparation techniques on soil erosion, soil productivity and downstream water quality, and evaluated the ability of the

SWAT model to simulate these interactions. This research has demonstrated the impacts of differing site preparation techniques on soil productivity and water quality, forming the foundation for ameliorating the environmental impacts of land management practices and climate change through pertaining to commercial forestry plantations. This research provides direction into improving our ability to model these impacts, and guides future research into the implementation of alternative and sustainable options, enabling better informed land-use management decisions, as we continue into an uncertain climatic future.

References

Albaugh, JM, Dye, PJ and King, JS. 2013. Eucalyptus and water use in South Africa. *International Journal of Forestry Research* 2013:1-11.

Auerswald, K, Kainz, M, Angermüller, S and Steindl, H. 1996. Influence of exchangeable potassium on soil erodibility. Soil Use and *Management* 12(3):117-121.

Bautista, S, Bellot, J and Vallejo, VR. 1996. Mulching treatment for postfire soil conservation in a semiarid ecosystem. *Arid Land Research and Management* 10(3):235-242.

Beasley, RS. 1979. Intensive Site Preparation and Sediment Losses on Steep Watersheds in the Gulf Coastal Plain 1. *Soil Science Society of America Journal* 43(2):412-417.

Beckedahl, HR and De Villiers, AB. 2000. Accelerated erosion by piping in the Eastern Cape Province, South Africa. *South African Geographical Journal* 82(3):157-162.

Blackburn, WH, Wood, JC and DeHaven, MG. 1986. Storm flow and sediment losses from site-prepared forestland in East Texas. *Water Resources Research* 22(5):776-784.

Bulcock, HH and Jewitt, GPW. 2012. Field data collection and analysis of canopy and litter interception in commercial forest plantations in the KwaZulu-Natal Midlands, South Africa. *Hydrology and Earth System Sciences* 16(10):3717-3728.

Buttafuoco, G, Conforti, M, Aucelli, PPC, Robustelli, G and Scarciglia, F. 2012. Assessing spatial uncertainty in mapping soil erodibility factor using geostatistical stochastic simulation. *Environmental Earth Sciences* 66(4):1111-1125.

Cantón, Y, Solé-Benet, A, De Vente, J, Boix-Fayos, C, Calvo-Cases, A, Asensio, C and Puigdefábregas, J, 2011. A review of runoff generation and soil erosion across scales in semiarid south-eastern Spain. *Journal of Arid Environments* 75(12):1254-1261.

Carpenter, SR, Caraco, NF, Correll, DL, Howarth, RW, Sharpley, AN and Smith, VH. 1998. Nonpoint pollution of surface waters with phosphorus and nitrogen. *Ecological applications* 8(3):559-568.

Cerda, A and Robichaud, P. 2009. Fire effects on soil infiltration. In: ed. Cerda, A and Robichaud, P, *Fire effects on soils and restoration strategies*, ch. 3, 81-104. Science Publishers, New Hampshire, USA.

Chaplot, V. 2007. Water and soil resources response to rising levels of atmospheric CO_2 concentration and to changes in precipitation and air temperature. *Journal of Hydrology* 337(1-2):159-171.

Chaplot, V, Brown, J, Dlamini, P, Eustice, T, Janeau, JL, Jewitt, G, Lorentz, S, Martin, L, Nontokozo-Mchunu, C, Oakes, E and Podwojewski, P. 2011. Rainfall simulation to identify the storm-scale mechanisms of gully bank retreat. *Agricultural Water Management* 98(11):1704-1710.

Chaplot, V, Le Brozec, EC, Silvera, N and Valentin, C. 2005. Spatial and temporal assessment of linear erosion in catchments under sloping lands of northern Laos. *Catena* 63(2-3):167-184.

Chaplot, V and Poesen, J. 2012. Sediment, soil organic carbon and runoff delivery at various spatial scales. *Catena* 88(1):46-56.

Clay, GD, Worrall, F and Fraser, ED. 2009. Effects of managed burning upon dissolved organic carbon (DOC) in soil water and runoff water following a managed burn of a UK blanket bog. *Journal of Hydrology 367*(1-2):41-51.

Clulow, A, Everson, CS and Gush, MB. 2011. *The Long-term Impact of Acacia Mearnsii Trees on Evaporation, Streamflow and Groundwater Resources: Report to the Water Research Commission.* Water Research Commission Report No. TT505/11, ISBN 978-1-4312-0020-3. Water Research Commission, Pretoria, South Africa.

Curriero, FC, Patz, JA, Rose, JB and Lele, S.,2001. The association between extreme precipitation and waterborne disease outbreaks in the United States, 1948–1994. *American journal of public health* 91(8):1194-1199.

da Silva, AM. 2004. Rainfall erosivity map for Brazil. *Catena* 57(3):251-259.

DeBano LF. 1981. Water repellent soils: a state of the art. Report no. General Technical Report PSW-46. Pacific Southwest Forest and Range Experiment Station, Berkeley, USA.

DeBano, LF, Savage, SM and Hamilton, DA. 1976. The Transfer of Heat and Hydrophobic Substances During Burning. *Soil Science Society of America Journal* 40(5):779-782.

Doerr, SH, Shakesby, RA and Walsh, RP. 1996. Soil hydrophobicity variations with depth and particle size fraction in burned and unburned *Eucalyptus globulus* and *Pinus pinaster* forest terrain in the Agueda Basin, Portugal. *Catena* 27(1):25-47.

Ekholm, P and Lehtoranta, J. 2012. Does control of soil erosion inhibit aquatic eutrophication? *Journal of Environmental Management* 93(1):140-146.

Everson CS, Clulow AD, Becker M, Watson A, Ngubo C, Bulcock H, Mengistu M, Lorentz S And Demlie M. 2014. *The long-term impact of Acacia mearnsii trees on evaporation, streamflow, low flows and ground water resources. Phase II: Understanding the controlling environmental variables and soil water processes over a full crop rotation*. WRC Report No. K5/2022. Water Research Commission, Pretoria, South Africa.

Fernández, C, Vega, JA, Gras, JM, Fonturbel, T, Cuinas, P, Dambrine, E and Alonso, M. 2004. Soil erosion after Eucalyptus globulus clearcutting: differences between logging slash disposal treatments. *Forest Ecology and Management* 195(1-2):85-95.

Fey, M. 2010. *Soils of South Africa*. Cambridge University Press, Cambridge, England.

Geißler, C, Kühn, P, Böhnke, M, Bruelheide, H, Shi, X and Scholten, T. 2012. Splash erosion potential under tree canopies in subtropical SE China. *Catena* 91:85-93.

Gillham, JS. 2016. Investigating the processes of erosion and sediment yield at different scales in commercial forestry – A case study at Two Streams, KwaZulu-Natal. Unpublished MSc Dissertation, Discipline of Geography, University of KwaZulu-Natal, Pietermaritzburg, South Africa.

Google Earth Pro version 7.1.8.3036, Google Inc., Mountain View, USA

Google Maps. 2018. [Internet]. Google Inc., Mountain View, USA. Available from: https://www.google.co.za/maps?q=29%C2%B012'13.1%22S+30%C2%B039'14.6%22E&rlz=1C1MSIM_enZA730ZA731&um=1&ie=UTF-8&sa=X&ved=0ahUKEwi_-9DN3a_aAhViI8AKHZZOD_8Q_AUICigB [Accessed 2 April 2018].

Govender, M and Everson, CS. 2005. Modelling streamflow from two small South African experimental catchments using the SWAT model. *Hydrological Processes: An International Journal 19*(3):683-692.

Guerra, A. 1994. The effect of organic matter content on soil erosion in simulated rainfall experiments in W. Sussex, UK. *Soil Use and Management* 10(2):60-64.

Gyamfi, C, Ndambuki, JM and Salim, RW. 2016. Application of SWAT model to the Olifants Basin: calibration, validation and uncertainty analysis. *Journal of Water Resource and Protection 8*(03):397.

Hardie, MA, Doyle, RB, Cotching, WE, Duckett, T and Zund, P. 2009. *Dispersive soils and their management*, Department of Primary Industries and Water, Hobart Tasmania.

Hartanto, H, Prabhu, R, Widayat, AS and Asdak, C. 2003. Factors affecting runoff and soil erosion: plot-level soil loss monitoring for assessing sustainability of forest management. *Forest Ecology and Management* 180(1-3):361-374.

Hewitson, BC and Crane, RG. 2006. Consensus between GCM climate change projections with empirical downscaling: precipitation downscaling over South Africa. *International Journal of Climatology* 26(10):1315-1337.

Jewitt, G. 2005. Water and forests. In: ed. Anderson, MG and McDonnell, JJ, *Encyclopedia of Hydrological Sciences*, ch. 186, 2897–2909. John Wiley & Sons Ltd, Chichester, UK.

Jewitt, GPW and Schulze, RE. 1999. Verification of the ACRU model for forest hydrology applications. *Water SA* 25(4):483-489.

Knoepp, JD and Swank, WT. 1993. Site preparation burning to improve southern Appalachian pine-hardwood stands: nitrogen responses in soil, soil water, and streams. *Canadian Journal of Forest Research 23*(10):2263-2270.

Knox, J, Morris, J and Hess, T. 2010. Identifying future risks to UK agricultural crop production: Putting climate change in context. *Outlook on Agriculture* 39(4):249-256.

Kort, J, Collins, M and Ditsch, D. 1998. A review of soil erosion potential associated with biomass crops. *Biomass and Bioenergy* 14(4):351-359.

Lakel, WA, Aust, WM, Bolding, MC, Dolloff, CA, Keyser, P and Feldt, R. 2010. Sediment trapping by streamside management zones of various widths after forest harvest and site preparation. *Forest Science* 56(6):541-551.

Laker, MC. 2004. Advances in soil erosion, soil conservation, land suitability evaluation and land use planning research in South Africa, 1978–2003. *South African Journal of Plant and Soil* 21(5):345-368.

Lal, R. 2001. Soil degradation by erosion. *Land Degradation & Development* 12(6):519-539.

Le Bissonnais, Y and Arrouays, D. 1997. Aggregate stability and assessment of soil crustability and erodibility: II. Application to humic loamy soils with various organic carbon contents. *European Journal of Soil Science* 48(1):39-48.

Le Bissonnais, Y, Benkhadra, H, Chaplot, V, Fox, D, King, D and Daroussin, J. 1998. Crusting, runoff and sheet erosion on silty loamy soils at various scales and upscaling from m2 to small catchments. *Soil and Tillage Research* 46(1-2):69-80.

Le Roux, JJ, Morgenthal, TL, Malherbe, J, Pretorius, DJ and Sumner, PD. 2008. Water erosion prediction at a national scale for South Africa. *Water SA* 34(3):305-314.

Le Roux, JJ, Newby, TS and Sumner, PD. 2007. Monitoring soil erosion in South Africa at a regional scale: review and recommendations. *South African Journal of Science* 103(7-8):329-335.

Le Roux, JJ, Sumner, PD, Lorentz, SA and Germishuyse, T. 2013. Connectivity aspects in sediment migration modelling using the Soil and Water Assessment Tool. *Geosciences* 3(1):1-12.

Le Roux, PAL, Hensley, M, Lorentz, SA, van Tol, JJ, Van Zijl, GM, Kuenene, BT, Bouwer, D, Freese, CS, Tinnefeld, M and Jacobs, CC. 2015. *Hydrology of South African Soils and Hillslopes*. WRC Report No. 2021/1/15. Water Research Commission, Pretoria, South Africa.

Mason, SJ, Waylen, PR, Mimmack, GM, Rajaratnam, B and Harrison, JM. 1999. Changes in extreme rainfall events in South Africa. *Climatic Change* 41(2):249-257.

Martin, DA and Moody, JA. 2001. Comparison of soil infiltration rates in burned and unburned mountainous watersheds. *Hydrological Processes* 15(15):2893-2903.

Mohammad, AG and Adam, MA. 2010. The impact of vegetative cover type on runoff and soil erosion under different land uses. *Catena* 81(2):97-103.

Montagnini, F and Nair, PKR. 2004. Carbon sequestration: an underexploited environmental benefit of agroforestry systems. *Agroforestry Systems* 61(3):281-295.

Morgan, RPC. 2009. *Soil Erosion and Conservation*. John Wiley & Sons, Hoboken, United States of America.

Morin, J and Benyamini, Y. 1977. Rainfall infiltration into bare soils. *Water Resources Research* 13(5):813-817.

Müller-Nedebock, D, Chivenge, P and Chaplot, V. 2016. Selective organic carbon losses from soils by sheet erosion and main controls. *Earth Surface Processes and Landforms* 41(10):1399-1408.

Nambiar, ES. 1999. Productivity and sustainability of plantation forests. *Bosque* 20(1):9-21.

Nanko, K, Hotta, N and Suzuki, M. 2004. Assessing raindrop impact energy at the forest floor in a mature Japanese cypress plantation using continuous raindrop-sizing instruments. *Journal of Forest Research* 9(2):157-164.

Nanko, K, Mizugaki, S and Onda, Y. 2008. Estimation of soil splash detachment rates on the forest floor of an unmanaged Japanese cypress plantation based on field measurements of throughfall drop sizes and velocities. *Catena* 72(3):348-361.

National Resources Conservation Service Soil Survey Staff, 1996. *National Soil Survey Handbook*. Handbook No. 430-VI, U.S. Government Printing Office, Washington, USA.

Nearing, MA. 2013. Soil erosion and conservation. In: ed. Wainwright, J, Mulligan, M, *Environmental Modelling: Finding Simplicity in Complexity*, ch. 22, 365-378. John Wiley & Sons, Hoboken, United States of America.

Neary, DG, Klopatek, CC, DeBano, LF and Ffolliott, PF. 1999. Fire effects on belowground sustainability: a review and synthesis. *Forest Ecology and Management* 122(1-2):51-71.

Obi, ME and Salako, FK. 1995. Rainfall parameters influencing erosivity in southeastern Nigeria. *Catena* 24(4):275-287.

Oeurng, C, Sauvage, S and Sánchez-Pérez, JM. 2011. Assessment of hydrology, sediment and particulate organic carbon yield in a large agricultural catchment using the SWAT model. *Journal of Hydrology* 401(3-4):145-153.

Oliveira, AH, Silva, MLN, Curi, N, Avanzi, JC, Klinke Neto, G and Araújo, EF. 2013. Water erosion in soils under eucalyptus forest as affected by development stages and management systems. *Ciência e Agrotecnologia* 37(2):159-169.

Panagopoulos, I, Mimikou, M and Kapetanaki, M. 2007. Estimation of nitrogen and phosphorus losses to surface water and groundwater through the implementation of the SWAT model for Norwegian soils. *Journal of Soils and Sediments 7*(4):223-231.

Parsons, AJ and Abrahams, AD. 1992. *Overland flow: hydraulics and erosion mechanics,* UCL Press, London, England.

Piirainen, S, Finér, L, Mannerkoski, H. and Starr, M, 2007. Carbon, nitrogen and phosphorus leaching after site preparation at a boreal forest clear-cut area. *Forest Ecology and Management* 243(1):10-18.

Pimentel, D, Harvey, C, Resosudarmo, P, Sinclair, K, Kurz, D, McNair, M, Crist, S, Shpritz, L, Fitton, L, Saffouri, R and Blair, R, 1995. Environmental and economic costs of soil erosion and conservation benefits. *Science* 267(5201):1117-1123.

Plumb Jr, RH. 1981. *Procedures for handling and chemical analysis of sediment and water Samples*. Technical Report EPA/CE-81-1. U.S Environmental Protection Agency/Corps of Engineers Technical Committee on Criteria for Dredge and Fill Material, Washington D.C., United States of America.

Podwojewski, P, Janeau, JL, Grellier, S, Valentin, C, Lorentz, S and Chaplot, V. 2011. Influence of grass soil cover on water runoff and soil detachment under rainfall simulation in a sub-humid South African degraded rangeland. *Earth Surface Processes and Landforms* 36(7):911-922.

Poore, MED 1955. The use of phytosociological methods in ecological investigations: I. The Braun-Blanquet system. *Journal of Ecology* 43(1):226-244.

Prats, SA, MacDonald, LH, Monteiro, M, Ferreira, AJ, Coelho, CO and Keizer, JJ. 2012. Effectiveness of forest residue mulching in reducing post-fire runoff and erosion in a pine and a eucalypt plantation in north-central Portugal. *Geoderma* 191:115-124.

Rickson, RJ 2014. Can control of soil erosion mitigate water pollution by sediments? *Science of the Total Environment* 468:1187-1197.

Rienks, SM, Botha, GA and Hughes, JC, 2000. Some physical and chemical properties of sediments exposed in a gully (donga) in northern KwaZulu-Natal, South Africa and their relationship to the erodibility of the colluvial layers. *Catena 39*(1):11-31.

Robichaud, PR and Waldrop, TA. 1994. A comparison of surface runoff and sediment yields from low-and high-severity site preparation burns. *Journal of the American Water Resources Association* 30(1):27-34.

Robichaud, PR, Lewis, SA, Wagenbrenner, JW, Ashmun, LE and Brown, RE. 2013. Post-fire mulching for runoff and erosion mitigation: Part I: Effectiveness at reducing hillslope erosion rates. *Catena* 105:75-92.

Rumpel, C, Ba, A, Darboux, F, Chaplot, V and Planchon, O. 2009. Erosion budget and process selectivity of black carbon at meter scale. *Geoderma* 154(1-2):131-137.

Rycroft, HB. 1947. A note on the immediate effects of veldburning on stormflow in a Jonkershoek stream catchment. *Journal of the South African Forestry Association* 15(1):80-88.

Salles, C and Poesen, J. 2000. Rain properties controlling soil splash detachment. *Hydrological Processes* 14(2):271-282.

Saá, A, Trasar-Cepeda, MC, Soto, B, Gil-Sotres, F and Diaz-Fierros, F., 1994. Forms of phosphorus in sediments eroded from burnt soils. *Journal of Environmental Quality* 23(4):739-746.

Schaller, N, Kay, AL, Lamb, R, Massey, NR, Van Oldenborgh, GJ, Otto, FE, Sparrow, SN, Vautard, R, Yiou, P, Ashpole, I and Bowery, A. 2016. Human influence on climate in the 2014 southern England winter floods and their impacts. *Nature Climate Change* 6(6):627.

Scott, DF. 1994. The hydrological effects of fire in South African catchments. Unpublished Doctoral dissertation, School of Agricultural Earth and Environmental Science, University of Natal, Pietermaritzburg, South Africa.

Scott, DF. 2000. Soil wettability in forested catchments in South Africa; as measured by different methods and as affected by vegetation cover and soil characteristics. *Journal of Hydrology* 231:87-104.

Scott, DF and Van Wyk, DB. 1990. The effects of wildfire on soil wettability and hydrological behaviour of an afforested catchment. *Journal of Hydrology* 121(1):239-256.

Scott-Shaw, BC, Hill, TR and Gillham, JS. 2020. Calibration of a modelling approach for sediment yield in a wattle plantation, KwaZulu-Natal, South Africa. *Water SA* 46(2):171-181.

Setegn, SG, Dargahi, B, Srinivasan, R and Melesse, AM. 2010. Modeling of Sediment Yield From Anjeni-Gauged Watershed, Ethiopia Using SWAT Model 1. *JAWRA Journal of the American Water Resources Association 46*(3):514-526.

Shakesby, RA and Doerr, SH. 2006. Wildfire as a hydrological and geomorphological agent. *Earth-Science Reviews* 74(3):269-307.

Singh, G, Babu, R, Narain, P, Bhushan, LS and Abrol, IP. 1992. Soil erosion rates in India. *Journal of Soil and water Conservation* 47(1):97-99.

Smets, T, Poesen, J and Knapen, A. 2008. Spatial scale effects on the effectiveness of organic mulches in reducing soil erosion by water. *Earth-Science Reviews* 89(1-2):1-12.

Snyman, HA. 2003. Short-term response of rangeland following an unplanned fire in terms of soil characteristics in a semi-arid climate of South Africa. *Journal of Arid Environments* 55(1):160-180.

Strydom, T. 2013. The Effect of Long-term Fire Frequencies on Soil Hydraulic Properties in Semi-arid Savannas in Kruger National Park. Unpublished MSc Hydrology Thesis, School of Agriculture, Earth and Environmental Sciences, University of Natal, Pietermaritzburg, RSA.

Swift Jr, LW, Elliott, KJ, Ottmar, RD and Vihnanek, RE. 1993. Site preparation burning to improve southern Appalachian pine–hardwood stands: Fire characteristics and soil erosion, moisture, and temperature. *Canadian Journal of Forest Research* 23(10):2242-2254.

Thompson, T, Sobsey, M and Bartram, J. 2003. Providing clean water, keeping water clean: an integrated approach. *International Journal of Environmental Health Research 13*:S89-S94.

Toucher, ML, Clulow, A, van Rensburg, SJ, Morris, F, Gray, B, Majozi, S, Everson, C, and Jewitt, EPW. 2016. Establishment of and Demonstration of the Potential of the Cathedral Peak Research Catchments as a Living Laboratory. Report No. 2236/1/16. Water Research Comission, Pretoria, South Africa.

Toy, TJ, Foster, GR and Renard, KG. 2002. Soil erosion: processes, prediction, measurement, and control. John Wiley & Sons, Hoboken, United States of America.

United Nations. 2015. Sustainable Development Goals. [Internet]. United Nations Department of Public Information, New York, USA. Available from: https://sustainabledevelopment.un.org/?menu=1300 [Accessed 16 April 2020].

University of New Hampshire. 2015. Randomized Complete Block Designs (RCBDs) and Latin Squares. [Internet]. University of New Hampshire, Durham, USA. Available from: http://www.unh.edu/halelab/BIOL933/Labs/Lab5.pdf [Accessed 19 April 2018].

Vacca, A, Loddo, S, Ollesch, G, Puddu, R, Serra, G, Tomasi, D and Aru, A. 2000. Measurement of runoff and soil erosion in three areas under different land use in Sardinia (Italy). *Catena* 40(1):69-92.

Valentin, C, Poesen, J and Li, Y. 2005. Gully erosion: impacts, factors and control. *Catena* 63(2-3):132-153.

Van Oost, K, Govers, G and Desmet, P. 2000. Evaluating the effects of changes in landscape structure on soil erosion water and tillage. *Landscape Ecology* 15:577-589.

Van Wyk, DB. 1986. The effects of catchment management on sediment and nutrient exports in the Natal Drakensberg. In: eds. Schulze, RE, *Second South African National Hydrology Symposium*, 266-274. Department of Agricultural Engineering, University of Natal, Pietermaritzburg, RSA.

Vandaele, K and Poesen, J. 1995. Spatial and temporal patterns of soil erosion rates in an agricultural catchment, central Belgium. *Catena* 25(1-4):213-226.

Vose, JM and Swank, WT. 1993. Site preparation burning to improve southern Appalachian pine–hardwood stands: aboveground biomass, forest floor mass, and nitrogen and carbon pools. *Canadian Journal of Forest Research* 23(10):2255-2262.

Wu, Y and Chen, J. 2009. Simulation of nitrogen and phosphorus loads in the Dongjiang River basin in South China using SWAT. *Frontiers of Earth Science in China 3*(3):273-278.

Youkhana, A. and Idol, T. 2009. Tree pruning mulch increases soil C and N in a shaded coffee agroecosystem in Hawaii. *Soil Biology and Biochemistry 41*(12):2527-2534.

Ziadat, FM. and Taimeh, AY. 2013. Effect of rainfall intensity, slope, land use and antecedent soil moisture on soil erosion in an arid environment. *Land Degradation and Development* 24(6):582-590.

Zinn, YL, Resck, DV and da Silva, JE. 2002. Soil organic carbon as affected by afforestation with Eucalyptus and Pinus in the Cerrado region of Brazil. *Forest Ecology and Management* 166(1-3):285-294.

Appendices

Appendix A

Treatment Photos

Plate A-1: Hot burn treatment.

Plate A-2: Cold burn treatment.

Plate A-3: Mulch treatment.

Plate A-4: Hot burn treatment runoff plot setup.

Plate A-5: Hot burn treatment micro-runoff plot setup.

Plate A-6: Cold burn treatment micro-runoff plot setup.

Plate A-7: Cold burn treatment runoff plot post-setup.

Plate A-8: Mulch treatment runoff plot setup.

Plate A-9: Mulch treatment micro-runoff plot setup.

Appendix B

Statistical Outputs

Table B-1: Parametric one-way ANOVA test of the precipitation of each rain gauge throughout the study period.

ANOVA						
Source of Variation	*SS*	*df*	*MS*	*F*	*P-value*	*F crit*
Between Groups	446.29294	6	74.38216	0.0910914	0.9970325	2.2311924
Within Groups	57159.625	70	816.5661			
Total	57605.918	76				

Table B-2: Parametric one-way ANOVA test of the top slope steepness across each treatment.

ANOVA						
Source of Variation	*SS*	*df*	*MS*	*F*	*P-value*	*F crit*
Between Groups	46.296296	1	46.296296	6.0679612	0.069443	7.7086474
Within Groups	30.518519	4	7.6296296			
Total	76.814815	5				

Table B-3: Parametric one-way ANOVA test of the bottom slope steepness across each treatment.

ANOVA						
Source of Variation	*SS*	*df*	*MS*	*F*	*P-value*	*F crit*
Between Groups	89.555556	2	44.777778	9.8292683	0.0127867	5.1432528
Within Groups	27.333333	6	4.5555556			
Total	116.88889	8				

Table B-4: Parametric one-way ANOVA test of the soil sample density across each treatment.

ANOVA						
Source of Variation	SS	df	MS	F	P-value	F crit
Between Groups	0.0287167	5	0.005743	0.480167	0.7845886	3.1058752
Within Groups	0.1435333	12	0.011961			
Total	0.17225	17				

Table B-5: Parametric one-way ANOVA test of the phosphorous content in the soil across each treatment.

ANOVA						
Source of Variation	SS	df	MS	F	P-value	F crit
Between Groups	257.83333	5	51.56667	2.659599	0.0766297	3.1058752
Within Groups	232.66667	12	19.38889			
Total	490.5	17				

Table B-6: Parametric one-way ANOVA test of the potassium content in the soil across each treatment.

ANOVA						
Source of Variation	*SS*	*df*	*MS*	*F*	*P-value*	*F crit*
Between Groups	40069.611	5	8013.922	3.434947	0.0370736	3.1058752
Within Groups	27996.667	12	2333.056			
Total	68066.278	17				

Table B-7: Parametric one-way ANOVA test of the calcium content in the soil across each treatment.

ANOVA						
Source of Variation	*SS*	*df*	*MS*	*F*	*P-value*	*F crit*
Between Groups	164689.61	5	32937.92	0.541188	0.7420215	3.1058752
Within Groups	730346.67	12	60862.22			
Total	895036.28	17				

Table B-8: Parametric one-way ANOVA test of the magnesium content in the soil across each treatment.

ANOVA						
Source of Variation	*SS*	*df*	*MS*	*F*	*P-value*	*F crit*
Between Groups	4095.1111	5	819.0222	0.451362	0.8045746	3.1058752
Within Groups	21774.667	12	1814.556			
Total	25869.778	17				

Table B-9: Parametric one-way ANOVA test of the soil acidity exchange across each treatment

ANOVA						
Source of Variation	*SS*	*df*	*MS*	*F*	*P-value*	*F crit*
Between Groups	2.4244944	5	0.484899	0.678961	0.6478427	3.1058752
Within Groups	8.5701333	12	0.714178			
Total	10.994628	17				

Table B-10: Parametric one-way ANOVA test of the total cations in the soil across each treatment.

ANOVA						
Source of Variation	*SS*	*df*	*MS*	*F*	*P-value*	*F crit*
Between Groups	4.4465778	5	0.889316	0.467053	0.7937059	3.1058752
Within Groups	22.8492	12	1.9041			
Total	27.295778	17				

Table B-11: Parametric one-way ANOVA test of the soil acidity across each treatment.

ANOVA						
Source of Variation	*SS*	*df*	*MS*	*F*	*P-value*	*F crit*
Between Groups	1924.6667	5	384.9333	1.199377	0.3662809	3.1058752
Within Groups	3851.3333	12	320.9444			
Total	5776	17				

Table B-12: Parametric one-way ANOVA test of the soil pH across each treatment.

ANOVA						
Source of Variation	*SS*	*df*	*MS*	*F*	*P-value*	*F crit*
Between Groups	0.3167778	5	0.063356	1.385831	0.2968217	3.1058752
Within Groups	0.5486	12	0.045717			
Total	0.8653778	17				

Table B-13: Parametric one-way ANOVA test of the zinc content in the soil across each treatment.

ANOVA						
Source of Variation	*SS*	*df*	*MS*	*F*	*P-value*	*F crit*
Between Groups	0.585	5	0.117	1.002857	0.45674	3.1058752
Within Groups	1.4	12	0.116667			
Total	1.985	17				

Table B-14: Parametric one-way ANOVA test of the manganese content in the soil across each treatment.

ANOVA						
Source of Variation	*SS*	*df*	*MS*	*F*	*P-value*	*F crit*
Between Groups	2591.1667	5	518.2333	1.500917	0.2608489	3.1058752
Within Groups	4143.3333	12	345.2778			
Total	6734.5	17				

Table B-15: Parametric one-way ANOVA test of the copper content in the soil across each treatment.

ANOVA						
Source of Variation	*SS*	*df*	*MS*	*F*	*P-value*	*F crit*
Between Groups	0.2444444	5	0.048889	1.333333	0.3149042	3.1058752
Within Groups	0.44	12	0.036667			
Total	0.6844444	17				

Table B-16: Parametric one-way ANOVA test of the Organic Carbon content in the soil across each treatment.

ANOVA						
Source of Variation	*SS*	*df*	*MS*	*F*	*P-value*	*F crit*
Between Groups	2.1711111	5	0.434222	1.915686	0.1652344	3.1058752
Within Groups	2.72	12	0.226667			
Total	4.8911111	17				

Table B-17: Parametric one-way ANOVA test of the Nitrogen content in the soil across each treatment.

ANOVA						
Source of Variation	*SS*	*df*	*MS*	*F*	*P-value*	*F crit*
Between Groups	0.08425	5	0.01685	2.412888	0.0980973	3.1058752
Within Groups	0.0838	12	0.006983			
Total	0.16805	17				

Table B-18: Parametric one-way ANOVA test of the Clay content in the soil across each treatment.

Source of Variation	*SS*	*df*	*MS*	*F*	*P-value*	*F crit*
Between Groups	159.33333	5	31.86667	1.732931	0.2016351	3.1058752
Within Groups	220.66667	12	18.38889			
Total	380	17				